WASHINGTON UNIVERSITY IN ST. LOUIS

Division of Biology and Biomedical Sciences

Evolution, Ecology, and Population Biology

Dissertation Examination Committee:
Jeffrey I. Gordon, Chair
Gautam Dantas
Daniel E. Goldberg
Scott Mangan
David Queller
Alan Templeton

A Gnotobiotic Mouse Model for Studying the Effect of Human Gut Community Ecology on a Pathobiont, *Bacteroides fragilis*

by

Vitas Wagner

A dissertation presented to the
Graduate School of Arts & Sciences
of Washington University in
partial fulfillment of the
requirements for the degree
of Doctor of Philosophy

August 2015

St. Louis, Missouri

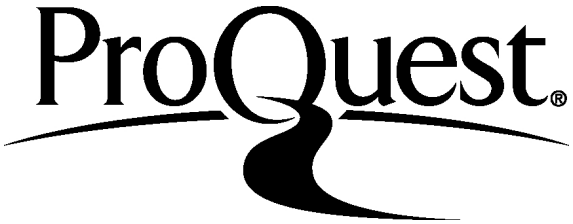

Table of Contents

Chapter 3

Regulators of gut motility revealed by a gnotobiotic model of travel-related diet changes

Chapter 4

Future Directions

Acknowledgements

I can confidently say that I could not have written the previous chapters of this thesis without the camaraderie and generosity displayed in the Gordon Lab, Washington University as a whole, and friends and family flung far and wide. Over the course of my doctoral research I have been surrounded by brilliant and extremely hardworking scientists that have pushed me to think and work harder on the problems my research has presented. My thesis advisor, Jeffrey Gordon, first and foremost deserves acknowledgement for giving me the opportunity to perform research in his laboratory. It is a rare occasion to work in an environment that provides the level of support found in this group of enthusiastic, collaborative, and bright scientists Jeff has assembled. His generosity, encouragement, and willingness to let me explore my professional development have been exceptional. My thesis committee also deserves an exceptional mention for the time and careful consideration they have displayed throughout the development of my thesis research, especially Dan Goldberg who has kindly served as my committee chair. I am very grateful to my committee's donation of their time and focus over the years, as we all know how valuable those resources are.

My development as a scientist began long before my entrance into graduate school. My middle school, high school, undergraduate science faculty, and employers were always, engaging, exceedingly supportive, and enthusiastic in my pursuit of studying the biological world. I find it hard to believe I would have found the passion to pursue doctoral research without their dedication to teaching and mentoring, and upon reflection, I was truly fortunate to string together such a fantastic series of teachers. Professor Delbert Hutchinson and Dr. Jerald Radich deserve particular acknowledgement for directing my enthusiasm and interest in evolutionary biology and focusing it toward questions concerning human health and disease.

My entry into lab was under Henning Seedorf where I was taught the mouse husbandry and metagenomic skills I would use throughout my time in lab. Doctors Andrew Goodman, Andrew Kau, Federico Rey, and Jeremiah Faith were also stalwart sources of information and guidance throughout my training. Dr. Neelendu Dey has also played an integral role in guiding me through

the process of writing and expanding my data analysis skills. I would be remiss if I forgot to mention Sabrina Wagoner, Janaki Lelwala-Guruge, Maria Karlsson, David O'Donnell, and Marty Meier. Sabrina is somehow able to keep the huge lab running smoothly while also donating enormous amounts of time and energy at the end of each mouse experiment. Janaki was integral in helping generate the culture collections that were central to chapters two and three of my thesis. David and Maria were enormous helps preparing for and helping me run my mouse experiments and were so welcoming to their home for car maintenance and coffee. Finally, Marty was a hero of our automation facility that allowed for the processing of thousands of samples generated over my time in the Gordon Lab. The Bill and Melinda Gates Foundation also deserves a special acknowledgement as it provided financial support for these projects, and their enthusiastic support for the work the lab does has been inspirational.

Aside from direct support in the laboratory, I have had wonderful encouragement from friends made here in St Louis as well as those gained throughout my life. Jessen Wabeke, Josh Kittrell, Jane Symington, Sarah Foyil, Chris Affolter, Matt Hibberd, and Joe Planer need particular acknowledgement in helping indulge my passions and hobbies outside of lab, as well as lending an ear when I would wax philosophical about the ups and downs of research.

Finally, my exceptional family has been here for me every step of the way. Paul and Ruta Wagner are unbelievable parents who have helped prepare me intellectually and emotionally for the pursuits I chased in life, and they gone above and beyond the call of duty raising their two sons. My younger brother, Justin, has also been a great source of camaraderie throughout our endeavors at balancing personal lives and professional goals. And the love bestowed upon me by all my grandparents–Jonas and Ona Motiejunas and Clarence and Dorothy Wagner–aunts, uncles, and cousins have been inspiring. The Wagner and Motiejunas families have been unbelievable sources of encouragement, entertainment, and motivation.

Thank you, to all those mentioned and unmentioned, for the support and time you have given to me—I would not have accomplished this body of work without it.

ABSTRACT OF THE DISSERTATION

A Gnotobiotic Mouse Model for Studying the Effect of Human Gut Community Ecology on a Pathobiont, *Bacteroides fragilis*

by

Vitas Wagner

Doctor of Philosophy in Biology and Biomedical Sciences

Evolution, Ecology, and Population Biology

Washington University in St. Louis, 2015

Professor Jeffrey I. Gordon, Chair

Childhood undernutrition represents a pressing global health challenge. Epidemiologic studies have shown that undernutrition is not due to food insecurity alone, but rather represents a complex set of interactions between intra- and intergenerational factors. The gut microbiota has been implicated as one such factor. This thesis tested the hypothesis that enteropathogen burden affects the structure and expressed functions of the gut microbiota, and reciprocally, the gut microbiota affects susceptibility to the effects of enteropathogen invasion. To examine this hypothesis, groups of adult germ-free C57Bl/6 mice were colonized with fecal microbiota sampled from two 24-month-old members of a birth-cohort living in an urban slum in the Mirpur district of Dhaka, Bangladesh: one child had a healthy growth phenotype as judged by anthropometry, and the undernourished child was severely stunted and underweight and exhibited relative microbiota immaturity. The microbiota of both children contained *Bacteroides fragilis*, a pathobiont. Both groups of colonized mice were fed three diets that embodied the diets consumed by the population from which the microbiota donors were selected. Mice harboring the intact uncultured microbiota from the stunted donor exhibited severe weight-loss, while those receiving the healthy donor's microbiota maintained weight on these diets. Clonally-arrayed, sequenced collections of cultured

anaerobic bacteria strains, generated from the donors' fecal microbiota, transmitted (i) the discordant weight phenotypes within and across generations of animals (in a diet-dependent fashion), as well as (ii) distinct host metabolic phenotypes (manifest by marked differences in tissue organic acid, amino acid and ceramide profiles as defined by mass spectrometry). The *B. fragilis* strain in the stunted donor's culture collection was enterotoxigenic (ETBF), while the two *B. fragilis* strains in the healthy donor's culture collection were non-toxigenic (NTBF). Through a series of experiments in which mice were colonized with either the stunted or healthy culture collection ± ETBF or ± NTBF, I demonstrated that ETBF was associated with weight loss as a member of the stunted donor's community, but not the healthy donor's community. Microbial RNA-Seq analysis revealed marked differences in ETBF gene expression in the two different community contexts, and as a function of the presence or absence of NTBF. Strikingly, ETBF induced expression of a large repertoire of virulence factor genes encoded in the genomes of the healthy culture collection members; these effects were mitigated when NTBF was present. The effects of ETBF on host metabolism were also community context-dependent. These results provide preclinical evidence that enteropathogen effects on host physiology and metabolism are greatly impacted by gut community ecology and illustrate the value of combining gnotobiotic mouse models, human diet embodiments, and 'personal' culture collections for dissecting microbial-microbial and microbial-host interactions. A parallel study using gnotobiotic mice and subsets of the culture collection from the healthy donor revealed how turmeric, a culturally relevant spice in the Bangladeshi diet, and microbial bile acid production/metabolism interact to impact gut motility.

Chapter 1

Introduction

Chapter 1: Introduction

The Gut Microbiota

The human gut microbiota is composed of tens of trillions of microorganisms from all three domains of life (Bacteria, Archaea, and Eukarya), plus their viruses. In healthy individuals, this microbial 'organ' takes approximately 2 years to assemble following birth (*1-3*). In healthy adults, it is dominated by members of the domain Bacteria, notably members of the phyla Bacteroidetes and Firmicutes. A study of healthy adult monozygotic and dizygotic twins and their mothers (*4*) revealed that family members had phylogenetically more similar bacterial assemblages compared to unrelated individuals. Moreover, monozygotic twin pairs did not exhibit significantly more similar overall phylogenetic configurations in their fecal microbiota compared to dizygotic pairs, implying that early environmental exposures are important determinants of microbial community structure in adults. In followup studies, Faith *et al.* conducted a time series study of these twin pairs: he demonstrated that on average 60% of the bacterial strains in a community remain present in an individual for at least five years (*5*). Specifically, the stability of an individual's microbiota fits a power-law function, leading to the proposal that once acquired, bacterial strains have the capability to persist for decades, and thus may have durable effects on our metabolic, physiologic, and immune phenotypes (*6*).

Even though there is significant interpersonal variation in the bacterial species and strains that comprise the human gut microbiota, a large proportion of microbial genes in our gut microbiomes are shared, including those involved in various facets of nutrient biosynthesis and metabolism (*3*, *4*). Disorders such as obesity have been associated with reductions in bacterial diversity in adulthood, while childhood undernutrition has, as noted below, been associated with perturbations in community assembly (development) (*4*, *7-11*).

Historical perspective

The fecal microbiota has long been recognized as important to the health of the host. The 4th Century Chinese writer Ge Hong described the use of fecal slurries as a treatment for patients with diarrhea and food poisoning (*12*). Theodor Escherich, discoverer of *E. coli*, recognized certain bacteria were essential for normal development of infants, while other bacteria would be indicative of an abnormal state (*13*). Escherich's contemporary, Élie Metchnikoff, postulated that lactic-acid fermenting bacteria in the human gut played a role in "prolonging life" through inhibition of putrefaction, the process of organic matter decomposition by bacteria. Today, fecal microbiota transplants (FMT) from healthy humans are used to treat patients suffering from the potentially lethal sequelae caused by *Clostridium difficile* infection (CDI), and preclinical experiments have demonstrated how the microbiota mediates resistance to CDI(*14*, *15*). Additionally, the effects of FMT on the activity of inflammatory bowel disease are now being tested (*16*). While the long-term impact of FMT remains unknown, these studies provide clinical proof-of-concept that the gut microbiota is causally related to disease pathogenesis and/or is a therapeutic target.

The advent of massively-parallel DNA sequencing has allowed culture-independent characterization of the microbiota and microbiomes associated with a variety of body habitats, at different stages of the human lifecycle, as a function of different lifestyles, geographic locations, and health states (*1*, *3*, *17-21*). These surveys focus primarily on bacteria and have allowed us to correlate the community composition with intra- and interpersonal variations in physiology, metabolism and/or immunity. However, despite the allure of descriptive studies, it is critical that this field advance to establish causal relationships between microbiota and microbiome configuration and expressed functions and host biology.

Establishing causal relationships between gut microbial community ecology and host biology using gnotobiotic mice

Gnotobiotic, from the Greek 'gnostos' meaning known and 'bios' signifying life, animals are raised germ-free (GF) in a sterile environment and can be subsequently colonized with determined

microbial communities. Plant physiologists pioneered this approach, with Émile Duclaux successfully growing germ-free peas and beans in a sterile environment (*22*). Duclaux's efforts were met with interest and inspired continued work by several researchers over the next 30 years. In 1895 Nuttall and Thierfelder used Caesarean section to deliver guinea pigs into a sterile environment in order to investigate whether life in the complete absence of microorganisms was possible (*23*). By 1914, Cohendy and Wollman had established nutritional protocols for maintaining healthy neonatal guinea pigs in a germ-free state, but it was not until 1936 that the Swedish researcher Gosta Glimstedt was able to perfect protocols for rearing guinea pigs in a sterile state for up to 2 months, producing the first account of differences between healthy germ-free and conventionally-raised animals (i.e., animals that acquired microbial communities in their body habitats from their environment beginning at birth) (*24*, *25*). Germ-free animal studies made substantial progress after James Arthur Reyniers, an instructor of bacteriology at Notre Dame University, described a germ-free rat model in 1946, unaware of the previous work in Europe (*26*). The 1950s saw Reyniers, in the United States, and Bengt Gustafsson, in Sweden, establish the first colonies of GF rats and mice (*27*, *28*).

Gnotobiotics remains a power tool for determining the specific contributions of the gut microbiota to host physiology. Broadly, microbial communities harvested from conventionally-raised (CONV-R) animals with defined genotypes and phenotypes are introduced to germ-free recipients. If a transmissible donor-specific phenotype is observed in recipient animals, further investigations can unlock microbe-microbe and microbe-host interactions. Comparisons of germ-free versus CONV-R animals have provided direct evidence for the role of the microbiota, and in some cases specific bacterial species, in shaping a large number of facets of host biology.

Growth and nutrition

While investigating the difference in physiology between CONV-R and germ-free rats, Wostmann and colleagues noted that lower O_2 consumption and cardiac output were significantly lower in the latter. Furthermore, for germ-free animals to achieve a growth rate comparable to, and an adult

body mass equivalent to their CONV-R counterparts, they had to consume 30% more calories/ day (*29*). Our lab supported these findings when Bäckhed and colleagues found that compared to CONV-R mice, germ-free animals were leaner and had lower oxygen consumption, yet consumed 29% more food (*30*, *31*). Sjorgren *et al.* showed that bone mass was increased in germ-free mice compared to their CONV-R counterparts; the mechanism remains unclear although they presented evidence for microbiota effects on specific immune cell populations in the bone marrow (*32*).

Carbohydrate metabolism

Humans have a limited capacity for digesting complex dietary carbohydrates (*29*) since our genomes lack the variety of genes encoding glycoside hydrolases and polysaccharide lyases needed to break down the dazzling array of glycoside linkages present in these glycans. While mono- and disaccharides are easily absorbed in the small intestine, most polysaccharides pass through the proximal gut undigested until they reach the distal gut. These predominantly plant-derived polysaccharides are fermented by members of the ileal and colonic microbiota: their genomes contain myriad carbohydrate active enzymes (CAZymes) (*33*). In the absence of these dietary polysaccharides, members of the distal gut microbiota are able to adaptively forage host mucosal glycans (*34*).

Diet appears to function as a selective force across generations of human hosts to shape microbial community structure in ways that promote this capacity for polysaccharide utilization. For example, De Fillipo *et al.* reported that children in rural Africa who consume a significantly higher fiber diet than their European counterparts, have microbiota that are significantly enriched for bacterial taxa and genes that specialize in metabolizing plant polysaccharides: they speculated that these features of their microbiota/microbiomes enhance energy intake and promote gut health(*17*).

Protein metabolism

CONV-R rodents were found to excrete lower levels of nitrogen compared to germ-free animals, suggesting a role of the gut microbiota in protein metabolism (*35*). In 1985, MacFarlane and

colleagues demonstrated that casein and bovine serum albumin were degraded by human fecal slurries, corroborating the hypothesis, based on observations that soluble protein, ammonia, and branched volatile fatty acids occurred throughout the colon, that the microbiota had proteolytic activity (*36*). MacFarlane went on to identify *Bacteroides* and *Propionibacterium* as predominant proteolytic members, with *Streptococcus, Clostridium, Bacillus*, and *Staphylococcus* species also exhibiting proteolytic activity. While the classification of proteases encoded by the gut microbiome is less advanced compared to CAZymes, the MEROPS database provides a valuable reference compilation of known proteases (*37*).

Microbial biotransformations of bile acids

Glycine- or taurine-conjugated bile acids are cholesterol derivatives synthesized in the liver and secreted into the small intestine; they facilitate solubilization and absorption of dietary lipids (*38*). Bile acids (BA) provide the primary route for cholesterol excretion(*39*). BA biosynthesis proceeds through two pathways: the 'classic' neutral pathway and the 'alternative' acidic pathway. Cholesterol 7-alpha-hydroxylase (also known as microsomal cytochrome P450 (Cyp7a1)) is the rate-limiting step in BA production via the neutral pathway. The products of Cyp7a1 are referred to as primary bile acids and differ between vertebrates: in humans and rats, the primary BAs are cholic and chenodeoxycholic acid, while in mice they are cholic and β-muricholic acid. To facilitate fat absorption, primary BAs are conjugated with glycine or taurine by the liver before secretion (*40*). Conjugated BAs (CBA) downregulate primary BA production through repression of Cyp7a1 expression and activity (*41*). Repression of primary BA production requires passage of CBAs through the intestine, suggesting a putative intestinal factor that detects the presence of BAs and mediates feedback regulation of BA synthesis (*42*). One pathway for modulation of bile acid production through primary BAs involves the nuclear farnesoid receptor (FXR), which is expressed in liver, adrenal cortex, kidney, and the gut. FXR was originally identified as interacting with farnesol metabolites (*43*, *44*). Intestinal FXR promotes secretion of fibroblast growth factor

15 (Fgf15), which is delivered to hepatocytes via the portal circulation which then interacts with fibroblast growth factor receptor 4 (Fgfr4) to inhibit Cyp7a1 (*45*).

Recovery of bile acids in the distal ileum occurs through the apical sodium-dependent bile acid transporter (ASBT) expressed in enterocytes: this process is highly efficient, with approximately 95% of BAs being reabsorbed. Enterohepatic circulation is based on this cycle of secretion and recovery and is essential for dietary lipid absorption (*46*). The gut microbiota acts upon the remaining 5% of bile acids not recovered in the terminal ileum in two principal ways: (i) converting conjugated BA, some of which which have strong microbicidal activities, to primary BA using bile salt hydrolases (BSH) and/or (ii) transforming primary BAs to secondary BAs using hydroxysteroid dehydrogenases (*45*, *47-49*). Because the gut microbiota can modify the BA pool, it is able to affect host cholesterol metabolism, regulate its own community structure, as well as alter gut motility (*50*) (see Chapter 3 of this thesis for details of how bacterial BSH activity influences motility)

Protection from enteropathogens

Disruption of the host microbial ecology through antimicrobial therapy can lead to infection by another pathogen or a normally non-pathogenic organism. Miller and colleagues highlighted this experimentally when they observed that animals receiving streptomycin were susceptible to infection with orders of magnitude fewer enteropathogenic *Salmonella* (*51*). The ability of a complex microbiota to serve as a barrier to invasion by enteropathogens was clearly delineated in gnotobiotic animals when it was shown that mono-colonization with common gut symbionts could not clear *Vibrio cholerae* from the mouse gut; however a community of *Escherichia coli, Proteus mirabilis,* and *Streptococcus faecalis* lead to the exclusion of *V. cholerae* from the host(*52*). More recently, studies have shown that (i) non-toxigenic *E. coli* can serve as a barrier to infection with Shiga toxin-producing *E. coli* O157:H7 and (ii) the gut microbiota mediates susceptibility to Salmonella-induced diarrhea (*53*, *54*). Fukuda *et al.* showed that production of acetate in the gut by *Bifidobacteria* protects from infection by *E. coli* O157:H7 (*55*). Together, these findings indicate that the gut microbiota plays an important role in mitigating enteropathogen infection either

through direct competition for niche space, or through production of metabolites that attenuate virulence.

Childhood Undernutrition, Stunting, and Enteric Disease

There are an estimated 805 million people in the world that experience chronic undernutrition (defined as the inability acquire enough nutrients from food to meet dietary energy requirements for a period of at least one year). Chronic undernutrition is particularly detrimental in children under five years of age where it accounts, either directly or indirectly, for almost 50% of deaths and where persistent sequelae such as stunting, impaired cognitive development, and immune dysfunction rob individuals of a chance to achieve their full potential. While there have been reductions in global food insecurity over the past two decades, the prevalence of stunting in children has remained largely unchanged, with little progress toward reduction (*56*).

Nutritional status in children is defined by anthropometric measurements (weight and height as a function of age), and referencing the results to a cohort of 8440 children with healthy growth phenotypes studied from birth in the World Health Organization's Multicentre Growth Reference Study (MGRS) (*57*). Members of this cohort lived in six countries with distinct geographic locations and cultural traditions. Specifically, the length/height and weight data collected from the MGRS was used to determine the distributions of healthy height-for-age and weight-for-age from which Z-scores for individual measurements can be assigned (HAZ and WAZ, respectively): i.e., a normalized Z-score can be calculated for any child to gauge his/her linear and ponderal growth phenotype.

Stunting in children less than 5 years of age is the most prevalent manifestation of undernutrition globally, with an estimated 165 million children being classified as stunted (i.e., have a HAZ score worse than -2) (*58*). Stunting manifests as a severe societal burden, pervasively harming developmental potential through the long-term impact on cognitive function and adult economic productivity (*59*, *60*). While undernutrition at any stage of development can have lasting consequences, a population analysis in the Philippines by Glewwe and King examined whether

cognitive deficits associated with stunting were correlated with when an episode of chronic undernutrition was experienced. They found that contrary to some arguments that the first six months represent the most critical window, undernutrition during the second year of life had a greater negative impact on cognitive development (*61*). Victora *et al.* examined WAZ, HAZ, and WHZ scores among children across 54 countries and found that a critical stage of growth faltering occurred between 9 and 24 months of age, where mean HAZ scores declined from -1 to -2 (*62*). Fortunately, Crookston and colleagues' analysis of a Peruvian cohort found evidence that cognitive deficits related to undernutrition-associated stunting can be remediated if catch-up growth occurs soon after faltering(*63*). It is important to emphasize that severe stunting and its sequelae are not attributable to chronic food-insecurity alone (*64-66*). There are often myriad other contributors including environmental enteropathy (see below), micronutrient deficiency (particularly vitamin A, zinc, iron, and iodine), and diarrheal disease.

Environmental Enteric Disease (EED), previously grouped with 'tropical enteropathy' or 'tropical sprue', is a subclinical chronic inflammatory condition of the small intestine (*67*, *68*). EED is characterized by decreased villus height and lymphocytic infiltration of the lamina propria and epithelium. Since obtaining small intestinal biopsy is not feasible in most children with undernutrition, there has been considerable controversy about what biomarkers to use in defining this entity. A constellation of biomarkers is currently used including lactulose:mannitol absorption test, fecal calprotectin, myeloperoxidase, alpha-1 anti-trypsin, and Reg1, as well as plasma IGF-1. EED has been implicated as a contributing factor to stunting, vaccine failure, and impaired development (*69*). The pathogenesis of EED remains ill-defined (see below). There is some evidence that EED is a reversible. Peace Corps workers who lived for a time in low income countries developed weight loss, diarrhea and small bowel histopathologic changes similar to that found in children with EED that were reversed when they moved back to the USA, while South Asians who moved to New York City became asymptomatic and manifested changes in their small intestinal morphology that resembed a 'Western' phenotype (*70*). Recently, Jones *et al.* studied the effects of treating undernourished children, diagnosed with EED, with mesalazine (5-aminosalicylic acid),

an agent used to treat inflammatory bowel disease. The results disclosed that treatment resulted in modest reductions of the inflammatory markers fecal calprotectin, plasma anti-endotoxin core immunoglobulin, and erythrocyte sedimentation rate compared to placebo (*71*).

EED has been associated with high burden of enteropathogens. Liu and colleagues developed a TaqMan Array Card (TAC) to detect 19 diarrhea-causing pathogens simultaneously (*72*): the assay targets viruses, a diverse set of bacteria (e.g., *Clostrium difficile*, *Vibrio cholerae*, and numerous *Escherichia coli* strains), as well as protozoans. In a worldwide multicenter study, they (i) found that their method had higher sensitivity, but similar specificity compared to other techniques, and (ii) demonstrated that a pathogen's strength of association with diarrheal disease was strongly correlated with higher load. In a prospective birth cohort study of 147 infants, Mondal *et* al. described that endotoxin core antibodies, a biomarker of EED, were associated with stunting pursuant increased incidence of diarrheal disease caused by enteropathogens (*73*). Petri and colleagues, have proposed that it may be possible to ameliorate EED through restoration of key bacteria that are present in the microbiota of healthy children (*7*, *69*).

Childhood Undernutrition and the Gut Microbiota

In a survey of the gut microbiomes of healthy children and adults representing three distinct socioeconomic/cultural/geographic contexts (i.e., three metropolitan areas in the USA, four rural villages in Southern Malawi, and Amerindians living in the Amazonas state in Venezuela), Yatsunenko *et al.* documented (i) a shared program of change during postnatal life in the proportional representation of microbial genes involved in various aspects of nutrient biosynthesis and metabolism (e.g., folate, cobalamin), (ii) distinct differences in the proportional representation of genes between the Western and non-Western population (e.g., those encoding enzymes involved in riboflavin biosynthesis and glycan metabolism), and (iii) a marked reduction in bacterial diversity in the USA compared to other two populations (*3*).

This set of observations led to the hypothesis that normal development of the microbiota/microbiome is essential for healthy growth and that perturbations to this developmental program

are involved in the pathogenesis of undernutrition. A corollary hypothesis, illustrated in **Figure 1,** is that EED represents the confluence of interacting/interrelated factors: (i) impairment of normal gut microbiota development is influenced by enteropathogen burden; (ii) enteropathogen invasion in turn is increased in the face of an immature microbiota; (iii) normal development of the gut mucosal immune system is impaired by an immature microbiota; and (iv) an immature mucosal immune system impedes further development of the microbiota, even in the face of therapeutic food interventions. Interactions between (i)-(iv) can manifest as an impaired growth phenotype, a perturbed metabotype, and disrupted gut barrier/absorptive function.

Smith and colleagues used a gnotobiotic mouse model of childhood undernutrition to demonstrate a causal link between the gut microbiota, diet, and weight loss (*8*). They colonized germ-free mice with fecal microbiota from Malawian twin-pairs discordant for severe acute malnutrition (SAM): one group of mice received the healthy co-twin's microbiota while the other received the SAM co-twin's microbial community. All mice were fed a prototypic macro- and micronutrient deficient Malawian diet. Mice colonized with the microbiota from the co-twin with SAM precipitously lost weight while mice receiving the healthy co-twin's microbiota maintained weight. The combination of a nutrient-deficient diet and a SAM microbiota were required for weight loss: mice harboring the same SAM donor microbiota but fed a nutrient sufficient diet maintained body weight. Moreover, Smith observed that when mice with a SAM microbiota where switched from their Malawian diet to a peanut-based ready-to-use therapeutic food (RUTF) used to treat children with SAM, there was transient albeit incomplete rescue of body weight and metabolic disturbances (including abnormalities in carbohydrate and amino acid metabolism, as well as disruption of the TCA cycle in host tissues). Moreover, the improvements produced with RUTF were not durable: they were lost when mice were switched back to the Malawian diet.

These findings in a preclinical model were intriguing for a number of reasons. A clinical study by Chang and colleagues found that children in Malawi successfully treated for moderate acute malnutrition (MAM) were still at risk for relapse and death during the year following initial recovery(*74*). A clinical trial, conducted by Trehan *et al.*, of a Malawian population demonstrated

that including antibiotic treatment with RUTF significantly decreased mortality and increased the rate of recovery, as measured by weight gain and mid-upper-arm circumference, in children with SAM (*75*).

Subramanian *et al.* used (i) 16S rRNA datasets generated from fecal samples collected monthly from birth through 24 months of age in a cohort of Bangladeshi children with healthy growth phenotypes (defined by anthropometry) and (ii) a machine learning algorithm (Random Forests) to identify a set of age-discriminatory bacterial strains that together describe normal gut microbiota development. The sparse 24-taxon Random Forests model they developed was used to create a metric, microbiota-for-age Z (MAZ) score, that defined microbiota 'maturity': i.e., the age of the gut microbiota in an index child compared to the microbiota configuration of chronologically-aged matched children from the reference Bangladeshi birth cohort with healthy growth phenotypes. Bangaldeshi children with SAM or MAM have significant microbiota immaturity, with MAZ scores being significantly worse (lower) in those presenting with SAM (*7*). Moreover children with SAM treated with either of two RUTFs exhibited incomplete and only transient recovery of their microbiota immaturity (*7*), suggesting that the persistent developmental abnormality exhibited by their gut microbiota may be causally related to their persistent stunting and other manifestations of undernutrition. A corollary was that durable repair of microbiota immaturity, either through food-based or microbial interventions, would be required to ameliorate some of the long-term sequelae of undernutrition.

Finally, Kau *et al.* provided additional support for the gut microbiota's causal role in childhood undernutrition. They used fluorescence activated cell-sorting (FACS) to separate members of the gut microbiota that were targeted by mucosal IgA responses from those that were not targeted (a method that was named 'BugFACS') (*10*). They found that gnotobiotic mice colonized with the fecal microbiota of twin-pairs discordant for SAM and fed either a nutritionally replete mouse diet, or the prototypic nutrient deficient Malawian diet exhibited diet-dependent differential IgA targeting of gut bacterial taxa. Specifically, mice receiving the SAM donor's microbiota had a strong IgA response to *Enterobacteriaceae* when fed the Malawian diet, despite its presence

in all four experimental groups (i.e., mice colonized with the healthy or SAM donor microbiota fed the nutrient-deficient or -sufficient diets), while mice colonized with the healthy twin's fecal microbiota fed a Malawian diet exhibited a distinctive IgA response to *Akkermansia muciniphila* and *Clostridium scindens.* Kau went on to perform experiments where IgA^+ microbes purified by BugFACS from the fecal microbiota of mice harboring a SAM community and fed a Malawian diet transmitted an enteropathy to germ-free mouse recipients fed the same Malawian diet. This phenotype was characterized by marked disruption of the small intestinal and colonic epithelium (the former more so than the latter) with resulting sepsis and death. In contrast, this enteropathy was not observed in mice receiving the IgA^+ fraction purified from the gut microbiota of mice harboring the healthy co-twin's gut community and fed the Malawian diet. Moreover, addition of the IgA-targeted fraction from the healthy co-twin, or a combination of *A. muciniphila* and *C. scindens* to the IgA^+ fraction purified from the SAM donor's microbiota prevented development of the lethal enteropathy. Kau *et al.* also applied BugFACS directly to human fecal samples. Studies of members of a Malawian birth cohort revealed IgA-targeted bacterial taxa at 6 months of age significantly correlate with HAZ at 18 months: the taxa include members of *Enterobacteriaceae*, *Veillonellaceae*, and *Lachnoclostridium* (the genus to which *C. scindens* belongs).

The Pathobiont Enterotoxigenic *Bacteroides fragilis*

Species belonging to the genus *Bacteroides* are critical to host nutrition as well as mucosal and systemic immunity (*76-79*). *B. fragilis* plays an important immunomodulatory role, but is also the leading anaerobic isolate in bloodstream infections and abdominal abscesses(*80-82*). One strain of *B. fragilis*, isolated when attempting to determine the etiology of acute diarrheal disease in newborn lambs in the Northern Rocky Mountains, provided the evidence that *B. fragilis* can be toxigenic. The proposed biologically active toxigenic factor was a heat-labile 20 kDa protein now known as *Bacteroides fragilis* Toxin (BFT) (*83*, *84*); strains positive for this protein family are known as Enterotoxigenic *Bacteroides fragilis* (ETBF). Initial animal studies noted that BTF ex-

hibited host species-specificity with the ilea of lambs and ceca of rabbits exhibiting the greatest secretory responses.

The first ETBF isolates from humans came from adults living in Montana and from Navajo infants living in the area around Tuba City, AZ. Diarrhea was self-limiting in most of these cases (*85*). The first controlled clinical study of the association of ETBF and diarrheal disease took place in 1992 in the clinics of the Apache Indian reservation at Whiteriver, AZ; the results revealed that children under 12 months old do not develop ETBF-associated diarrhea, while children 1-5 years of age had ETBF isolates associated with diarrhea(*86*). Followup studies have found a wide variance in ETBF carriage rates among symptomatic and asymptomatic populations(*87-91*). Aside from inducing acute diarrhea, recent evidence suggests that chronic subclinical ETBF carriage could be a risk factor in colon cancer by promoting colitis through induction of inflammatory $CD4^+$ $Th17^+$ lymphocytes (*92*, *93*).

BFT is a 20 kDa metalloprotease encoded by a gene located within a pathogenicity island. Three alleles ('subtypes') are known: *bft—1*, *2*, and *3,* named in the order in which they were characterized (*84*, *94*, *95*). While all three alleles have a cosmopolitan distribution, *bft-3* is dominant in *B. fragilis* strains isolated from Southeast Asian populations (*96*). There is a second putative metalloprotease encoded within the BFT pathogenicity island; it is not clear whether it is biologically active, necessary for the production of BFT, or even expressed *in vivo* (*97*).

The biologic activity of BFT has been assayed only in epithelial cell lines, (largely intestinal) which are capable of forming polarized monolayers. Addition of BFT to these monolayers results in rapid morphological changes with swelling, rounding, and loss of cell-cell contact occurring within 15 minutes of exposure (*98*). The accumulated evidence points to BFT being non-lethal and non-cytotoxic, as cellular protein synthesis is stimulated and DNA synthesis remains unaltered in its presence (*99*, *100*). Interestingly, BFT exhibits 'polar activity' characterized by increasing permeability more rapidly when administered basolaterally compared to presentation at the apical

membranes of monolayers. BFT results in basolateral release of proinflammatory cytokines along with NF-κB (*101*).

The molecular mechanisms through which BFT produces colitis and diarrhea are not thoroughly understood. The only known cellular protein demonstrated to be cleaved by BFT in the colonic epithelium is the zonula adherens associated protein E-cadherin. Cleavage of E-cadherin has only been observed in intact living cells as the proteolytic event requires cellular ATP(*102*). Proteolysis in response to BFT induces nuclear localization of β-catenin, *c-myc* transcription and cellular proliferation (*103*). ETBF induction of intestinal inflammation likely happens through two pathways: submucosal inflammation through exposure to luminal bacterial antigens due to increased intestinal permeability, along with BFT-stimulated release of proinflammatory IL-8, CCL2, MCP-1, and CXCL1 (*101*, *104*).

Sears proposed a mechanism of action for ETBF (*97*) where adherence of the bacterium to the colonic mucosa results in local secretion of BFT, its binding to apical membrane proteins present in colonic epithelial cells, cleavage of E-cadherin, beta-catenin translocation to the nucleus and induction of a variety of transcriptional cascades. E-cadherin cleavage along with reorganization of the actin cytoskeleton results in epithelial morphologic changes that result in increased permeability, allowing gut mucosal immune cells access to luminal bacterial antigens, thereby promoting chemokine expression and inflammatory responses. Finally, it is important to note that BFT is not implicated in pathogenesis outside of its direct role in affecting colonic epithelial cell biology. The epidemiology of ETBF carriage compared to the occurrence of clinical symptoms, together with this proposed model for ETBF-induced colitis/diarrhea suggest that this organism operates as a pathobiont whose virulence is related to a number of factors. This thesis tests the hypothesis that one such factor is the configuration of the gut microbiota.

Examining the role of the gut microbial ecology in defining the pathologic effects of *B. fragilis*

This thesis describes the development of a gnotobiotic mouse model that examines the interactions of members of the gut microbiota of healthy versus stunted Banglaldeshi children, their diet and ETBF. Mice received intact uncultured microbiota from one of two 24-month-old children: one with a healthy growth phenotype and a normal MAZ score; the other with severe stunting with significant microbiota immaturity. The ability of their microbiota to effect the weight, metabolic and immune phenotypes of gnotobiotic mice was tested in the context of three embodiments of a Bangladeshi diet that I designed based on diet records obtained from the donor population. A key strategy was to determine whether the phenotypes transmissible by the intact uncultured microbiota were also transmissible using the culturable components of these donor's microbiota (*105*, *106*). To do so, I generated clonally arrayed collections of anaerobic bacterial strains from each donor and sequenced all members of each collection – in essence capturing the history of microbial exposures and bacterial strain co-evolution that had transpired in a given host. The results revealed that the undernourished child harbored a strain of ETBF while the child with the healthy growth phenotype possessed two strains of NTBF. It is notable that the ETBF was not detected through standard pathogen screens.

Mice receiving the intact microbiota or culture collection from the severely stunted donor exhibited marked weight loss; this phenotype could be transmitted across generations of gnotobiotic mice and was diet-dependent. The two microbiota also transmitted discordant metabolic phenotypes with the stunted donor community producing pronounced and reproducible effects on lipid, amino acid and ceramide metabolic profiles. The clonally-arrayed culture collections allowed me to deliberately manipulate the community context in which ETBF existed: i.e., germ-free mice were colonized with the healthy community containing NTBF, or with ETBF substituted for NTBF, or with both ETBF and NTBF strains, or with the stunted community with or without ETBF. The community context in which ETBF was delivered had marked effects on the commu-

nity's expression of virulence factors (and other expressed functional features of the community meta-transcriptome), as well as on community and host metabolism.

The approaches used in Chapter 2 are applied in the study described in Chapter 3, where subsets of the healthy donor's culture collection are introduced into germ-free animals to determine the effects of the interaction between (i) turmeric, a commonly used culturally relevant spice in the Bangladeshi diet, and (ii) bacterial strains with and without bile salt hydrolase activity, on gut transit time. Together, these experiments show how microbial community context and diet define the expressed properties and host effects of gut bacterial strains. Given the remarkable strain level diversity that exists in the human gut microbiota, the experimental approaches that I describe in this thesis should be useful for addressing a number of fundamental questions related to community assembly, dynamic operations, and responses to various perturbations of the microbiota. In principle, they should also provide an opportunity for developing new ways to deliberately manipulate bacterial community properties in order to improve health.

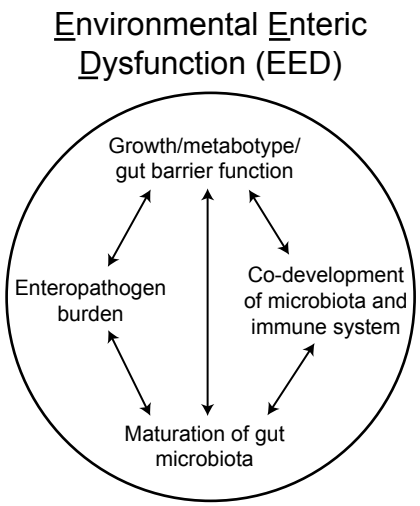

Figure 1. A view of the pathogenesis of Environmental Enteric Dysfunction (EED). In this conceptualization, EED represents the confluence of interacting/interrelated factors: (i) impairment of normal gut microbiota development is influenced by enteropathogen burden; (ii) enteropathogen invasion in turn is increased in the face of an immature microbiota; (iii) normal development of the gut mucosal immune system is impaired by an immature microbiota; and (iv) an immature mucosal immune system impedes further development of the microbiota, even in the face of therapeutic food interventions. Interactions between (i)-(iv) result in impaired growth, perturbed host metabolic phenotypes, and disrupted gut barrier and absorptive function.

References

1. C. Palmer, E. Bik, D. DiGiulio, D. Relman, P. Brown, Development of the human infant intestinal microbiota, *PLoS Biol* **5**, e177 (2007).

2. S. Mueller *et al.*, Differences in Fecal Microbiota in Different European Study Populations in Relation to Age, Gender, and Country: a Cross-Sectional Study, *Applied and Environmental Microbiology* **72**, 1027–1033 (2006).

3. T. Yatsunenko *et al.*, Human gut microbiome viewed across age and geography, *Nature* (2012), doi:10.1038/nature11053.

4. P. J. Turnbaugh *et al.*, A core gut microbiome in obese and lean twins, *Nature* **457**, 480–484 (2009).

5. J. J. Faith *et al.*, The Long-Term Stability of the Human Gut Microbiota, *Science* **341**, 1237439–1237439 (2013).

6. J. J. Faith, P. P. Ahern, V. K. Ridaura, J. Cheng, J. I. Gordon, Identifying Gut Microbe-Host Phenotype Relationships Using Combinatorial Communities in Gnotobiotic Mice, *Science Translational Medicine* **6**, 220ra11–220ra11 (2014).

7. S. Subramanian *et al.*, Persistent gut microbiota immaturity in malnourished Bangladeshi children, *Nature* (2014).

8. M. Smith *et al.*, Gut microbiomes of Malawian twin pairs discordant for kwashiorkor, *Science* **339**, 548–554 (2013).

9. E. Le Chatelier *et al.*, Richness of human gut microbiome correlates with metabolic markers, *Nature* **500**, 541–546 (2013).

10. A. L. Kau *et al.*, Functional characterization of IgA-targeted bacterial taxa from undernourished Malawian children that produce diet-dependent enteropathy, *Science Translational Medicine* **7**, 276ra24–276ra24 (2015).

11. J. Suez *et al.*, Artificial sweeteners induce glucose intolerance by altering the gut microbiota, *Nature*, 1–17 (2014).

12. H. B. Zhou, *G. Hong (Donjin Dynasty)* (Tianjin Science & Technology, Tianjin, 2000).

13. T. Escherich, K. S. Bettelheim, The Intestinal Bacteria of the Neonate and Breast-Fed Infant, *Reviews of Infectious Diseases* **10**, 1220–1225 (1988).

14. E. van Nood *et al.*, Duodenal Infusion of Donor Feces for Recurrent Clostridium difficile, *N Engl J Med* **368**, 407–415 (2013).

15. C. G. Buffie *et al.*, Precision microbiome reconstitution restores bile acid mediated resistance to Clostridium difficile, *Nature* **517**, 205–208 (2014).

16. R. J. Colman, L. Rubert, Fecal microbiota transplantation as therapy for inflammatory bowel disease: A systematic review and meta-analysis, *Journal of Crohn's and Colitis* **8**, 1569–1581 (2014).

17. C. De Filippo *et al.*, Impact of diet in shaping gut microbiota revealed by a comparative study in children from Europe and rural Africa, *Proceedings of the National Academy of Sciences* (2010), doi:10.1073/pnas.1005963107.

18. M. J. Claesson *et al.*, Gut microbiota composition correlates with diet and health in the elderly, *Nature* **488**, 178–184 (2012).

19. J. Ravel *et al.*, Vaginal microbiome of reproductive-age women, *Proc Natl Acad Sci U S A* **108 Suppl 1**, 4680–4687 (2011).

20. P. Gajer *et al.*, Temporal dynamics of the human vaginal microbiota, *Science Translational Medicine* **4**, 132ra52–132ra52 (2012).

21. E. A. Grice *et al.*, Topographical and temporal diversity of the human skin microbiome, *Science* **324**, 1190–1192 (2009).

22. P. E. Duclaux, *Sur la germination dans un sol riche en matiéres organiques, mais exempt de microbes* (Comptes rendus de l'Académie des Sciences, 1885), pp. 66–68.

23. G. Nuttal, *Thierisches Leben ohne Bacterien im Verdauungskanal* (Hoppe Seyler's Zeitschrift Physiological Chemistry, 1895), pp. 109–112.

24. M. Cohendy, E. Wollman, *Expériences sur la vie sans microbes. Élevage aseptique de cobayes.* (Comptes rendus de l'Académie des Sciences, 1914), p. 1283.

25. G. Glimstedt, H. A. Moberg, E. M. Widmark, Der Stoffwechsel bakterienfreier Tiere, *Skandanavian Archive of Physiology* **73**, 148–157 (1936).

26. J. A. Reyniers, P. C. Trexler, R. F. Ervin, *Rearing Germ-free albino rats* (Lobund Resports, 1946).

27. J. A. Reyniers, M. R. Sacksteder, *Observations on the survival of germfree C3H mice and their resistance to a contaminated environment* (Proceedings of the Animal Care Panel, 1957), pp. 41–53.

28. B. E. Gustafsson, Lightweight Stainless Steel Systems for Rearing Germ-Free Animales, *Annals of the New York Academy of Sciences* **78**, 17–28 (1959).

29. B. S. Wostmann, C. Larkin, A. Moriarty, E. Bruckner-Kardoss, *Dietary intake, energy metabolism, and excretory losses of adult male germfree Wistar rats* (Laboratory Animal Science, 1983), pp. 46–50.

30. F. Bäckhed *et al.*, The gut microbiota as an environmental factor that regulates fat storage, *Proc Natl Acad Sci U S A* **101**, 15718–15723 (2004).

31. V. Tremaroli, F. Bäckhed, Functional interactions between the gut microbiota and host metabolism, *Nature* **489**, 242–249 (2012).

32. K. Sjögren *et al.*, The gut microbiota regulates bone mass in mice, *J Bone Miner Res* **27**, 1357–1367 (2012).

33. A. A. Salyers, S. E. West, J. R. Vercellotti, T. D. Wilkins, Fermentation of mucins and plant polysaccharides by anaerobic bacteria from the human colon, *Applied and Environmental Microbiology* **34**, 529–533 (1977).

34. E. C. Martens, H. C. Chiang, J. I. Gordon, Mucosal Glycan Foraging Enhances Fitness and Transmission of a Saccharolytic Human Gut Bacterial Symbiont, *Cell Host & Microbe* **4**, 447–457 (2008).

35. S. M. Levenson, B. Tennant, *16th Proceedings of the International Congress of Zoology, 1963* (International Congress of Zoology, 1963), pp. 148–153.

36. G. T. Macfarlane, J. H. Cummings, C. Allison, Protein degradation by human intestinal bacteria, *J. Gen. Microbiol.* **132**, 1647–1656 (1986).

37. N. D. Rawlings, A. J. Barrett, A. Bateman, MEROPS: the database of proteolytic enzymes, their substrates and inhibitors, *Nucleic Acids Research* **40**, D343–D350 (2011).

38. A. F. Hofmann, B. Borgström, The Intraluminal Phase of Fat Digestion in Man: The Lipid Content of the Micellar and Oil Phases of Intestinal Content Obtained during Fat Digestion and Absorption*, *J Clin Invest* **43**, 247–257 (1964).

39. G. A. Graf *et al.*, ABCG5 and ABCG8 Are Obligate Heterodimers for Protein Trafficking and Biliary Cholesterol Excretion, *Journal of Biological Chemistry* **278**, 48275–48282 (2003).

40. D. E. Cohen, L. S. Leighton, M. C. Carey, Bile salt hydrophobicity controls vesicle secretion rates and transformations in native bile, *Am. J. Physiol.* **263**, G386–95 (1992).

41. M. Crestani, W. G. Karam, J. Y. Chiang, Effects of bile acids and steroid/thyroid hormones on the expression of cholesterol 7 alpha-hydroxylase mRNA and the CYP7 gene in HepG2 cells, *Biochem. Biophys. Res. Commun.* **198**, 546–553 (1994).

42. W. M. Pandak, D. M. Heuman, P. B. Hylemon, J. Chiang, Failure of intravenous infusion of taurocholate to down-regulate cholesterol 7α-hydroxylase in rats with biliary fistulas, *Gastroenterology* (1995).

43. B. M. Forman *et al.*, Identification of a nuclear receptor that is activated by farnesol metabolites, *Cell* **81**, 687–693 (1995).

44. M. Makishima *et al.*, Identification of a Nuclear Receptor for Bile Acids, *Science* **284**, 1362–1365 (1999).

45. T. Inagaki *et al.*, Regulation of antibacterial defense in the small intestine by the nuclear bile acid receptor, *Proc Natl Acad Sci U S A* **103**, 3920–3925 (2006).

46. M. H. Wong, P. Oelkers, A. L. Craddock, Expression cloning and characterization of the hamster ileal sodium-dependent bile acid transporter, ... *of Biological Chemistry* (1994).

47. B. V. Jones, M. Begley, C. Hill, C. G. M. Gahan, J. R. Marchesi, Functional and Comparative Metagenomic Analysis of Bile Salt Hydrolase Activity in the Human Gut Microbiome, *Proceedings of the National Academy of Sciences of the United States of America* **105**, 13580–13585 (2008).

48. A. F. Hofmann, L. Eckmann, How Bile Acids Confer Gut Mucosal Protection against Bacteria, *Proceedings of the National Academy of Sciences of the United States of America* **103**, 4333–4334 (2006).

49. I. A. Macdonald, B. A. White, P. B. Hylemon, Separation of 7 alpha- and 7 beta-hydroxysteroid dehydrogenase activities from clostridium absonum ATCC# 27555 and cellular response of this organism to bile acid inducers, *J Lipid Res* **24**, 1119–1126 (1983).

50. C. Jiang *et al.*, Intestinal farnesoid X receptor signaling promotes nonalcoholic fatty liver disease, *J Clin Invest* **125**, 386–402 (2015).

51. C. P. Miller, M. Bohnhoff, D. RIFKIND, The effect of an antibiotic on the susceptibility of the mouse's intestinal tract to Salmonella infection, *Trans. Am. Clin. Climatol. Assoc.* **68**, 51–5– discussion 55–8 (1956).

52. C. E. Miller, J. C. Feeley, Competitive effects of intestinal microflora on Vibrio cholerae in gnotobiotic mice, **25**, 454–458 (1975).

53. M. P. Leatham *et al.*, Precolonized Human Commensal Escherichia coli Strains Serve as a Barrier to E. coli O157:H7 Growth in the Streptomycin-Treated Mouse Intestine, *Infection and Immunity* **77**, 2876–2886 (2009).

54. K. Endt *et al.*, C. E. Stebbins, Ed. The Microbiota Mediates Pathogen Clearance from the Gut Lumen after Non-Typhoidal Salmonella Diarrhea, *PLoS Pathog* **6**, e1001097 (2010).

55. S. Fukuda *et al.*, Bifidobacteria can protect from enteropathogenic infection through production of acetate, *Nature* **469**, 543–547 (2011).

56. Food And Agriculture Organization, Food and Agriculture Organization of the United Nations, *The State of Food Insecurity in the World 2014* (Food and Agriculture Organization, 2014).

57. World Health Organization, U. N. C. Fund, World Health Organization Department of Nutrition for Health and Development. WHO child growth standards growth velocity based on weight, length and head circumference: methods and development, *World Health Organization*, 1–262 (2009).

58. A. J. Prendergast, J. H. Humphrey, The stunting syndrome in developing countries, *Paediatrics and International Child Health* **34**, 250–265 (2014).

59. W. E. C. O. P. S. T. U. A. I. O. Anthropometry, *Physical status : the use and interpretation of anthropometry : report of a WHO Expert Committee.* (Geneva : World Health Organization, 1995).

60. M. Pradhan, D. E. Sahn, S. D. Younger, Decomposing world health inequality, *Journal of Health Economics* **22**, 271–293 (2003).

61. P. Glewwe, E. M. King, The Impact of Early Childhood Nutritional Status on Cognitive Development: Does the Timing of Malnutrition Matter? *The World Bank Economic Review* **15**, 81–113 (2001).

62. C. G. Victora, M. de Onis, P. C. Hallal, M. Blossner, R. Shrimpton, Worldwide Timing of Growth Faltering: Revisiting Implications for Interventions, *PEDIATRICS* **125**, e473–e480 (2010).

63. B. T. Crookston *et al.*, Children Who Recover from Early Stunting and Children Who Are Not Stunted Demonstrate Similar Levels of Cognition, *J Nutr* **140**, 1996–2001 (2010).

64. M. Lazzerini, L. Rubert, P. Pani, Specially formulated foods for treating children with moderate acute malnutrition in low- and middle-income countries (Review),, 1–155 (2013).

65. S. A. Richard *et al.*, Modeling environmental influences on child growth in the MAL-ED cohort study: opportunities and challenges, *CLIN INFECT DIS* **59 Suppl 4**, S255–S260 (2014).

66. L. E. Caulfield *et al.*, Infant feeding practices, dietary adequacy, and micronutrient status measures in the MAL-ED study, *CLIN INFECT DIS* **59 Suppl 4**, S248–S254 (2014).

67. W. O'Brien, Tropical sprue: a review, *J R Soc Med* **72**, 916–920 (1979).

68. P. S. Korpe, W. A. Petri Jr, Environmental enteropathy: critical implications of a poorly understood condition, *Trends in Molecular Medicine* **18**, 328–336 (2012).

69. W. A. Petri Jr, C. Naylor, R. Haque, Environmental enteropathy and malnutrition: do we know enough to intervene?, 1–5 (2014).

70. G. T. Keusch *et al.*, Environmental Enteric Dysfunction: Pathogenesis, Diagnosis, and Clinical Consequences, *CLIN INFECT DIS* **59**, S207–S212 (2014).

71. K. D. Jones *et al.*, Mesalazine in the initial management of severely acutely malnourished children with environmental enteric dysfunction: a pilot randomized controlled trial,, 1–14 (2014).

72. J. Liu *et al.*, A Laboratory-Developed TaqMan Array Card for Simultaneous Detection of 19 Enteropathogens, *Journal of Clinical Microbiology* **51**, 472–480 (2013).

73. D. Mondal *et al.*, Contribution of Enteric Infection, Altered Intestinal Barrier Function, and Maternal Malnutrition to Infant Malnutrition in Bangladesh, *CLIN INFECT DIS* **54**, 185–192 (2012).

74. C. Y. Chang *et al.*, Children Successfully Treated for Moderate Acute Malnutrition Remain at Risk for Malnutrition and Death in the Subsequent Year after Recovery, *J Nutr* **143**, 215–220 (2013).

75. I. Trehan *et al.*, Antibiotics as part of the management of severe acute malnutrition, *N Engl J Med* **368**, 425–435 (2013).

76. P. B. Eckburg *et al.*, Diversity of the human intestinal microbial flora, *Science* **308**, 1635–1638 (2005).

77. S. K. Mazmanian, C. H. Liu, A. O. Tzianabos, D. L. Kasper, An Immunomodulatory Molecule of Symbiotic Bacteria Directs Maturation of the Host Immune System, *Cell* **122**, 107–118 (2005).

78. S. K. Mazmanian, J. L. Round, D. L. Kasper, A microbial symbiosis factor prevents intestinal inflammatory disease, *Nature* **453**, 620–625 (2008).

79. J. L. Sonnenburg *et al.*, Glycan Foraging in Vivo by an Intestine-Adapted Bacterial Symbiont, *Science* **307**, 1955–1959 (2005).

80. B. Lassmann, D. R. Gustafson, C. M. Wood, J. E. Rosenblatt, Reemergence of Anaerobic Bacteremia, *CLIN INFECT DIS* **44**, 895–900 (2007).

81. B. F. Polk, D. L. Kasper, Bacteroides fragilis subspecies in clinical isolates, *Ann Intern Med* **86**, 569–571 (1977).

82. M. C. Redondo, M. D. Arbo, J. Grindlinger, D. R. Snydman, Attributable mortality of bacteremia associated with the Bacteroides fragilis group, *CLIN INFECT DIS* **20**, 1492–1496 (1995).

83. L. L. Myers, B. D. Firehammer, D. S. Shoop, Bacteroides fragilis: a possible cause of acute diarrheal disease in newborn lambs, *Infection and ...* (1984).

84. C. L. Sears, The toxins of Bacteroides fragilis, *Toxicon* **39**, 1737–1746 (2001).

85. L. L. Myers *et al.*, Isolation of enterotoxigenic Bacteroides fragilis from humans with diarrhea, *Journal of Clinical Microbiology* **25**, 2330–2333 (1987).

86. R. B. Sack *et al.*, *Enterotoxigenic Bacteroides Fragilis: Epidemiologic Studies of its Role as a Human Diarrhoeal Pathogen* (ICDDR,b, 1992), pp. 4–9.

87. M. J. Albert, A. S. Faruque, S. M. Faruque, R. B. Sack, D. Mahalanabis, Case-control study of enteropathogens associated with childhood diarrhea in Dhaka, Bangladesh, *Journal of Clinical Microbiology* **37**, 3458–3464 (1999).

88. P. Pathela *et al.*, Enterotoxigenic Bacteroides fragilis: Associated Diarrhea in Children 0-2 Years of Age in Rural Bangladesh, *The Journal of Infectious Diseases* **191**, 1245–1252 (2005).

89. N. Kato *et al.*, Prevalence of enterotoxigenic Bacteroides fragilis in children with diarrhea in Japan, *Journal of Clinical Microbiology* **37**, 801–803 (1999).

90. G. Zhang, B. Svenungsson, A. Kärnell, A. Weintraub, Prevalence of Enterotoxigenic Bacteroides fragilis in Adult Patients with Diarrhea and Healthy Controls, *CLIN INFECT DIS* **29**, 590–594 (1999).

91. A. Pantosti *et al.*, Detection of enterotoxigenic Bacteroides fragilis and its toxin in stool samples from adults and children in Italy, *CLIN INFECT DIS* **24**, 12–16 (1997).

92. S. Rabizadeh *et al.*, Enterotoxigenic Bacteroides fragilis: A potential instigator of colitis, *Inflammatory Bowel Diseases* **13**, 1475–1483 (2007).

93. S. Wu *et al.*, A human colonic commensal promotes colon tumorigenesis via activation of T helper type 17 T cell responses, *Nature Medicine* **15**, 1016–1022 (2009).

94. A. A. Franco *et al.*, Cloning and characterization of the Bacteroides fragilis metalloprotease toxin gene, *Infection and Immunity* **65**, 1007–1013 (1997).

95. N. Kato *et al.*, A new subtype of the metalloprotease toxin gene and the incidence of the three bft subtypes among Bacteroides fragilis isolates in Japan, *FEMS Microbiol Lett* **182**, 171–176 (2000).

96. A. S. S. d'Abusco, M. Del Grosso, S. Censini, A. Covacci, A. Pantosti, The alleles of the bft gene are distributed differently among enterotoxigenic Bacteroides fragilis strains from human sources and can be present in double copies, *Journal of Clinical Microbiology* **38**, 607–612 (2000).

97. C. Sears, Enterotoxigenic Bacteroides fragilis: a rogue among symbiotes, *Clinical Microbiology Reviews* **22**, 349–369 (2009).

98. R. F. Saidi, C. L. Sears, Bacteroides fragilis toxin rapidly intoxicates human intestinal epithelial cells (HT29/C1) in vitro, *Infection and Immunity* **64**, 5029–5034 (1996).

99. C. L. Wells *et al.*, Bacteroides fragilis enterotoxin modulates epithelial permeability and bacterial internalization by HT-29 enterocytes, *YGAST* **110**, 1429–1437 (1996).

100. R. J. Obiso, A. O. Azghani, T. D. Wilkins, The Bacteroides fragilis toxin fragilysin disrupts the paracellular barrier of epithelial cells, *Infection and Immunity* **65**, 1431–1439 (1997).

101. S. Wu *et al.*, Bacteroides fragilis Enterotoxin Induces Intestinal Epithelial Cell Secretion of Interleukin-8 through Mitogen-Activated Protein Kinases and a Tyrosine Kinase-Regulated Nuclear Factor- B Pathway, *Infection and Immunity* **72**, 5832–5839 (2004).

102. S. Wu, K. C. Lim, J. Huang, R. F. Saidi, C. L. Sears, Bacteroides fragilis enterotoxin cleaves the zonula adherens protein, E-cadherin, *Proc Natl Acad Sci U S A* **95**, 14979–14984 (1998).

103. S. Wu, P. J. Morin, D. Maouyo, C. L. Sears, Bacteroides fragilis enterotoxin induces c-Myc expression and cellular proliferation, *Gastroenterology* **124**, 392–400 (2003).

104. L. Sanfilippo *et al.*, Bacteroides fragilis enterotoxin induces the expression of IL-8 and transforming growth factor-beta (TGF-beta) by human colonic epithelial cells, *Clin Exp Immunol* **119**, 456–463 (2000).

105. A. L. Goodman *et al.*, Extensive personal human gut microbiota culture collections characterized and manipulated in gnotobiotic mice, *Proceedings of the National Academy of Sciences*, 1–6 (2011).

106. V. Ridaura *et al.*, Gut microbiota from twins discordant for obesity modulate metabolism in mice, *Science* **341**, 1241214 (2013).

Chapter 2

Gut microbiota-pathobiont interactions in a gnotobiotic mouse model of childhood undernutrition

Gut microbiota-pathobiont interactions in a gnotobiotic mouse model of childhood undernutrition

Vitas E. Wagner[1,2,7], Neelendu Dey[1,2,3,7], Ansel Hsiao[1], Sathish Subramanian[1,2], Janaki Guruge[1,2], Jiye Cheng[1,2], Philip Ahern[1,2], Olga Ilkayeva[4], Christopher Newgard[4], William Petri[5], Rashidul Haque[6], Tahmeed Ahmed[6], and Jeffrey I. Gordon[1,2*]

[1]Center for Genome Sciences and Systems Biology, [2]Center for Gut Microbiome and Nutrition Research, and [3]Department of Medicine, Washington University School of Medicine, St. Louis, MO 63108, USA.

[4]Sarah W. Stedman Nutrition and Metabolism Center, Duke University School of Medicine, Durham, NC 27710, USA.

[5]Departments of Medicine, Microbiology and Pathology, University of Virginia School of Medicine, Charlottesville, Virginia 22908, USA.

[6]Centre for Nutrition and Food Security, International Centre for Diarrhoeal Disease Research, Dhaka 1212, Bangladesh.

[7]Contributed equally

*Correspondence: jgordon@wustl.edu

ABSTRACT

Childhood undernutrition is a pressing global health challenge representing a complex set of interacting factors including those involving the gut microbiota. To examine how the effects of enteropathogens are impacted by gut microbial community structure, we colonized groups of germ-free C57BL/6 mice with intact uncultured fecal microbiota samples obtained from two 24-month old members of a Bangladeshi birth-cohort, one with a healthy growth phenotype and the other severely stunted and underweight, or with members of clonally-arrayed, sequenced collections of cultured anaerobic bacterial strains generated from these microbiota. Mice were fed diets that embodied those consumed by the population from which the donors were selected. The gut community from the stunted/underweight but not healthy donor transmitted a weight loss phenotype to recipient animals and subsequently to their offspring. The discordant weight phenotypes were accompanied by discordant host metabolic phenotypes. The *Bacteroides fragilis* strain in the stunted/underweight donor's culture collection was enterotoxigenic (ETBF), while the two *B. fragilis* strains in healthy donor's culture collection were non-toxigenic (NTBF). A series of experiments in which mice were colonized with either the stunted/underweight culture collection with and without ETBF, or the healthy culture collection with and without ETBF, revealed that ETBF was causally related to weight loss as a member of the stunted/underweight donor's culture collection but not when introduced into the healthy donor's community. Microbial RNA-Seq revealed marked differences in ETBF gene expression in the two different community contexts, as a function of the presence or absence of NTBF. Strikingly, ETBF induced expression of a large repertoire of virulence factor genes encoded in the genomes of healthy culture collection members that was mitigated when NTBF was present. The effects of ETBF on host metabolism were also community context-dependent. These results demonstrate how *B. fragilis* acts as a pathobiont and illustrate a generalizable way of dissecting intra- and interspecies interactions that define niche space (the sum of functional occupancies) of enteropathogens in a gut community.

INTRODUCTION

Undernutrition is the leading cause of childhood mortality worldwide and reflects a broad and complex set of interrelated factors that operate within and across generations (*1-4*). The gut microbiota is a metabolic organ that develops in an age-dependent fashion (*5*). A recent culture-independent study of Bangladeshi birth cohorts identified age-dependent changes in the representation of bacterial strains that occurred during the first two years of postnatal life in biologically unrelated healthy infants/children. These age-discriminatory strains together defined a developmental program for the microbiota (*6*). Remarkably, children with moderate or severe undernutrition exhibit disruptions in this program that result in microbial communities which appear younger than those of chronologically age-matched healthy individuals. Moreover, this microbiota immaturity is not repaired by existing food-based therapeutic interventions.

A large enteropathogen burden is a major risk factor for undernutrition (*7*, *8*). Deciphering the effects of perturbations in gut microbial community development on enteropathogen invasion and burden, and reciprocally, the effects of enteropathogens on the gut microbiota and host in children who have healthy growth phenotypes versus those that are undernourished, is challenging. Preclinical models are needed to help dissect the complex and dynamic interactions between enteropathogens, members of the microbiota, and host in order to obtain insights about disease pathogenesis, and develop new strategies for disease treatment and ultimately prevention.

Bacteroides species provide attractive 'subjects' for such preclinical studies. They are not only critical for processing a variety of dietary polysaccharides but also influence maturation and function of the immune system (*9*, *10*). They function as pathobionts. For example, non-toxigenic *B. fragilis* (NTBF) strains are prominently represented in the initial phase of recovery following *Vibrio cholera* infection in adults (*11*). This recovery recapitulates the normal pattern of initial assembly of the gut microbiota in healthy infants and adults. In contrast, enterotoxigenic *B. fragilis* (ETBF) strains are endemic to countries such as Bangladesh (*12*) where the burden of undernutrition is great, and are associated with diarrheal disease in children (*13*). ETBF produces diarrhea

and gut inflammation through BFT (also known as fragilysin), a zinc-dependent metalloprotease that cleaves E-cadherin at epithelial cell adherence junctions (*14*).

"Niche space" can be defined as the sum of functional occupancies of a species/strain in a community – a context-dependent view where a strain influences and is influenced by competitors, resources, and host traits (*15*, *16*). The present study describes a gnotobiotic mouse model for defining the niche space occupied by *B. fragilis*. We started with fecal samples collected from Bangladeshi children who were participants in a previously completed birth-cohort study (*17*). Using anthropometric metrics to define healthy growth versus stunting and wasting (*18*), and a PCR-based assay that targeted *bft*, we selected two chronologically age-matched individuals, one markedly stunted, underweight, and ETBF-positive, and the other ETBF-negative (and NTBF-positive) with a healthy growth phenotype. We transplanted intact fecal microbiota samples, collected from these two children at 24-months-of-age, into germ-free mice; mice were fed cooked diets containing ingredients embodying those consumed by the population from which the microbiota donors were selected. Finding that these microbiota transmitted discordant weight phenotypes to recipient animals and subsequently to their offspring, we performed follow-up transplant studies using clonally arrayed collections of sequenced anaerobic bacterial strains cultured from the donors' intact uncultured fecal samples. These culture collections allowed us to dissect microbe-microbe and host-microbe interactions by testing the effects of (i) removing the ETBF strain from the stunted donor's cultured community, and (ii) introducing the ETBF strain into the healthy donor's culture collection together with or in lieu of its own NTBF strains, on microbiota community structure and gene expression, microbial and host metabolism, plus body weight and immune phenotypes. Our approach demonstrates how ETBF functions as a pathobiont with markedly different effects produced in the healthy versus undernourished donor community contexts.

RESULTS

We used anthropometric data collected from members of a now completed birth cohort study of 100 children living in Mirpur *thana* in Dhaka, Bangladesh, to define whether they were healthy or

undernourished. Those with height-for-age Z (HAZ) scores greater than or equal to -2 were classified as 'healthy' while those with scores less than or equal to -3 were deemed severely stunted: at 18 months, 30 and 25 children satisfied these criteria for healthy versus severely stunted, respectively, while at 24 months, 27 and 20 received these designations; the remaining children were classified as moderately stunted (HAZ scores between -2 and -3).

A PCR-based screen for ETBF was performed using DNA isolated from fecal samples that had been collected from these children at 18 months and 24 months of age; the PCR primers targeted all three fragilysin gene subtypes (*14*). The results revealed that ETBF was variably present across individuals and within a given individual over time, with a total of 25% of 18-month old and 14% of 24-month old children having a positive test (**Table S1**): there was no significant difference in HAZ score associated with ETBF carriage at either age (p=0.8 and p=0.4 at 18 and 24 months, respectively; two-tailed Student's t-test).

Using the anthropometric and PCR data, we selected fecal samples collected at 24 months from two individuals: (i) a healthy child (ID 7114 in **Table S1**) with an HAZ of -0.71, a weight-for-age Z (WAZ) score of -1.49, and weight-for-height Z (WHZ) score of -1.62 who was ETBF-negative at the two time points tested, and (ii) a severely stunted and moderately underweight child (ID 7004) with a HAZ of -3.02, a WAZ of -2.51, WHZ =-1.34 who was ETBF-positive at both time points. Of the 35 individuals with a positive ETBF test at either time point, only this stunted/underweight child was positive at both 18 and 24 months of age.

To create a representative gnotobiotic mouse model to determine the effects of these microbiota on host biology, we generated three embodiments of the diets consumed by the population represented by the donors. To design these embodiments, we first selected ingredient types (e.g., cereals, leafy vegetables, fruits, meat) and determined their relative daily caloric contributions based on a study by Arsenault and coworkers (*19*). Selection of specific food items as representative of each ingredient type was based on consumption incidence surveys tabulated by Islam et al (*20*) and incorporated into a database consisting of 54 food ingredients. Using the R statistical

programming language, we filtered this database to remove items consumed by <20% of households and categorized each of the remaining 39 items (see *Methods* for details). From the resulting diet ingredient matrix, we randomly sampled (without replacement) one item each from cereals, pulse vegetables, roots/tubers, leafy vegetables, fruits, and fish, plus three non-leafy vegetables, to populate three separate diet lists. Using the USDA National Nutrient Database for Standard References (*21*), we determined the caloric information for each ingredient and subsequently calculated proportions required to match the pre-determined contributions of each ingredient type. Food items were cooked in a manner intended to simulate Bangladeshi practices, and the resulting three embodiments of a Bangladeshi diet were sterilized by irradiation prior to administration to germ-free mice. The composition and nutritional analyses of the three Bangladeshi diet embodiments are described in **Table S2A**. The nutritional requirements of mice and children are compared in **Table S2B**.

Separate groups of 8-9 week old germ-free male C57BL/6 mice were gavaged with the intact uncultured fecal microbiota samples obtained from the healthy or stunted/underweight donors. Gavage occurred 2 days after mice had been switched from an irradiated, nutritionally complete, low-fat/high plant polysaccharide (LF/HPP) mouse chow that they had received since weaning to the first of the three embodiments of the Bangladeshi diet. Animals were subsequently fed embodiment 1 (*ad libitum*) for one week, followed by embodiment 2 for one week, followed by embodiment 3 for one week, with frequent sampling of their fecal microbiota during the course of each diet (n=4 singly-housed mice/donor microbiota/experiment; 2 independent experiments; see **Figure S1A** for time points when fecal samples were collected and mice were weighed). Sequencing PCR amplicons generated from variable region 4 (V4) of bacterial 16S rRNA genes present in the donor fecal sample and in fecal samples collected over time from recipient gnotobiotic mice provided an *in vivo* assay of bacterial viability/colonization efficiency for each human donor sample. 16S rRNA sequencing reads were grouped into operational taxonomic units based on a threshold of ≥97% nucleotide sequence identity (97%ID OTUs; **Table S3**). The results revealed that at the conclusion of the experiment 65.8±2.5% of OTUs in the stunted/underweight donor's fecal micro-

biota sample and 68.4±8.8% of the OTUs in the healthy donor's microbiota were detectable in recipient mice (i.e., each OTU had a relative abundance of ≥0.1% in ≥1% of fecal samples obtained from the mice; **Table S3B**).

While gnotobiotic animals colonized with the healthy donor's fecal microbiota maintained weight, recipients of the severely stunted/underweight donor's microbiota exhibited progressive and significant weight loss ($p<0.005$, paired two-tailed Student's *t*-test, comparing final versus initial weights; **Figure 1A**). Mice that received the stunted donor's microbiota first exhibited statistically significant degrees of weight loss by 11 days post gavage (dpg), during consumption of diet embodiment 2; weight loss worsened progressively reaching 31±6% of original starting weight by dpg 17 ($p<0.0001$; repeated measures ANOVA in which weight was the dependent variable while 'dpg' and 'microbiota' were within-group and between-group variables, respectively; **Figure 1A**). Importantly, food consumption was not different between the two treatment groups when their weight phenotypes diverged significantly. Mice were sacrificed on dpg 17 based on the extent of weight loss allowable by our approved animal studies protocol and the fact that animals harboring the stunted/underweight community had begun to exhibit reductions in feeding in the preceding 1-2 days.

The relative abundance of *B. fragilis*, defined by V4-16S rRNA sequencing, was significantly greater in mice colonized with the stunted/underweight donor microbiota than in mice colonized with the healthy donor microbiota ($p=1.9\text{x}10^{-6}$, Student's two-tailed *t*-test; **Figure 1B**). The negative correlation between relative abundance of *B. fragilis* and weight (the latter expressed as a proportion of the baseline value just prior to colonization) was significant ($p=0.01$, rho = -0.55, Spearman's rank correlation; **Figure S2B**).

Assaying the functional properties of clonally-arrayed collections of anaerobic bacterial strains cultured from healthy and stunted/underweight donor microbiota

The 16S rRNA sequence data did not allow us to distinguish the number of NTBF versus ETBF OTUs that had been transferred to gnotobiotic mice, nor would transplantation of intact uncul-

tured microbiota allow us to (i) describe the contribution of individual strains in the transplanted community to the community meta-transcriptome or (ii) test the effects of deliberately adding or subtracting individual members on community structure, community function, or host biology. Therefore, to further characterize microbe-microbe and microbe-host interactions, anaerobic bacterial strains were cultured from the healthy and stunted/underweight donors' fecal samples (*22*, *23*). Each collection of cultured strains was clonally arrayed in multi-well plates so that each well contained a monoculture of a given bacterial isolate (*22*). Each culture collection consisted of organisms that had co-existed in a single donor's gut and thus were the products of the donor's history of environmental exposures to various microbial reservoirs (including those of family members and various enteropathogens endemic to the Mirpur *thana*), as well as the selective pressures and evolutionary events (e.g., immune, antibiotic, food, horizontal gene transfers) placed on and operating within their microbiota.

Individual isolates in the clonally arrayed culture collection were grouped into 'strains' if they shared an overall level of nucleotide sequence identity of >96% across their assembled draft genomes. Based on this criteria and the results of full length and V4-16S rRNA sequencing of the isolates, we determined that the healthy and stunted donors' culture collections contained 53 and 37 strains, respectively, representing 21 and 17 of the 97%ID OTUs captured in mice receiving the intact uncultured human donor fecal samples. Only one strain was shared between the two culture collections: *Bifidobacterium breve* hVEW9. (See **Table S4A,B** for a list of all isolates in the culture collection derived from the stunted/underweight child plus a summary of KEGG-based annotations of their sequenced genomes, and (*23*) for details about the healthy donor's culture collection.)

ETBF strains contain one of three alleles of the toxin-encoding gene *bft* (*bft1, bft2, bft3*) in their 6 kb pathogenicity island (BfPAI). Two *B. fragilis* strains present in the healthy donor's culture collection (*B. fragilis* hVEW46 and hVEW47) lacked a BfPAI and were therefore classified as NTBF. The stunted donor's collection contained a single *B. fragilis* strain (*B. fragilis* mVEW4);

its genome contained a *bft-3* allele (**Table S1A**). ETBF strains of this type are globally distributed, most commonly in Southeast Asia (*24*).

We colonized 8-week-old adult male germ-free C57BL/6 mice with all members of either of these two culture collections (n=6 singly caged mice/culture collection; all mice receiving a given culture collection were maintained in a single gnotobiotic isolator). As a control, we also colonized mice with the corresponding intact uncultured fecal microbiota samples; they were housed in separate isolators from those used for the culture collection transplants. All mice were given each of the three embodiments of the Bangladeshi diet, each for one week, in the same order described for the previous experiments.

As with the intact uncultured microbiota, the corresponding culture collections transmitted discordant weight phenotypes to recipient animals (p<0.0001, repeated measures ANOVA; **Figure 1C**). Moreover, the weight phenotypes (change in body weight over time as a percentage of initial weight before gavage) between mice receiving intact fecal microbiota or the derivative culture collection from the same human donor were not significant (p>0.05, repeated measures ANOVA; **Figure 1C**).

The weight phenotypes first became statistically significantly different between the two groups of mice midway through consumption of diet embodiment 2 and again were not attributable to differences in food consumption; the differences continued to increase into the final phases of diet embodiment 3 where in the terminal days of the experiment mice harboring the stunted/underweight but not healthy donor culture collection manifested reduced food intake (**Figure 1C**).

To test whether the discordant weight phenotype was sensitive or robust to diet embodiment-type, the complete clonally-arrayed bacterial culture collections from the healthy or stunted/underweight donors were gavaged into separate groups of 8-week-old adult male germ-free C57BL/6 mice who were monotonously fed Bangladeshi diet embodiment 1, 2, *or* 3 for three weeks (n=6 singly caged recipient mice/culture collection/diet embodiment). The discordant weight phenotype observed previously was preserved irrespective of the Bangladeshi diet embodiment consumed

(p<0.0001, repeated measures ANOVA comparing recipients of the healthy versus stunted/underweight culture collections across all three diet embodiments; n=18 mice/culture collection; **Figure 1E**). Moreover, no significant differences in weights were noted between groups of mice colonized with the same culture collection but fed different diet embodiments (repeated measures ANOVA; Tukey-adjusted p=0.75, p=0.99, and p=0.61 for embodiments 1 versus 2, 1 versus 3, and 2 versus 3 for mice receiving the stunted/underweight donor's culture collection, respectively, and adjusted p=0.99 for each of these three comparisons in mice colonized with the healthy donor's culture collection; **Figure 1E**). We concluded that in our model, the gut microbiota was a more significant determinant of body weight phenotype than the particular diet embodiment consumed.

Transmission of strains was defined by short read shotgun sequencing of DNA isolated from fecal samples collected at the end of the experiment. This method, known as COmmunity PROfiling by Sequencing (COPRO-Seq), maps reads onto the draft genome assemblies of community members; at the depth of sequencing employed (354,352 ± 23,216 (mean ± s.e.m.); 50 nt unidirectional reads/fecal DNA sample), it can reliably detect strains whose relative abundance is ≥0.1% (for further details, see (*25*) and *Methods)*. COPRO-Seq demonstrated that transplantation of the culture collections was efficient and reproducible, with 98.1 ± 0.6% and 94.5 ± 1.6% (mean ± s.e.m.) of strains in the collections derived from the healthy and stunted donors, appearing in recipient animals, respectively. The abundance of ETBF in the fecal microbiota of mice containing the stunted/underweight donor's culture collection was significantly greater than the cumulative relative abundance of the two NTBF strains in recipients of the healthy culture collection (**Figure 2B**). This difference in the total relative abundance was significant irrespective of the diet embodiment consumed (p=2.8x10^{-9}, two-tailed Student's t-test; **Figure S2C**), and abundance negatively correlated with weight relative to baseline (p=5.4x10^{-5}, rho = -0.45, Spearman's rank correlation; **Figure S2B**). Moreover, the relative abundances of the ETBF strain in recipients of the stunted/underweight donor's culture collection, the two NTBF strains in the healthy donor's collection, and all other *Bacteroides* species did not differ significantly between diet embodiments (p>0.5, ANOVA; illustrated using indicator species analysis (*26-28*) in **Figure S2C**).

To assess whether this discordant weight loss phenotype was transmissible across generations of mice, two males from the transplant experiment, one containing the stunted/underweight donor's intact uncultured microbiota or derived culture collection, the other the healthy donor's intact microbiota or derived culture collection, were switched to and subsequently maintained on an irradiated nutritionally enhanced mouse breeder chow from 21 to 48 days post-colonization, at which time they were each co-housed with two germ-free 6-week old females that had received breeder chow since weaning. Seven days after co-housing, each male mouse was withdrawn from each mating trio, and the females were subsequently maintained on breeder chow throughout their pregnancy and as their pups completed the suckling period (**Figure S1B**). Male pups (n=3-4/litter) were then weaned onto an irradiated, nutritionally sufficient LF/HPP chow until they were 9-weeks old, at which time they were switched to the Bangladeshi diets (10 days/diet; order of sequential presentation of the embodiments as before). The efficiency of transmission of 97% ID OTUs from mothers to offspring was high: e.g., 96±1.8% and 88±2.3% (mean ± s.e.m.) in the case of the healthy and stunted/underweight donor's intact uncultured donor microbiota, respectively (**Figure S3**).

Mice born to mothers colonized with either of these intact uncultured fecal microbiota or arrayed culture collections experienced identical weight gain profiles while consuming the nutritionally complete LF/HPP chow (p=0.9, two-tailed Student's t-test comparing weights between the two treatment groups; **Table S5**). However, once they were transitioned to the sequence of three Bangladeshi diet embodiments (consumed from postnatal days 56 to 86), a discordant weight loss phenotype was again observed with mice born to mothers harboring a stunted/underweight microbiota exhibiting significantly greater weight loss (p<0.001; repeated measures ANOVA). In mice colonized with the culture collections, the efficiency of ETBF and NTBF transmission from parents to pups was 100%: the total relative abundance of the two NTBF strains in fecal samples obtained from recipients of the healthy donor's culture collection was 4.2±0.7% at the conclusion of the LF/HPP diet period and 4.6±0.9% at the conclusion of the Bangladeshi diet embodiment sequence, while the relative abundance of ETBF for these two time points were 34.3±4.2% and

50.0±0.7%, respectively, in mice colonized with the stunted/underweight donor's culture collection. Based on these results, we concluded that the weight loss phenotype was transmissible across generations and evocable by embodiments of a Bangladeshi diet.

We used targeted mass spectrometry to quantify levels of amino acids, organic acids, acylcarnitines, and acyl-CoAs in liver and serum harvested from mice in the two treatment groups, each of which had been monotonously fed diet embodiment 2. Animals were not fasted prior to euthanasia.

The combination of this embodiment of the Bangladeshi diet and a stunted/underweight culture collection was associated with significant increases in hepatic levels of succinate, malate, and fumarate compared to mice colonized with the healthy culture collection ($p<0.03$; **Figure S4A**), indicating that the former group had impaired TCA cycle activity. Pyruvate, the end product of glycolysis that feeds into the TCA cycle, was also significantly decreased, as was lactate, which is converted to pyruvate in energy-deficient states ($p<0.005$; **Figure S4A**) (*29*).

Long-chain fatty acid (LCFA) CoA synthetase converts fatty acids to fatty acylCoAs, a carnitine-dependent first step in fatty acid transport through the outer and inner membranes of mitochondria into the mitochondrial matrix (*30*). Undernutrition is associated with carnitine deficiency (*31*) and decreased ability to utilize LCFAs (*29*): carnitines are converted to acylcarnitines in the mitochondrial inter-membrane space as part of LCFA transport. Carnitine can be synthesized from lysine and methionine (*32*). Compared to mice harboring the healthy donor culture collection, those colonized with the ETBF-containing stunted/underweight donor culture collection exhibited (i) increased concentrations of lauroyl-, myristoyl-, palmitoyl-, oleoyl-, and linoleoyl-CoAs in their livers ($p<0.03$, FDR-adjusted Student's two-tailed *t*-test; **Figure S4C**), (ii) significantly lower levels of C2, C6, and C20 acylcarnitines in their livers ($p<0.05$, FDR-adjusted Student's two-tailed *t*-test; **Figure S4D**), plus (iii) significantly lower levels of methionine in their serum ($p<0.0005$, FDR-adjusted Student's two-tailed *t*-test; **Figure S4B**). These results are consistent with a decreased capacity for acylCoA utilization.

Niche space dictates the effects of the pathobiont ETBF on microbiota community structure and function

Figure 3 describes a series of manipulations we performed involving (i) removal of the ETBF strain from the stunted/underweight donor's culture collection (to allow comparison of the responses of the community as well as host to its presence or absence), and (ii) addition of the ETBF strain to the healthy donor's culture collection with or without subtraction of its two NTBF strains (to ascertain community/host responses to ETBF, the ability of NTBF to modulate ETBF effects, and the effects of ETBF on NTBF). C57BL/6 male mice in each of the five different treatment groups were 8-9 weeks of age at the time of colonization; all were placed on diet embodiment 2 for two days prior to gavage and subsequently maintained on this diet for 13 days until they were euthanized (n=5 animals/treatment group; all singly caged; treatment groups maintained separate gnotobiotic isolators). Fecal samples were collected as described in **Figure S1D**. Host weight, metabolic, and immune phenotypes were defined. Microbial communities were characterized structurally by COPRO-Seq analysis of fecal samples, and functionally by RNA-Seq and mass spectroscopic analyses of cecal samples.

Host phenotypes – Removal of the ETBF strain from the complete stunted/underweight donor's culture collection prevented the transmissible weight loss phenotype (**Figure 2C**; p<0.0002, Tukey-corrected repeated-measures ANOVA). However, addition of the ETBF strain to the healthy donor's culture collection did not produce significant weight loss, regardless of whether the NTBF strains were present or absent (p=0.9, repeated-measures ANOVA; **Figure 2C**).

The metabolic effects of these microbial community manipulations were studied by assaying serum, liver, gastrocnemius muscle, and cecal contents by targeted mass spectrometry. Results are summarized in **Table S6H**. Mice colonized with the complete (unmanipulated) stunted/underweight donor's culture collection were unique among the treatment groups in having elevated hepatic levels of two known inhibitors of mitochondrial electron transport complex IV, C16 and d18:1/16:0 ceramides, (p<0.0006 and p<0.05, respectively, using FDR-adjusted Student's two-

tailed *t*-test; **Figure 2D**), and significantly elevated levels of lactate in their gastrocnemius muscle ($p<0.04$, FDR-adjusted Student's two-tailed *t*-test) consistent with decreased oxidative metabolism. Ceramides are involved in key intracellular stress response pathways (*33*), including those associated with immuno-inflammatory responses (*34*) (see below).

The effects of removing ETBF from the stunted/underweight donor's culture collection and of adding ETBF to the healthy donor's culture collection included changes in multiple metabolite classes (**Table S6H)**. Among the >100 metabolites characterized by targeted mass spectrometry, including multiple bile acid species, the presence of ETBF in these two community contexts resulted in just one identified common metabolic response - a significant increase in cecal levels of acetate ($p<0.02$, FDR-adjusted Student's two-tailed *t*-test) but not other short-chain fatty acids (e.g. propionate, butyrate). Intriguingly, acetate has been linked to the regulation of virulence, as illustrated by its effect on Shiga toxin-producing *E. coli* in gnotobiotic mice co-colonized with an age-discriminatory bacterial species in the developing human gut microbiota, *Bifidobacterium longum* (*35*). Such a limited metabolic signature of ETBF might be explained by the fact that two communities that only shared only one member.

To assess the effects of ETBF on host immune phenotype, we performed FACS analysis of immune cell populations in the colons, mesenteric lymph nodes, and spleens of four groups of mice: those colonized with the stunted/underweight donor's culture collection with or without ETBF; and those containing the transplanted unmanipulated healthy donor's culture collection or the manipulated collection where ETBF had been substituted for NTBF. Consistent with a previous study of gnotobiotic mice mono-colonized with an ETBF isolate (*36*), colonic $CD4^+$ $Th17^+$ T-lymphocyte populations were significantly increased in animals colonized with ETBF(+) healthy and ETBF(+) stunted/underweight culture collections compared to ETBF(–) healthy and ETBF(–) stunted culture collections ($p<0.001$ and $p<0.02$ for, respectively, Student's *t*-test; **Figure S5B**). The presence of ETBF was not associated with significant differences in the size of the anti-inflammatory $FoxP3^+$ regulatory T-cell population in mesenteric lymph nodes in either the stunted/underweight or healthy community contexts ($p>0.05$, ANOVA corrected for multiple hypotheses;

Figure S5C). Based on these cellular phenotypes, the immune response to the presence of ETBF could not be readily correlated with the observed weight loss phenotypes.

Microbial community responses to ETBF – COPRO-Seq analysis revealed that recipients of the unmanipulated stunted donor's culture collection had fecal microbiota dominated by ETBF (relative abundance 62.3±4.0%). Removal of ETBF led to significant increases in the relative abundances of *Bifidobacterium breve*, *Bifidobacterium*, *Enterococcus lactis*, and *Enterococcus gallinarum* ($p<0.02$, two-tailed Student's *t*-test; **Figure 4A**). (Note that no other *Bacteroides* species were present in this culture collection).

In contrast, the fecal microbiota of recipients of the unmanipulated ETBF(–) NTBF(+) healthy donor's culture collection were dominated by (i) the two NTBF strains [total *B. fragilis* relative abundance 14.5±3.0% (mean ± s.e.m.), with strains *Bacteroides fragilis* hVEW46 and *Bacteroides fragilis* hVEW47 comprising 1.1% and 13.5%, respectively; **Figure 4A**] and (ii) two other *Bacteroides* (*B. thetaiotaomicron* and *B. caccae*), plus *Bifidobacterium breve* and *Enterococcus*. Addition of ETBF to the healthy donor's culture collection did not produce significant changes in the relative abundance of the *B. fragilis* component of the recipient's microbiota [*B. fragilis* strains comprised 18.4±0.9% (mean ± s.e.m.) of the community, with the NTBF and ETBF equivalently represented at relative abundances 8.9±0.5% and 9.5±0.4% respectively]. Remarkably, this relative abundance value for *B. fragilis* held (i.e. was not significantly different) in all three versions of the transplanted healthy donor community examined (the unmanipulated ETBF(–) NTBF(+), plus the manipulated ETBF(+) NTBF(–), and ETBF(+) NTBF(+) types) was remarkable (**Figure 4A**; $p>0.5$, two-tailed Student's *t*-testing) suggesting that a restricted niche space for *B. fragilis* is imposed by other members of this healthy donor's culture collection. In line with this notion, we observed that the fecal microbiota of mice colonized with the ETBF(+) NTBF(–) manipulated healthy culture collection had significantly higher relative abundances of *B. thetaiotaomicron, B. caccae*, and *Bifidobacterium breve*, and significantly lower relative abundance of *Enterobacteriaceae* compared to the fecal microbiota of mice harboring the manipulated ETBF(+) NTBF(+) version ($p<0.05$, Student's two-tailed *t*-test; **Figure 4A**).

Integrating the weight phenotypes with these observations also suggested that both intra-species and inter-species interactions are critical in determining whether ETBF colonization results in weight loss. Therefore, we turned to microbial RNA-Seq to assess (i) the effects of the stunted/underweight versus the healthy community on ETBF, (ii) the effects of intra-species competition (NTBF on ETBF and vice versa) in the healthy community context, and (iii) the effects of co-colonization with ETBF on other *Bacteroides* and other bacterial members that do not belong to this genus in the healthy community context.

The results of a comparison of the ETBF transcriptome in the transplanted unmanipulated stunted/underweight versus the manipulated ETBF(+) NTBF(–) healthy donor cultures collection are summarized in **Figure 5** in the form of a volcano plot where the x-axis represents the fold-difference in expression of ETBF genes in the context of the two communities and the y-axis shows the FDR-corrected *p*-value of the significance of the difference as determined by the exact negative binomial test, as well as a heatmap where rows show Z-score normalized transcript levels (read counts per million reads) of differentially expressed transcripts whose protein products had assignable Pfam annotations. A variety of ETBF genes involved in carbohydrate uptake, metabolism and biosynthesis were differentially expressed, including components of polysaccharide utilization loci (PULs) and capsular polysaccharide biosynthesis (*CPS*) loci (**Figures 5B** and **S6**).

Intriguingly, our transcriptional analysis of ETBF responses showed that expression of its key virulence and colonization determinant, *bft-3* (*37-39*), varied significantly based on community context. In a manipulated healthy community where ETBF was present but NTBF was absent, *bft-3* expression in the cecal meta-transcriptome was increased 120-fold compared to a community where both ETBF and NTBF were present ($p<1x10^{-21}$, **Figure S6C**, **Table S7B**).The importance of *bft* in colonization and virulence was further highlighted when we abrogated fragilysin (*bft-3*) expression within ETBF isolate mB11 through insertional mutagenesis (**Figure S10**). Though this mutant grew robustly *in vitro*, when we attempted to colonize germ-free gnotobiotic mice (n=5) with a manipulated version of the stunted donor's culture collection where the isogenic *bft*-knockout strain had been substituted for the existing wild-type ETBF strain, we saw no ETBFΔ*bft-3*

colonization of the mutant: the number of reads mapping to the *bft* knockout strain was no greater than background; failed colonization (as opposed to low level colonization) was confirmed by a negative PCR assay that used *B. fragilis*-specific *bft* primers (*40*).

Given the critical role played by ETBF in mediating our weight-loss phenotype, we turned to our transcriptomic data for insights into how NTBF might be mediating regulation of the key colonization/virulence factor *bft-3* in ETBF. Comparing the healthy community with or without its NTBF strains revealed that the presence of the two NTBF strains affected a number of features of ETBF gene expression (**Table S7B**). One of these factors is LuxQ, which serves as a key signaling protein in the detection of the quorum-sensing molecule AI-2 (Autoinducer-2). We observed that expression of three of the four *luxQ* homologs in ETBF were decreased when NTBF was present in the context of the healthy donor's culture collection ($p<0.005$, $\log_2$(fold-change) of -2.8, -4.4, -9.5; **Table S7B**): comparing the mice colonized with the unmanipulated NTBF(+) with the manipulated ETBF(+), NTBF(+) versions of the healthy donor's culture collection revealed differential regulation of three other *luxQ* transcripts encoded by *Bacteroides* members of the healthy community (one each in *B. thetaiotaomicron hVEW3, B. caccae* hVEW52*,* and *B. caccae* hVEW52, **Table S7D**). Recent studies in gnotobiotic mice have (i) demonstrated that AI-2 signaling by members of the human gut microbitoa can alter the virulence factor expression of enteropathogens (*11*) and (ii) linked AI-2 signaling modulation of levels of Bacteroidetes in the gut (*41*). The healthy culture collection contains a total of five *Bacteroides* strains; two representatives of *B. fragilis*, one of *B. thetaiotaomicron* and two *B. caccae* (**Table S4A**). Intriguingly, the relative abundances of the latter three strains but not the NTBF strains were significantly altered when ETBF was added (see above).

The AI-2 signaling system in *Bacteroides* has not been well characterized. Genomic analysis of the type strains of six *Bacteroides* species revealed that majority of their genomes did not encode the AI-2 synthase luxS, but did contain many luxQ homologs. Furthermore, this analysis revealed few putative downstream *luxP*, *luxU*, and *luxO* genes (*11*). While much work remains to be done to characterize the mechanisms behind how AI-2 regulates gene expression and fitness of

Bacteroides in the gut, the changes in species-level abundances and expression of components of quorum-sensing regulatory systems which occur in the context of ETBF-NTBF interactions in the healthy donor's community suggest that cell-cell communication may play a role in the communities structural and functional configuration in the gut.

The volcano plot and heatmaps shown in **Figure S7** summarize the myriad effects of ETBF on the NTBF transcriptome. As with ETBF, NTBF responds to the presence of its conspecific (ETBF) strain by changing expression of multiple features of carbohydrate utilization and biosynthesis, including several of its capsular polysaccharide biosynthesis (*CPS*) loci and polysaccharide utilization loci (PULs) (**Figure S7B**).

The effects of incorporating ETBF in lieu of the two strains of NTBF in the transplanted healthy culture collection on *B. thetaiotaomicron* and *B. caccae* are depicted in **Figures S8** and **S9** and include significant increases in expression of a *luxQ* locus in *B. thetaiotaomicron* and decreased expression of two *luxQ* loci in one of the two strains of *B. caccae* (*B. caccae* hVEW51) plus induction and suppression of several PULs and *CPS* loci (also see **Table S7D**).

Effects of ETBF on gene expression by other members of the microbiota – We proceeded to further elucidate the transcriptional responses in the community during its reorganization as a result of pathogenic ETBF invasion. To do this, we examined genes known to be related to infection, colonization, and virulence in pathogenic organisms by BLAST searches of the genomes of members of both culture collections for genes within the Virulence Factor (VF) database (putative virulence factor representation by strain listed in **Table 1**).

We used our microbial RNA-Seq data to compare the expression of genes related to virulence processes in five different transplanted cultured community contexts: the stunted/underweight donor's community with or without ETBF; the un-manipulated ETBF(–) NTBF(+) healthy donor's community; and the manipulated healthy donor's community with ETBF and NTBF, or with ETBF in lieu of NTBF. None of the 105 genes with annotations in the VF database encoded in the genomes of the members of the transplanted stunted/underweight donor's culture collection

underwent significant changes in expression when ETBF was not present (**Figure 4B** and **Table S8B**). Addition of ETBF to the healthy donor's culture collection when its NTBF strains were present produced only 7 (0.7%) significant changes in gene expression *in vivo* in four of its 53 member strains (**Table S8D**). In stark contrast, removal of the two NTBF strains 'allowed' ETBF to have a very large and generalized effect on community expression, with 254 (25%) of the 993 VF database annotated genes encoded by 9 of the 53 members of this manipulated community exhibiting significant changes in their expression (**Table S8D**). The distribution of these ETBF-induced virulence factors among community members is shown in **Table 1** and **Figure 4B,** with the majority of those induced present in *Enterobacteriaceae* hVEW34 (134 of its 320 encoded VFs) and *Enterococcus gallinarum* hVEW37 (36 of its 292 VFs) (**Table 1, Table S8**), and the majority of those suppressed belonging to *Bifidobacterium breve* hVEW45 (11 of its 14 virulence factors).

We identified numerous genes related to stress responses, including the key general stress response sigma factor *rpoS* (*42*), and genes related to DNA repair such as *recD*, suggesting that community members may undergo a regulated general stress response to ETBF invasion that is ameliorated by the presence of NTBF.

Genes responsible for iron acquisition and metabolism were also upregulated during invasion by ETBF, suggesting one possible area of species competition leading to metabolic stress within the community. An *Enterobacteriaceae* homolog of the *E. coli* BasSR system component BasS that is induced under high iron conditions is also repressed during ETBF invasion (*43*). This is also concordant with previous work in model bacterial systems suggesting that RpoS positively controls carbon source transport and iron acquisition (*44*), suggesting that competition with ETBF for iron by members of the health donor's-derived community is important during ETBF invasion.

Intriguingly, numerous genes related to prophage and mobile DNA element biology were also up-regulated as a response to ETBF invasion (**Figure 4B**). Prophage activation in bacteria as a function of stress has been shown previously, with some studies postulating that phage induction and subsequent lysis of resident commensal microbes may lead to a shift in community structure to favor an increased proportion of pathobionts via "community shuffling" (*45*).

The mechanisms by which NTBF can suppress the effects of ETBF on gene expression in other community members are unclear, including the role played by inter-species quorum sensing (e.g. by *luxQ* regulation). Nonetheless, these changes reveal/report inter-specific interactions that are profoundly shaped by intra-specific competition (*46*, *47*).

DISCUSSION

The approach described in this study, involving generation of sequenced, clonally arrayed culture collections from the fecal microbiota of 24-month old healthy and stunted/underweight Bangladeshi children and subsequently introducing these consortia, with or without addition or subtraction of *B. fragilis* strains, into germ-free mice fed embodiments of the diets consumed by the microbiota donors, allowed us to characterize how an enterotoxigenic strain functions as a pathobiont in a microbial community context-dependent manner.

In ecology, zero net-growth isoclines (ZNGI) are used to describe the conditions necessary for a habitat to sustain a given population size of a given species; they can also be used to predict what alterations could be made to extirpate an organism from the niche described by the ZNGI. The parameters required to calculate a ZNGI for a given species are the abundance of competitors and/or resource availability. Gnotobiotic mouse models like that created for the present set of experiments provide a way to model a ZNGI for various members of the human gut microbiota including pathobionts such as ETBF (*16*).

The ability of the community of bacterial strains cultured from the healthy donor's gut microbiota to accommodate ETBF is vividly illustrated by the intraspecific interactions between NTBF and ETBF: simulating invasion of ETBF into a healthy host's community by introducing it into the culture collection prior to colonization of mice a regulated stress and iron metabolism response that was only apparent when NTBF was removed. The power of marrying gnotobiotics with clonally arrayed culture collections to deliberately and systematically alter the membership of communities assembled in mouse models of human donors' gut ecosystems creates an opportunity to conduct future experiments in which (i) ETBF is added to various subsets of the healthy

donor's culture collection ± NTBF and introduced into germ-free mice to identify the intra- and interspecific interactions that lead to or prevent different pathological outcomes and how diet shapes this rich community transcriptional response. Similarly, testing the ability of other NTBF strains, cultured from different Bangladeshi children living in Mirpur or other geographic locations within Bangladesh to mitigate ETBF effects, or reciprocally, examining different isolated ETBF strains in the presence of a given NTBF strain in this healthy donor's community context, should be informative. An analogous series of combinatorial experiments could also be performed involving introduction of different NTBF strains (in the context of various ETBF strains) into the stunted/underweight donor's culture collection. Other levels of generalization can be envisioned with this approach: our study was limited to characterizing the microbiota of two donors representing a single population where the burden of childhood undernutrition is great; clonally arrayed culture collections obtained from healthy and undernourished donors from other populations where burden of disease is also great, could be used for these types of addition/subtraction/subset experiments to better understand how inter/intra-specific competition and niche space determine the effects of enteropathogens in different diet contexts on disease pathogenesis. One hoped for outcome from these types of analyses is development of new food and microbe-based interventions that more effectively treat and ultimately help prevent childhood undernutrition.

MATERIALS AND METHODS

Birth cohort study

The birth cohort study design and sample collection protocols have been described previously (*17*).

bft PCR assay

Confirmation of blastn results of *B. fragilis* toxin (*bft*) in *B. fragilis* strains in the stunted donor's culture collection and screening DNA isolated from fecal samples collected at 18 and 24 months of age from members of the birth-cohort was achieved by PCR using primer pair: 5'-GAACCTAAAACGGTATATGT-3' (GBF-201) and 5'-GTTGTAGACATCCCACTGGC-3' (GBF-210) (*48*)

and OneTaq 2x master mix (New England Biolabs) under the following thermocycling conditions: after initial melting at 95°C for 30 s, 30 cycles of 95°C for 30 s, 53°C for 30 s, and 68°C for 30 s, with a final annealing time of 7 min at 68°C.

Preparation of human fecal samples for transplantation

Under anaerobic conditions (77%N_2, 20%CO_2, 3%H_2), 1 g aliquots of previously frozen fecal samples were resuspended in 15 mL of gut microbiota medium (GMM) (*22*) and homogenized at the 'high' setting in a sterilized blender (Waring, Torrington, CT). Homogenates were clarified by passage through 100 μm pore-diameter nylon filters (BD Falcon, Franklin Lakes, NJ). Five mL of sterile 2 mm-diameter glass beads were added and remaining cell clumps were disrupted by vortexing (four on/off cycles, each 30 s). A final filtration through a 40 μm pore-diameter nylon filter (BD Falcon, Franklin Lakes, NJ) was performed before storage in GMM with 15% glycerol at -80°C in 2 mL amber glass vials with a crimp-top butyl septum (Wheaton Scientific, Millville, NJ).

Production of Bangladeshi Diet Embodiments

Diet embodiments were prepared in 15 kg batches, with ingredient composition and nutritional content given in **Table S1**. Tilapia fish filets (Whole Foods Markets, St. Louis, MO) were simmered for 30 min in a 20 L stainless steel pot over a Corning hotplate (temperature setting 4). Fruits and vegetables were combined and simmered in a separate pot for 45 min on a Corning hotplate (temperature set at '4'). Parboiled rice (Delta Star, Stuttgart, AR) was cooked in a rice cooker (KRUPS, Medford, MA). Lentils were simmered for 90 min (temperature set at '2'). All ingredients for a given diet embodiment were combined in a vertical cutter-mixer (Robot Coupe Model R23, Jackson, MS) and pureed for 5 min. Aliquots were cooled for 12 hours in large plastic containers at 4°C; thereafter, 500 g aliquots were vacuum-sealed in 8"x10" plastic bags (U-line, Pleasant Prairie, WI). The vacuum-sealed food paste was placed in a second 8"x10" plastic bag (as an added barrier against incidental contamination), and the contents of the packages were sterilized by irradiation (20-50 kGy) within 24 h of food production (Steris Co, Chicago, IL). Sterility was verified by culturing samples of the irradiated diet in BHI medium for 5 days at 37°C under

anaerobic and aerobic conditions as described previously (*23*). In addition, *B. subtilis* spore strips that had been included along with the food during the irradiation were cultured under the same conditions. Final nutritional profiles of the diets were obtained by submitting 100 g samples of each embodiment to Nestle Purina Analytical Labs (St Louis, MO).

Clonally arrayed bacterial culture collections

Clonally arrayed bacterial culture collections were generated from frozen fecal samples using previously published methodologies (*22*). Diluted bacterial cultures were arrayed in Coy chambers under strict anaerobic conditions (77%N_2, 20%CO, 3%H_2) using protocols executed on a Precision XS liquid handling robot (BioTek, Winooski, VT). The bacteria occupying each well were first grouped into 100%ID OTUs based on the results of V4-16S rRNA amplicon sequencing. Most OTUs were observed more than once across an arrayed library. Next, 3-4 isolates representing each OTU were picked robotically from the 384-well arrays and struck out individually onto 8-well agar plates containing GMM (*22*): DNA from isolates was subjected to whole genome shotgun sequencing, plus sequencing of full-length 16S rRNA gene amplicons generated by primer pairs 8F and 1391R. Isolates sharing ≥99% nucleotide sequence identity in their 16S rRNA genes, and ≥96% sequence identity throughout their genomes (as determined by NUCmer (*49*) were defined as a unique strain. Full-length 16S rRNA sequences were used to define taxonomy (Ribosomal Database Project (RDP) version 2.4 classifier (*50*)). Whole genome shotgun sequencing was performed using an Illumina HiSeq 2000 instrument (101 nt paired-end reads) or a MiSeq machine (150 nt paired-end reads). Sequences were assembled using MIRA (*51*), version 4.02 (parameters: "-NW:cnfs=warn, -NW:cmrnl=no, –GE:not=4"; template_size = "150 500 autorefine"). Coverage of strains from the severely stunted/underweight donor's culture collection was 38.6±5.0-fold (mean±SEM) with an N50 contig length of 28.5±3.5kb (mean±SEM) (Table S3B). The corresponding values for members of the healthy donor's collection are described in (*23*). Genes were annotated using Prokka v1.10 (*52*). Predicted genes in each isolate's genome assemblies were mapped to KEGG pathways and assigned KEGG Ortholog (KO) groups by querying the KEGG

reference database (release 72.1) (BLAST 2.2.29+, blastp E-value $\leq 10^{-10}$, single best hit defined by E-value and bit score) (*53*, *54*).

Clonally arrayed, sequenced culture collections were stored in GMM/15% glycerol at 80° C in 96-well plates (TPP Tissue Culture Test Plates, Switzerland).

Generation of a bft-3:pGERM mutant in the ETBF strain cultured from the stunted donor's microbiota — *Bft* gene disruption was accomplished using the *Bacteroides* suicide vector pGERM (*55*). We introduced a 380-bp fragment of the 5' end of *bft-3* into BamH1-digested pGERM suicide vector using the Gibson Assembly Cloning Kit (NEB) (*56*). Primers to create the PCR product for the Gibson reaction were created using the NEBuilder Assembly Tool (v1.7.2). Assembled constructs were introduced by electroporation into kanamycin-resistant, electrocompetent E. *coli* DH5-α RK231 (*57*). Transformants were plated on LB-agar containing IPTG/Xgal (SigmaAldrich, St. Louis, MO) and ampicillin (100 μg/mL). Individual colonies were picked and grown in ampicillin-treated LB medium; successful transformation was verified by PCR. The pGERM-transformed *E. coli* DH5-α RK231 and the ETBF strain were conjugated by filter-mating on BHI-blood agar plates incubated under anaerobic conditions at 37° C for 24h (*58*). A scraping of the resultant lawn was plated on BHI agar plates containing erythromycin/gentamycin (25 μg/mL and 100 μg/mL, respectively) which were incubated under anaerobic conditions at 37° C for 48 h. Picked colonies were sequenced to confirm successful pGERM insertion into *bft-3* and positive colonies were stored as TYG/15% glycerol stock.

The mutant and wild-type strains were cultured in TYG liquid media to mid-log phase in medium at 37°C under anaerobic conditions. Cells were harvested, and RNA was extracted using Trizol reagent (Life Technologies, Carlsbad, CA). To confirm that *bft* expression had been disrupted, cDNA was generated from the extracted RNA (see RNA-Seq section below) to enable a PCR-based assay for detection of *bft* transcripts *in vitro*. PCR was performed using ReddyMix PCR Mastermix (ThermoFisher Scientific, Waltham, MA) under the following thermocycler conditions: 94°C for 10 minutes followed by 30 cycles of 94°C for 30 seconds, 56°C for 30 seconds, 72°C

for 60 seconds, with a final extension of 72°C for 5 minutes, and the following primers were used: forward primer that spans the vector insertion site and 5'-ATGAAGAATGTAAAGTTACTTTTA-ATGCTAGGAACCG-3' and the reverse primer that is 3' to the crossover site in order to confirm successful *bft* disruption 5'-CTCCACTTTGTACTTTATACTACTGAATATGCTTG-3'.

Assembling consortia of cultured bacterial strains for gavage

Archived 96-well culture collection plates were thawed in an anaerobic chamber and aliquots of each well inoculated into 600 μL of GMM in 1 mL 96-deep-well culture plates (ThermoScientific, Rochester, NY). Cultures were grown anaerobically to stationary phase at 37°C before pooling 100 μL aliquots of selected isolates using a Precision XS liquid handling robot (BioTek, Winooski, VT). For healthy culture collection pools where ETBF was to be added, separate cultures of ETBF were grown under the same conditions as the 96-well format and added in the same volume to the pool manually. Final pools were mixed 1:1 with sterile PBS (15% glycerol final concentration) and aliquoted (1 mL each) into 2 mL butyl septum-stoppered amber glass vials (Wheaton, Melville NJ).

Gnotobiotic mouse experiments

All mouse experiments were performed using protocols approved by Washington University Animal Studies Committee. Prior to the initiation of experiments, germ-free adult male C57BL/6 mice were maintained in plastic flexible film gnotobiotic isolators under a strict 12-hour light cycle and fed an autoclaved low-fat, high-plant polysaccharide (LF/HPP) chow *ad libitum* (B&K Universal, East Yorkshire, U.K; diet 7378000).

Feeding Bangladeshi diet embodiments was initiated two days prior to colonization with either uncultured fecal microbiota samples or pools generated from arrayed bacterial culture collections. Diets were extruded as a paste from their plastic bags into food trays. Fresh 30 g aliquots of the paste were provided to each singly caged animal/day; this amount was never fully consumed . In the final 1-2 days of a given experiment, the amount of residual diet in the cages of mice already experiencing weight loss rose to represent up to 50% of the administered daily volume.

Due to the paste-like consistency of these diet embodiments, exact quantification of the amount of consumed diet versus diet discarded from the tray into the bedding could not be performed. For experiments where diet embodiments were changed, autoclaved Aspen hardwood lab bedding (NEPCO, Warrensburg, NY) was replaced at the start of each embodiment transition to minimize carryover of ingredients between embodiment exposures.

For the intergenerational transmission experiments, male pups (*n*=3-4/ for intact donor microbiota communities; *n*=5/culture collections), representing the combined litter from trio matings were weaned onto LF/HPP chow and transitioned to the three Bangladeshi diet embodiments at 8 weeks of age (embodiments 1→2→3; 10 d/diet phase).

Microbial community profiling

Multiplex sequencing of 16S rRNA PCR amplicons — Genomic DNA was extracted from mouse fecal pellets and snap-frozen cecal contents using a phenol-chloroform and beat-beating protocol previously described (*50*, *59*). Barcoded 16S primers 515F and 806R were used to generate PCR amplicons covering the V4 region of 16S rRNA genes present in the samples. Equimolar pools of these sample-barcoded V4-16S rRNA amplicon libraries underwent multiplex sequencing via the Illumina MiSeq platform to generate 250 bp paired-end Illumina reads, which were trimmed *in silico* to 200 bases using prinseq-lite v0.15 (in order to retain only the highest-quality base calls) (*60*), assembled with the software FLASH v1.2.11 (*61*), and de-multiplexed in QIIME v1.8.0 (*62*).

QIIME v1.8.0 was used to analyze the resulting V4-16S rRNA datasets (*63*). The 16S rRNA sequence datasets were first analyzed using open-reference OTU picking (97%ID OTUs) utilizing uclust-ref against the Greengenes reference database (*64*). 98.7% of the 26,419,497 sequences that passed QIIME's default quality filters were successfully clustered with a reference sequence of ≥97%ID. For all subsequent analyses, OTU tables were rarefied to 4000 reads per sample and filtered to retain only those OTUs whose relative abundances in fecal microbiota were ≥0.1% in ≥1% of all samples sequenced. Taxonomies were assigned using RDP classifier 2.4 trained on the manually curated Greengenes database 'Isolated named strains 16S' (*64*).

Community profiling by sequencing (COPRO-Seq) in mice colonized with unmanipulated and manipulated culture collections – 75-nt unidirectional reads were obtained by sequencing fecal and cecal DNA samples on an Illumina MiSeq platform and trimmed to 50 nt to preserve the highest quality reads before mapping onto the genomes of culture community members. The analytic pipeline is described in (*25*) and freely available at https://github.com/nmcnulty/COPRO-Seq.

Microbial RNA-Seq - Procedures for performing microbial RNA-Seq are described in-depth in previous publications (*25*, *65*, *66*). Cecal contents aliquots (~50 mg), collected at sacrifice (14 days post colonization) and stored at -80° C, were suspended in 500 µL of extraction buffer (200 mM NaCl, 20 mM EDTA), 210 µL of 20% SDS, 500 µL phenol:chloroform:isoamyl alcohol (pH 4.5, 125:24:1, Ambion/Life Technologies, Carlsbad, CA), and 150 µL acid-washed glass beads (212-300 µm diameter, Sigma-Aldrich, St. Louis, MO). Cells were lysed by mechanical disruption using a bead beater (maximum setting; 5 min at room temperature; BioSpec Products, Bartlesville, OK), followed by phenol:chloroform:isoamyl alcohol extraction and isopropanol precipitation on ice. After treatment with RNAse-free TURBO-DNAse (Ambion/Life Technologies, Carlsbad, CA), MEGAClear columns (Life Technologies, Carlsbad, CA) were utilized to remove 5S rRNA and tRNAs. A second DNAse treatment (Baseline-Zero DNAse; Epicentre/Illumina, San Diego, CA) was performed before a second MEGAClear purification followed by rRNA depletion using the Ribo-zero rRNA removal kits (Epicentre/Illumina, San Diego, CA). cDNA was synthesized using SuperScript II (Invitrogen/Life Technologies, Carlsbad, CA), and the second strand synthesis was performed using RNAaseH, *E. coli* DNA polymerase and *E. coli* DNA ligase (all from New England Biolabs). cDNA libraries were prepared by shearing samples using a BioRuptor Pico sonicator (Diagenode, Denville, NJ); then size-selecting 150-200 base-pair fragments for blunting, A-tailing, and ligating sample-specific barcoded sequencing adapters; and finally PCR enrichment.

cDNA libraries were pooled for multiplex sequencing using an Illumina NextSeq instrument (13.4 ±4.1 million unidirectional 75 nucleotide reads/cecal sample). Analysis was performed

as described in previous publications (*50*), using a custom reference database consisting of the genomes of the strains that comprised the communities.

Florescence-activated cell sorting

Cell isolation — Cells from the spleen, MLN and colonic lamina propria were isolated as described previously with minor modifications (*67*). Spleens and mesenteric lymph nodes were harvested and placed in ice-cold Hank's Balanced Salt Solution (HBSS; Gibco c/o Life Technologies, Carlsbad, CA) containing 0.1% (w/v) bovine serum albumin (BSA) (Sigma-Aldrich, St. Louis, MO). Single-cell suspensions were prepared by passage through a cell strainer (70-µm-diameter pores; BD Falcon, Franklin Lakes, NJ) and resuspension in HBSS/0.1% BSA. Splenocytes were pelleted by centrifugation at 453g for 5 min, and the supernatant was removed. Pellet was resuspended by gentle flicking of the tube, and red blood cells were removed by addition of 700 µl of prewarmed (37°C) ammonium-chloride-potassium lysis buffer (Gibco c/o Life Technologies, Carlsbad, CA) to splenocytes followed by immediate vortexing. After a 3-min incubation at room temperature, ~10 ml of HBSS/0.1% BSA was added to halt the lysis, the cell suspension was passed through a cell strainer (70 um-diameter pores) and centrifuged at 453g for 5 min, and the supernatant was removed. Spleen and mesenteric lymph node cell suspensions were stored on ice until further use. Colonic lamina propria cells were isolated using a previously described protocol with modifications (50). The colon was harvested immediately after sacrifice and opened longitudinally with scissors. Luminal contents were removed by gentle scraping, and the colon was trimmed of fat/mesentery. The remaining tissue was minced into small pieces (~2 to 3 mm^3), and the fragments were placed on ice in ~10 ml of HBSS/0.1% BSA until further processing. HBSS/0.1% BSA was aspirated, and the tissue fragments were placed in 15 ml of complete HBSS containing penicillin (100 U/ml; CellGro, Manassas, VA) and EDTA (5 mM; CellGro, Manassas, VA). The mixture was shaken at 180 rpm for 20 min (at 37°C) in an orbital shaker, after which time the medium was aspirated. This step was repeated once, and the colonic tissue was washed of excess EDTA by placing in 10 ml of complete RPMI [RPMI 1640 (Gibco c/o Life Technologies, Carlsbad, CA) containing heat-inactivated fetal bovine serum (5% (v/v); Gibco c/o Life Technologies, Carls-

bad, CA), penicillin (100 U/ml; CellGro, Manassas, VA), streptomycin (100 mg/ml; Gibco c/o Life Technologies, Carlsbad, CA), L-glutamine (2.0 mM; CellGro, Manassas, VA), and Hepes (20 mM; CellGro, Manassas, VA)] at room temperature for 5 min, after which time the medium was removed by aspiration. This step was repeated once, and the colonic tissue fragments were digested by placing in 10 ml of complete RPMI supplemented with collagenase type VIII (0.3 mg/ml) (Sigma-Aldrich, St. Louis, MO) and dispase (0.075 U/ml) (BD Biosciences, San Jose, CA) for 60 min at 37°C with shaking at 180 rpm. Tissue fragments were vortexed and then allowed to settle briefly, and the supernatant was collected by passing through a cell strainer (BD Falcon, Franklin Lakes, NJ; 100-µm pore diameter); an equal volume of complete RPMI with EDTA (5 mM) was used to wash the strainer and added to the harvested cell suspension to ensure that digestion was terminated. Cells were pelleted by centrifugation at 453g, the supernatant was discarded, the pellet was resuspended by flicking, and cells were stored on ice in 10 to 20 ml of HBSS/0.1% BSA. The colonic tissue fragments that remained from this initial round of digestion were subjected to an identical second round of digestion, and the resulting cells were pooled with those from the first digestion. No Percoll enrichment step was performed.

Cell re-stimulation — Intracellular cytokine staining was performed on cell suspensions from the spleen, MLN and colonic lamina propria following restimulation in round bottom 96 well plates in complete RPMI containing β-mercaptoethanol (0.05 mM; Sigma-Aldrich, St. Louis, MO) supplemented with 50 ng/ml phorbol-myrisotol-acetate (Sigma-Aldrich, St. Louis, MO), 750 ng/ml ionomycin (Sigma-Aldrich, St. Louis, MO) and Brefeldin A (eBioscience, San Diego, CA) diluted as per manufacturers recommendations. Cells were restimulated at 37°C for 3 h in a CO_2 humidified tissue culture incubator.

Flow cytometry — Cells were washed of re-stimulation media using HBSS. Cells were first incubated in HBSS containing anti-CD16/CD32 [Fc block (2.4G2); BD Pharmingen, San Jose, CA] and Live/Dead Fixable Aqua Dead Cell Stain (Life Technologies, Carlsbad, CA) at 4°C for 30 min. Cells were pelleted by centrifugation at 453g for 5 min (4°C). The resulting supernatant was discarded, and the pelleted cells were surface-stained (with anti-CD4, TCR-β) by resuspend-

ing in HBSS/0.1% BSA containing the indicated cocktail of fluorophore-conjugated antibodies. Cells were stored at 4°C in the dark for 20 min and were then washed by adding 200 µl of HBSS/ 0.1% BSA followed by centrifugation at 453g for 5 min. The supernatant was discarded, and the cell pellets were washed a second time with 250 ml of HBSS/0.1% BSA. Pellets were resuspended by vortexing and fixed in 100 ml of Fixation/Permeabilization Buffer (eBioscience, San Diego, CA). Cells were stored overnight at 4°C in the dark. For intracellular staining, 200 µl of HBSS/0.1% BSA was added, and the cells were centrifuged at 652g for 5 min. The supernatant was discarded, cells were resuspended by vortexing, and the step was repeated a second time. 100 µL of permeabilization buffer (eBioscience, San Diego, CA) supplemented with normal rat serum [Sigma-Aldrich, St. Louis, MO; 2% (v/v)] was added, and the cells were mixed by pipetting, placed in the dark for 60 min at 4°C, and centrifuged at 652g for 5 min; the resulting supernatant was discarded, and the cells were resuspended in permeabilization buffer containing anti-IL-17A or supplier-matched isotype control antibody. Cells were subsequently mixed by pipetting and stored at 4°C for 30 min (or room temperature for 20 min). Cells were washed by addition of 200 µl of permeabilization buffer and centrifuged at 652g for 5 min; the supernatant was discarded, and the cells were resuspended by vortexing. This wash step was repeated twice: first with permeabilization buffer and subsequently with HBSS/0.1% BSA. Cells were then resuspended in HBSS/0.1% BSA and analyzed with an Aria III flow cytometer (BD Biosciences, San Jose, CA). Data were analyzed with FlowJo software. The following antibodies were used: CD4 eFluor 450 (GK1.5; eBioscience, San Diego, CA), CD8a allophycocyanin (53-6.7; eBioscience, San Diego, CA), IL-17A phycoerythrin (TC11-18H10.1; Biolegend, San Diego, CA), TCR-β Alexa Fluor 488 (H57-597; Biolegend, San Diego, CA).

Mass spectrometry

Amino acids, acylcarnitines, organic acids, acyl CoAs, and ceramides were analyzed using stable isotope dilution techniques. Amino acids and acylcarnitine measurements were made by flow injection tandem mass spectrometry using sample preparation methods described previously (*68*, *69*). The data were acquired using a Waters Acquity UPLC system (Waters, Milford, MA) equipped

with a TQ (triple quadrupole) detector and a data system controlled by MassLynx 4.1 operating system (Waters, Milford, MA). Organic acids were quantified using methods described previously (*70*) employing Trace Ultra GC coupled to ISQ MS operating under Xcalibur 2.2 (Thermo Fisher Scientific, Austin, TX). Acyl-CoAs were extracted and purified as described previously (*71-73*), and analyzed by flow injection analysis using positive electrospray ionization on Xevo TQ-S, triple quadrupole mass spectrometer (Waters, Milford, MA). Heptadecanoyl CoA was employed as an internal standard. Ceramides were extracted as described previously (*74*) and analyzed by flow injection tandem mass spectrometry using a Xevo TQS spectrometer (Waters, Milford, MA) for precursors of *m*/*z* 264.

REFERENCES

1. P. Katona, J. Katona-Apte, The interaction between nutrition and infection, *CLIN INFECT DIS* **46**, 1582–1588 (2008).

2. D. You, G. Jones, T. Wardlaw, Levels and Trends in Child Mortality, (2011).

3. M. Smith *et al.*, Gut microbiomes of Malawian twin pairs discordant for kwashiorkor, *Science* **339**, 548–554 (2013).

4. A. L. Kau *et al.*, Functional characterization of IgA-targeted bacterial taxa from undernourished Malawian children that produce diet-dependent enteropathy, *Science Translational Medicine* **7**, 276ra24–276ra24 (2015).

5. T. Yatsunenko *et al.*, Human gut microbiome viewed across age and geography, *Nature* (2012), doi:10.1038/nature11053.

6. S. Subramanian *et al.*, Persistent gut microbiota immaturity in malnourished Bangladeshi children, *Nature* (2014).

7. G. T. Keusch et al., Environmental Enteric Dysfunction: Pathogenesis, Diagnosis, and Clinical Consequences, CLIN INFECT DIS 59, S207–S212 (2014).

8. The MAL-ED Network Investigators *et al.*, The MAL-ED Study: A Multinational and Multidisciplinary Approach to Understand the Relationship Between Enteric Pathogens, Malnutrition, Gut Physiology, Physical Growth, Cognitive Development, and Immune Responses in Infants and Children Up to 2 Years of Age in Resource-Poor Environments, *CLIN INFECT DIS* **59**, S193–S206 (2014).

9. L. V. Hooper, J. I. Gordon, Commensal host-bacterial relationships in the gut, *Science* **292**, 1115–1118 (2001).

10. S. K. Mazmanian, J. L. Round, D. L. Kasper, A microbial symbiosis factor prevents intestinal inflammatory disease, *Nature* **453**, 620–625 (2008).

11. A. Hsiao *et al.*, Members of the human gut microbiota involved in recovery from Vibrio cholerae infection, *Nature* **515**, 423–426 (2014).

12. P. Pathela *et al.*, Enterotoxigenic Bacteroides fragilis: Associated Diarrhea in Children 0-2 Years of Age in Rural Bangladesh, *The Journal of Infectious Diseases* **191**, 1245–1252 (2005).

13. C. Sears, Enterotoxigenic Bacteroides fragilis: a rogue among symbiotes, *Clinical Microbiology Reviews* **22**, 349–369 (2009).

14. C. L. Sears, The toxins of Bacteroides fragilis, *Toxicon* **39**, 1737–1746 (2001).

15. G. E. Hutchinson, Concluding Remarks, *Cold Spring Harbor Symposia on Quantitative Biology* **22**, 415–427 (1957).

16. J. Chase, M. Leibold, *Ecological Niches* (University of Chicago Press, 2003).

17. D. Mondal *et al.*, Contribution of Enteric Infection, Altered Intestinal Barrier Function, and Maternal Malnutrition to Infant Malnutrition in Bangladesh, *CLIN INFECT DIS* **54**, 185–192 (2012).

18. World Health Organization, U. N. C. Fund, World Health Organization Department of Nutrition for Health and Development. WHO child growth standards growth velocity based on weight, length and head circumference: methods and development, *World Health Organization*, 1–262 (2009).

19. J. Arsenault *et al.*, The current high prevalence of dietary zinc inadequacy among children and women in rural Bangladesh could be substantially ameliorated by zinc biofortification of rice, *The Journal of nutrition* **140**, 1683 (2010).

20. S. N. Islam, N. I. Khan, Akhtaruzzaman, A Food Composition Database for Bangladesh with Special reference to Selected Ethnic Foods,, 1–118 (2010).

21. U. D. O. Agriculture, A. R. Service, N. D. Lab, USDA National Nutrient Database for Standard Reference, Release 27, 1–154 (2015).

22. A. L. Goodman *et al.*, Extensive personal human gut microbiota culture collections characterized and manipulated in gnotobiotic mice, *Proceedings of the National Academy of Sciences*, 1–6 (2011).

23. N. Dey, V. Wagner, J. I. Gordon, Regulators of gut motility revealed by a gnotobiotic mouse model of human travel-related diet changes, *Cell*.

24. A. S. S. d'Abusco, M. Del Grosso, S. Censini, A. Covacci, A. Pantosti, The alleles of the bft gene are distributed differently among enterotoxigenic Bacteroides fragilis strains from human sources and can be present in double copies, *Journal of Clinical Microbiology* **38**, 607–612 (2000).

25. N. P. McNulty *et al.*, The impact of a consortium of fermented milk strains on the gut microbiome of gnotobiotic mice and monozygotic twins, *Science Translational Medicine* **3**, 106ra106–106ra106 (2011).

26. M. De Cáceres, P. Legendre, Associations between species and groups of sites: indices and statistical inference, *Ecology* **90**, 3566–3574 (2009).

27. M. De Cáceres, D. Sol, O. Lapiedra, P. Legendre, A framework for estimating niche metrics using the resemblance between qualitative resources, *Oikos* **120**, 1341–1350 (2011).

28. M. De Cáceres, P. Legendre, S. K. Wiser, L. Brotons, R. B. O'Hara, Ed. Using species combinations in indicator value analyses, *Methods Ecol Evol* **3**, 973–982 (2012).

29. R. A. H. Ph. D, R. A. Harvey, D. R. Ferrier, *Biochemistry* (Lippincott Williams & Wilkins, 2011).

30. S. Eaton, Control of mitochondrial b-oxidation flux, *Progress in Lipid Research*, 1–43 (2002).

31. L. Khan, M. S. Bamji, Plasma carnitine levels in children with protein-calorie malnutrition before and after rehabilitation, *Clin. Chim. Acta* **75**, 163–166 (1977).

32. C. J. Rebouche, E. P. Bosch, C. A. Chenard, K. J. Schabold, S. E. Nelson, Utilization of dietary precursors for carnitine synthesis in human adults, *The Journal of nutrition* **119**, 1907–1913 (1989).

33. Y. A. Hannun, Functions of ceramide in coordinating cellular responses to stress, *Science* **274**, 1855–1859 (1996).

34. M. I. Pörn-Ares, S. C. Chow, J. P. Slotte, S. Orrenius, Induction of apoptosis and potentiation of TNF- and Fas-mediated apoptosis in U937 cells by the xanthogenate compound D609, *Exp Cell Res* **235**, 48–54 (1997).

35. S. Fukuda *et al.*, Bifidobacteria can protect from enteropathogenic infection through production of acetate, *Nature* **469**, 543–547 (2011).

36. S. Wu *et al.*, A human colonic commensal promotes colon tumorigenesis via activation of T helper type 17 T cell responses, *Nature Medicine* **15**, 1016–1022 (2009).

37. L. L. Myers, D. S. Shoop, J. E. Collins, W. C. Bradbury, Diarrheal disease caused by enterotoxigenic Bacteroides fragilis in infant rabbits, *Journal of Clinical Microbiology* **27**, 2025–2030 (1989).

38. R. J. Obiso, A. O. Azghani, T. D. Wilkins, The Bacteroides fragilis toxin fragilysin disrupts the paracellular barrier of epithelial cells, *Infection and Immunity* **65**, 1431–1439 (1997).

39. K. J. Rhee *et al.*, Induction of Persistent Colitis by a Human Commensal, Enterotoxigenic Bacteroides fragilis, in Wild-Type C57BL/6 Mice, *Infection and Immunity* **77**, 1708–1718 (2009).

40. A. Pantosti *et al.*, Detection of enterotoxigenic Bacteroides fragilis and its toxin in stool samples from adults and children in Italy, *CLIN INFECT DIS* **24**, 12–16 (1997).

41. J. A. Thompson, R. A. Oliveira, A. Djukovic, C. Ubeda, K. B. Xavier, Manipulation of the Quorum Sensing Signal AI-2 Affects the Antibiotic-Treated Gut Microbiota, *CellReports* **10**, 1861–1871 (2015).

42. A. Battesti, N. Majdalani, S. Gottesman, The RpoS-Mediated General Stress Response in Escherichia coli*, *Annu Rev Microbiol* **65**, 189–213 (2011).

43. D. HAGIWARA, T. YAMASHINO, T. MIZUNO, A Genome-Wide View of the Escherichia coliBasS–BasR Two-component System Implicated in Iron-responses, *Bioscience, Biotechnology and Biochemistry* **68**, 1758–1767 (2014).

44. T. Dong, M. G. Kirchhof, H. E. Schellhorn, RpoS regulation of gene expression during exponential growth of Escherichia coli K12, *Mol Genet Genomics* **279**, 267–277 (2007).

45. S. Mills *et al.*, Movers and shakers, *gutmicrobes* **4**, 4–16 (2014).

46. F. Harrison, J. Paul, R. C. Massey, A. Buckling, Interspecific competition and siderophore-mediated cooperation in Pseudomonas aeruginosa, *The ISME Journal* **2**, 49–55 (2007).

47. A. Trejo-Hernández, A. Andrade-Domínguez, M. Hernández, S. Encarnación, Interspecies competition triggers virulence and mutability in Candida albicans-Pseudomonas aeruginosa mixed biofilms, *The ISME Journal* **8**, 1974–1988 (2014).

48. N. Kato *et al.*, Prevalence of enterotoxigenic Bacteroides fragilis in children with diarrhea in Japan, *Journal of Clinical Microbiology* **37**, 801–803 (1999).

49. S. Kurtz *et al.*, Versatile and open software for comparing large genomes, *Genome Biology* ... **5**, R12 (2004).

50. V. Ridaura *et al.*, Gut microbiota from twins discordant for obesity modulate metabolism in mice, *Science* **341**, 1241214 (2013).

51. B. Chevreux, T. Wetter, S. Suhai, Genome Sequence Assembly Using Trace Signals and Additional Sequence Information, *German Conference on Bioinformatics* (1999).

52. T. Seemann, Prokka: rapid prokaryotic genome annotation, *Bioinformatics* **30**, 2068–2069 (2014).

53. M. Kanehisa, S. Goto, KEGG: kyoto encyclopedia of genes and genomes, *Nucleic Acids Research* **28**, 27–30 (2000).

54. M. Kanehisa *et al.*, Data, information, knowledge and principle: back to metabolism in KEGG, *Nucleic Acids Research* **42**, D199–D205 (2014).

55. A. A. Salyers, G. Bonheyo, N. B. Shoemaker, Starting a New Genetic System: Lessons from Bacteroides, *Methods* **20**, 35–46 (2000).

56. D. G. Gibson *et al.*, Enzymatic assembly of DNA molecules up to several hundred kilobases, *Nature Publishing Group* **6**, 343–345 (2009).

57. N. B. Shoemaker, C. Getty, J. F. Gardner, Tn4351 transposes in Bacteroides spp. and mediates the integration of plasmid R751 into the Bacteroides chromosome, ... *of bacteriology* (1986).

58. D. G. Guiney, P. Hasegawa, C. E. Davis, Plasmid transfer from Escherichia coli to Bacteroides fragilis: differential expression of antibiotic resistance phenotypes, *Proc Natl Acad Sci U S A* **81**, 7203–7206 (1984).

59. P. J. Turnbaugh *et al.*, A core gut microbiome in obese and lean twins, *Nature* **457**, 480–484 (2009).

60. R. Schmieder, R. Edwards, Quality control and preprocessing of metagenomic datasets, *Bioinformatics* **27**, 863–864 (2011).

61. T. Magoč, S. L. Salzberg, FLASH: fast length adjustment of short reads to improve genome assemblies, *Bioinformatics* **27**, 2957–2963 (2011).

62. J. Caporaso, C. Lauber, W. Walters, Global patterns of 16S rRNA diversity at a depth of millions of sequences per sample, *Proceedings of the ...* (2010).

63. J. G. Caporaso *et al.*, correspondence, *Nature Publishing Group* **7**, 335–336 (2010).

64. T. Z. DeSantis *et al.*, Greengenes, a chimera-checked 16S rRNA gene database and workbench compatible with ARB, *Applied and Environmental Microbiology* **72**, 5069–5072 (2006).

65. J. Faith, N. McNulty, F. Rey, J. Gordon, Predicting a Human Gut Microbiota's Response to Diet in Gnotobiotic Mice, *Science* **333**, 101 (2011).

66. F. Rey *et al.*, Dissecting the in vivo metabolic potential of two human gut acetogens, *Journal of Biological Chemistry* (2010).

67. J. J. Faith, P. P. Ahern, V. K. Ridaura, J. Cheng, J. I. Gordon, Identifying gut microbe-host phenotype relationships using combinatorial communities in gnotobiotic mice, *Science Translational Medicine* **6**, 220ra11 (2014).

68. J. An *et al.*, Hepatic expression of malonyl-CoA decarboxylase reverses muscle, liver and whole-animal insulin resistance, *Nature Medicine* **10**, 268–274 (2004).

69. C. T. Ferrara *et al.*, E. T. Dermitzakis, Ed. Genetic Networks of Liver Metabolism Revealed by Integration of Metabolic and Transcriptional Profiling, *PLoS Genetics* **4**, e1000034 (2008).

70. M. V. Jensen *et al.*, Compensatory responses to pyruvate carboxylase suppression in islet beta-cells. Preservation of glucose-stimulated insulin secretion, *J. Biol. Chem.* **281**, 22342–22351 (2006).

71. C. Magnes, F. M. Sinner, W. Regittnig, T. R. Pieber, LC/MS/MS Method for Quantitative Determination of Long-Chain Fatty Acyl-CoAs, *Anal. Chem.* **77**, 2889–2894 (2005).

72. J. Deutsch, E. Grange, S. I. Rapoport, A. D. Purdon, Isolation and quantitation of long-chain acyl-coenzyme A esters in brain tissue by solid-phase extraction, *Analytical Biochemistry* (1994).

73. P. E. Minkler, J. Kerner, S. T. Ingalls, C. L. Hoppel, Novel isolation procedure for short-, medium-, and long-chain acyl-coenzyme A esters from tissue, *Analytical Biochemistry* **376**, 275–276 (2008).

74. A. H. Merrill Jr, M. C. Sullards, J. C. Allegood, S. Kelly, E. Wang, Sphingolipidomics: High-throughput, structure-specific, and quantitative analysis of sphingolipids by liquid chromatography tandem mass spectrometry, *Methods* **36**, 207–224 (2005).

Acknowledgments: We thank David O'Donnell, Maria Karlsson, Sabrina Wagoner, and Justin Serugo for assistance with gnotobiotic husbandry, plus Marty Meier, Su Deng, and Jessica Hoisington-Lopez, for superb technical assistance; Ansel Hsiao, Mark Charbonneau, and Michael Barratt provided valuable insights during the course of this study. This study was supported by the Bill & Melinda Gates Foundation and the NIH (DK30292).

Author Contributions: V.E.W. and J.I.G. designed the experiments. R.H., T.A. and B.P. directed the clinical study design, enrollment, plus clinical data and sample collection for the Bangladeshi birth cohort. V.E.W., N.D., J.G., J.C., P.A., and O.I. performed experiments. V.E.W., N.D., A.H., S.S., J.C., P.A., O.I., C.N., and J.I.G. analyzed the data. V.E.W., N.D., and J.I.G. wrote the paper.

Competing financial interests: J.I.G. is co-founder of Matatu, Inc., a company characterizing the role of diet-by-microbiota interactions in health in animals. The other authors declare that they have no competing interests.

Data and Materials Availability: 16S rRNA datasets, whole genome shotgun sequencing datasets from cultured bacterial strains, microbial RNA-Seq datasets, and assembled contigs of bacterial strains are available through the European Nucleotide Archive (ENA Study Accession Number PRJEB9703).

FIGURE LEGENDS

Figure 1. Weight phenotypes are transmissible via transplantation of intact uncultured human fecal microbiota samples and derivative culture collections into germ-free mice. (**A)** In adult germ-free mice serially fed three embodiments of a Bangladeshi diet, transplantation of intact uncultured fecal microbiota from a severely stunted donor (red) was associated with significantly greater weight loss than a fecal microbiota from a donor with consistently healthy anthropometry (blue). (**B)** Mean relative abundances (± s.e.m.) of 97%ID OTUs representing ≥1% of the total community in mice receiving intact fecal microbiota. OTUs present at lower abundances are not shown and account for the proportion not represented in each stacked barplot. (**C**) Transplantation of culture collections (dashed lines) generated from the fecal microbiota of healthy (blue) or stunted/underweight (red) donors recapitulate the weight phenotype seen with the corresponding intact uncultured microbiota (solid lines). (**D)** Relative abundances of bacterial strains summarized by species (as determined by COPRO-Seq) representing ≥1% of the fecal communities of mice colonized with the culture collections derived from either the healthy or stunted donors. Taxa present at low abundances are not represented and account for the proportion not represented in each stacked barplot. (**E)** The weight-loss phenotype observed in recipients of the stunted/underweight donor's culture collection is robust to all three Bangladeshi diet embodiments. Significant weight differences were seen between mice colonized with culture collections produced from the stunted/unhealthy versus healthy donors in all three diet embodiment contexts (**F)** Out-of-bag (OOB) error rates of Random Forests models generated to predict the culture collection that was transplanted into mice or diet embodiment administered based on microbiota- or diet-discriminatory input OTU abundances, respectively. OOB error rates are high when predicting diet, suggesting that the three diet embodiments do not significantly differ in their impact on the microbiota. Statistical significance was determined using repeated measures ANOVA; *, $p<0.05$.

Figure 2. Enterotoxigenic *Bacteroides fragilis* (ETBF) is necessary but not alone sufficient for diet-induced weight loss. (**A.**)Schematic illustrating the different treatment groups (and numbers of mice per treatment group) generated by manipulating the presence/absence of ETBF and NTBF

within the stunted/underweight or healthy donors' culture collections. (**B)** Representation of cultured *Bacteroides* species in healthy and stunted culture collections ± ETBF ± NTBF. (**C)** Removal of ETBF prevents weight loss in mice colonized with the stunted/underweight donor's culture collection. In contrast, addition of ETBF with the simultaneous removal of NTBF does not significant impact weight in mice colonized with the culture collection derived from the healthy child. **D.** The liver ceramides C16, d18.1.C16, and d18.1.C24.1 are present at significantly higher levels in mice colonized with an ETBF(+) NTBF(–) stunted culture collection compared to an ETBF(–) NTBF(–) stunted culture collection. The former two (red font) remain significantly different in a comparison between mice that lost weight (i.e., those colonized with an ETBF(+) NTBF(–) stunted culture collection) and all other groups depicted in **(C)**.

Figure 3. Schematic depicting the various comparisons between treatment groups and the underlying experimental questions.

Figure 4. The effects of intra-specific NTBF-ETBF interactions on community structure and gene expression. All mice in all treatment groups were monotonously fed diet embodiment 2. Cecal samples collected at the time of sacrifice 14 days after initial colonization were analyzed by COPRO-Seq and microbial RNA-Seq. (**B)** Differential expression of selected genes by members of the transplanted healthy culture collection ± ETBF ± NTBF. The loci depicted comprise the set of loci with the listed putative functions differentially expressed between two versions of the healthy donor's culture collection: ETBF(–) NTBF(+) and ETBF(+) NTBF(–). Loci that are also expressed in the meta-transcriptome of the stunted culture collection are denoted by an asterisk (*). No VF database genes showed significant differences in their expression in mice colonized with the stunted/underweight donor's culture collection ± ETBF. Strains are color-coded on the left; UniProt database annotations shown on the right.

Figure 5. Changes in the ETBF transcriptome between different community contexts. A. Volcano plot illustrating pathways represented by differentially expressed ETBF genes in the context of being in the transplanted healthy donor's (upper right) or stunted/underweight (upper left)

donors culture collections. RNA-Seq datasets were generated from cecal samples obtained from mice that had been monotonously fed the Bangladeshi diet embodiment 2 (*n*=5 mice/treatment group). The x-axis represents $\log_2$(expression fold-difference) in mice colonized with manipulated ETBF(+) NTBF(–) healthy donor culture collection compared to the unmanipulated ETBF(+) NTBF(–) stunted/underweight donor culture collection; the y-axis represents $\log_{10}$(FDR-corrected *p*-value of the significance of the difference as determined by the exact negative binomial test). Purple dots indicate transcripts with Pfam and KEGG annotations; the associated numbers reference the superscripted numbers next to the corresponding annotation for that transcript in the heatmap shown in panel B. (**B**) Z-score normalized transcript levels (counts per million) of differentially expressed transcripts represented in panel **A** that are annotated in both the Pfam and KEGG databases. Each row represents a locus (with Pfam IDs listed in parentheses, and numerical superscript indicating the associated purple dots in panel **A)**. Each column represents a single mouse. Full Pfam and KEGG annotations are provided in **Table S7A**.

FIGURES

Figure 1.

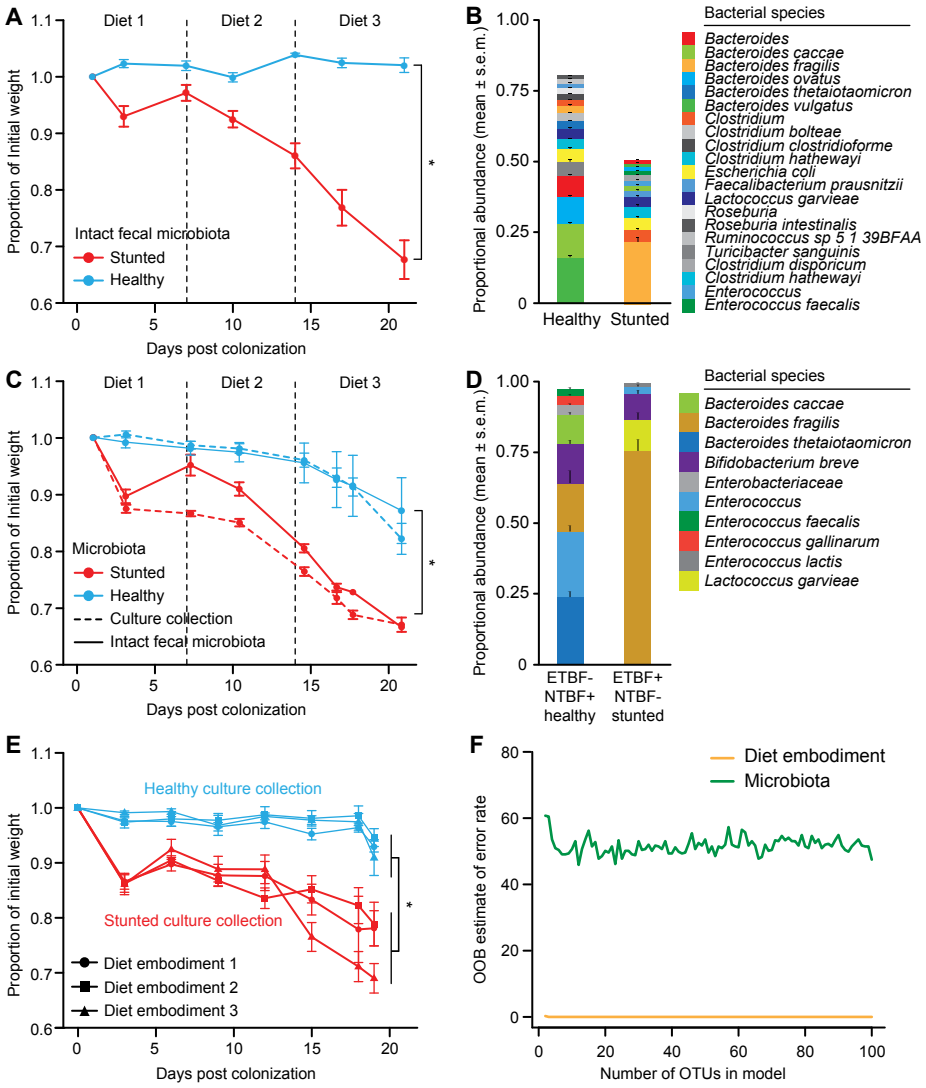

Figure 2.

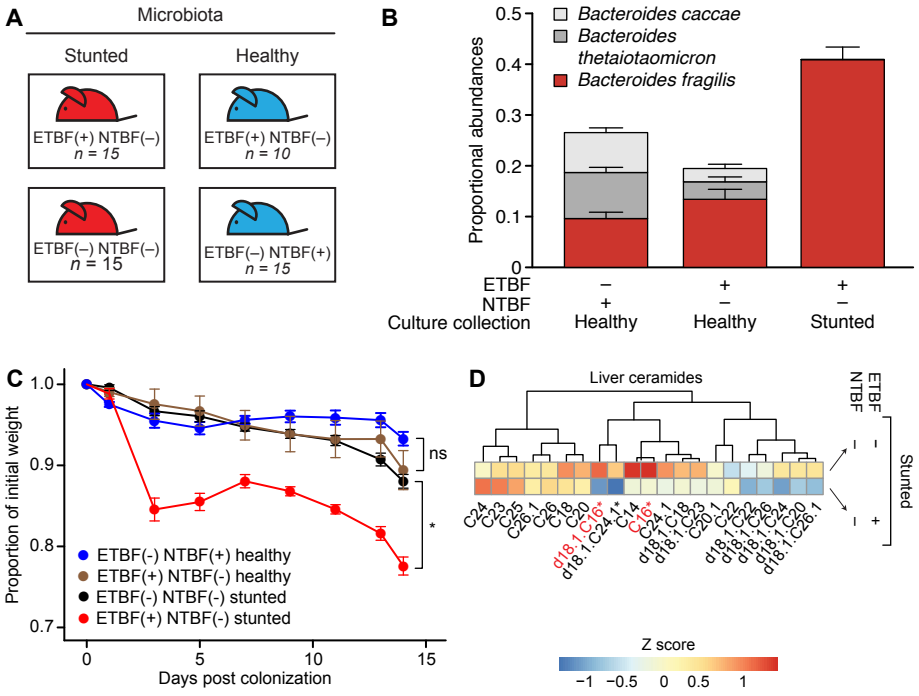

Figure 3.

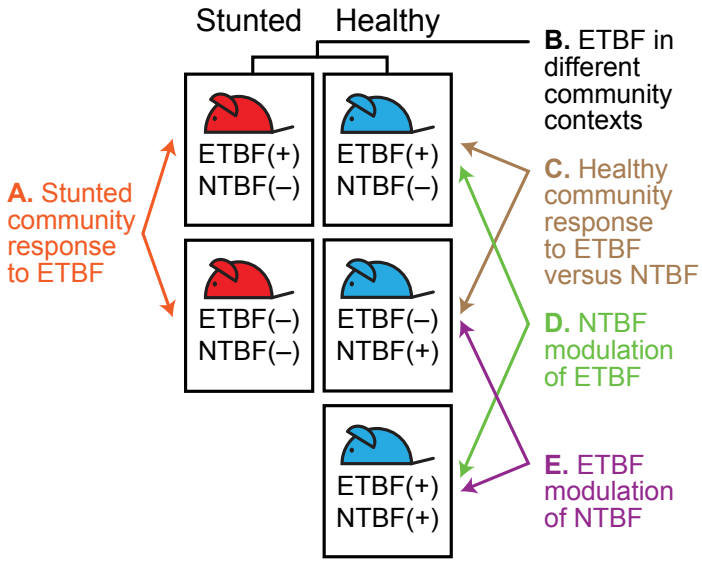

Figure 4.

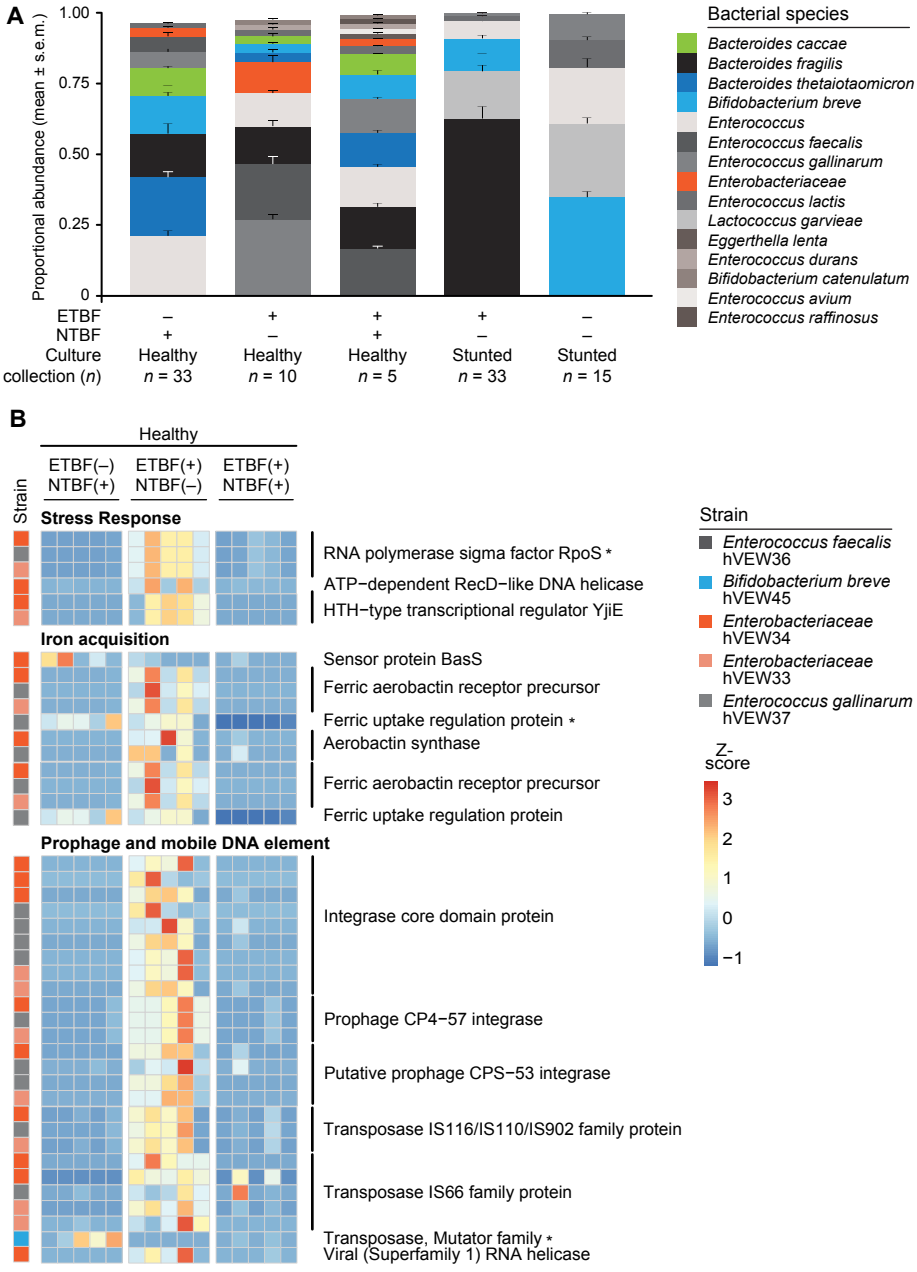

Figure 5.

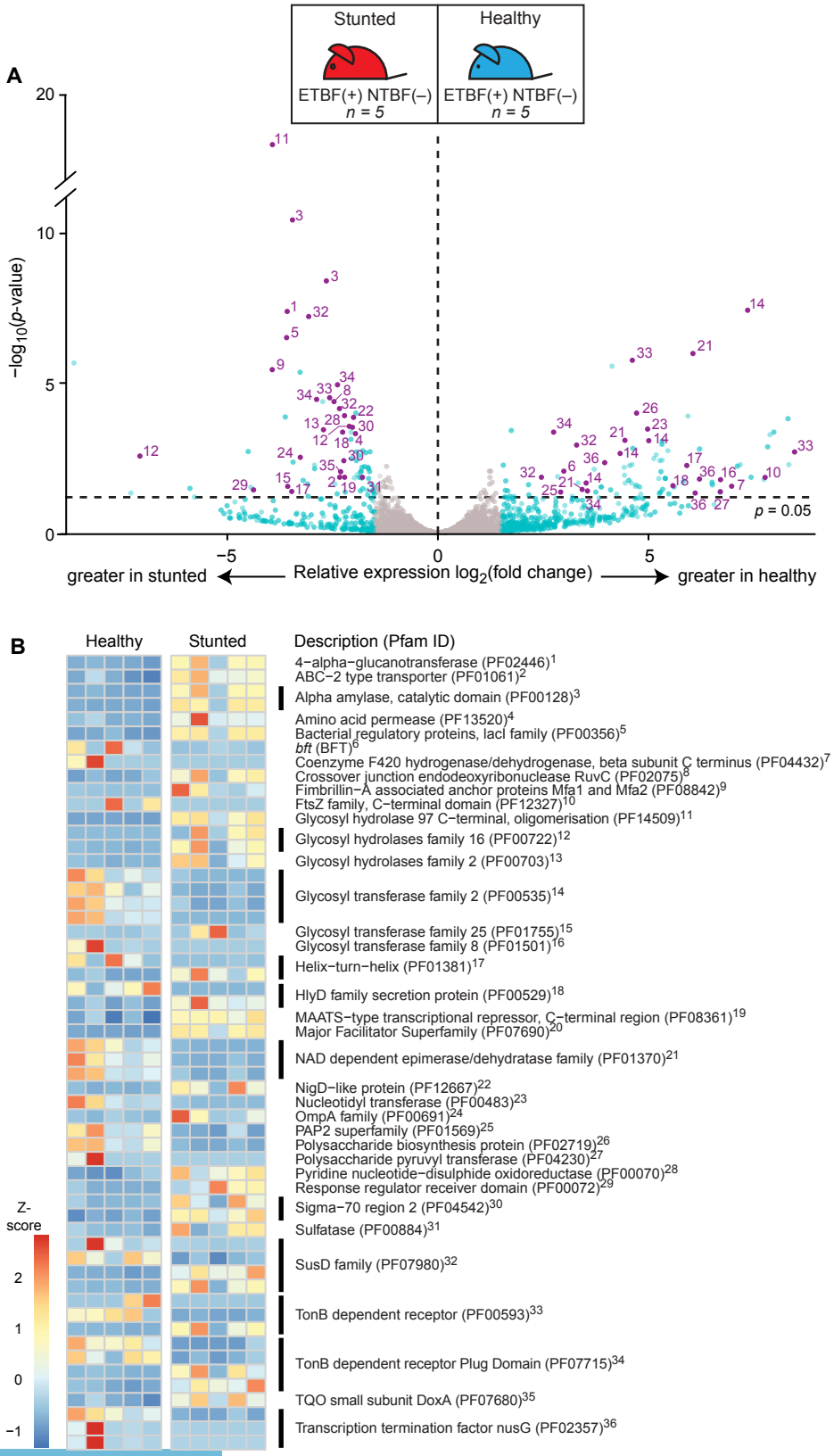

TABLE LEGENDS

Table 1. Summary of putative virulence factor (VF) representation, expression, and differential expression in the the cecal meta-transcriptomes of mice colonized with the stunted/ underweight donor's culture collection ± ETBF or with the healthy donor's culture collection ± ETBF. Mice were monotonously fed Bangladeshi diet embodiment 2. Virulence factors were defined as loci in the genomes of the indicated community members with BLAST hits (E-value $< 10^{-17}$) against the Virulence Factor database. Expressed VFs are defined as loci having non-zero counts after mapping RNA-Seq reads via bowtie to the custom database of genome sequences. Differentially expressed VFs were identified using a negative binomial exact test with FDR-correction.

SUPPLEMENTAL MATERIALS

SUPPLEMENTAL FIGURE LEGENDS

Figure S1. Experimental designs. (A) Schematic of experimental design of groups of adult gnotobiotic C57BL/6 mice (*n*=4-6 mice per group) colonized with either intact uncultured fecal microbiota or derivative culture collections. (**B)** Schematic of gnotobiotic experiments examining whether intergenerational transmission of intact uncultured fecal microbiota or derived culture collections from one generation of mice to another recapitulates the weight phenotype of the parental generation. **(C)** Test of whether weight-loss phenotype is robust to the three different Bangladesh diet embodiments. (**D**) Test of whether ETBF alone is not sufficient to induce weight loss.

Figure S2. Relative abundances of the ETBF and NTBF strains plus other *Bacteroides* in the fecal microbiota of gnotobiotic mice a function of donor community. (A) *Bacteroides* species relative abundances (mean ± s.e.m.) in mice colonized with the intact fecal microbiota from two human donors. V4-16S rRNA analyses were performed on fecal samples collected at the time of sacrifice when mice were consuming diet embodiment 3 after animals had be subjected to a sequence of weekly exposures to embodiments 1, 2 and finally 3. *B. fragilis* is the most abundant *Bacteroides* species in mice harboring the transplanted intact uncultured fecal microbiota from the stunted/underweight donor. (**B)** *B. fragilis* abundances are inversely proportional to mouse weights. Green, groups of mice colonized with intact uncultured fecal microbiota from the two donors; orange, groups of mice colonized with the two derived unmanipulated culture collections. Data for mice harboring the uncultured communities were generated from fecal samples collected at sacrifice while mice were on embodiment 3, having completed the sequence of being fed all three embodiments, while data for mice with culture communities was generated from fecal samples collected after two weeks of monotonous consumption of embodiment 2. (**C)** While *B. fragilis* strain abundances (one ETBF strain highlighted in red, two NTBF strains highlighted in blue) distinguish culture collections derived from healthy versus stunted donors, indicator species analysis discloses that they are not specific for diet embodiment. The heatmap on the left shows

relative abundances of all strains in mice colonized with these culture collections; the heatmap on the right represents indicator scores for each strain in a given diet embodiment setting.

Figure S3. Transfer of 97%ID OTUs present in the intact uncultured human donor microbiota from one generation of recipient mice to another. Heatmap: rows plot the Z-score normalized relative abundances in the fecal microbiota of recipient; each column represents one mouse. Data were by V4-16S rRNA analysis of fecal samples collected at sacrifice after mice had completed the sequence of exposure to all three diet embodiments. *Bacteroides* species are highlighted in orange.

Figure S4. Mass spectrometry-based analyses of metabolism in mice harboring the unmanipulated and manipulated healthy donor or stunted/underweight donor culture collections. Analyses were performed on the indicated biospecimens obtained at sacrifice after 2 weeks of consumption of diet embodiment 2. Z-score normalized peak intensities or concentrations are given for **(A)** organic acids, **(B)** amino acids, **(C)** acyl-CoA metabolites, and **(D)** acylcarnitines in selected organs (liver, gastrocnemius, or serum).

Figure S5. The effect of ETBF on the representation of $Th17^+$ and regulatory T cell ($FoxP3^+$) cells in the colon or mesenteric lymph notes of mice colonized with four different types of culture collections. (**A)** Representative flow cytometry plots showing IL-17A expression in CD4+ T cells isolated from the colonic lamina propria of mice containing the indicated culture collections. The percentages shown represent frequency in the gate. (**B**) Colonic $Th17^+$ $CD4^+$ T cell populations are increased in mice colonized with ETBF in the context of both the healthy and stunted/underweight donors' culture collections. (**C)** $FoxP3^+$ $CD4^+$ regulatory T cells from mesenteric lymph nodes

Figure S6. Differentially expressed ETBF genes in healthy versus stunted microbial community contexts. (A) Changes in the expression of SusC and SusD paralogs present in two PULs. (**B.)** Changes in the expression of genes present in two of its capsular polysaccharide biosynthesis (CPS) loci. (**C**) Changes in the expression of fragilysin when ETBF is colonized in healthy donor-derived culture collection ±NTBF; expression levels in the context of the manipulated versions of

the healthy donor's culture collection were normalized to levels in mice colonized with the unmanipulated stunted donor's culture collection.

Figure S7. Multiple pathways represented in the NTBF transcriptome are altered by ETBF. **(A)** Volcano plot illustrating pathways represented by differentially expressed NTBF genes in the cecal microbiota of mice that had received two versions of the healthy donor's culture collection: ETBF(+) NTBF(+) (upper right) or ETBF(–) NTBF(+) (upper left). The x-axis represents $\log_2$(expression fold-difference) between ETBF(+) NTBF(+) versus ETBF(–) NTBF(+) with the latter serving as the reference; the y-axis represents $\log_{10}$(FDR-corrected *p*-value of the significance of the difference as determined by the exact negative binomial test). Purple dots indicate transcripts with Pfam and KEGG annotations, with associated numbers indicating the annotation listed in superscript in panel B. (**B)** Z-score normalized transcript levels (counts per million) of differentially expressed transcripts represented in panel A that have both Pfam and KEGG annotations. Each row represents a transcript, with Pfam IDs listed in parentheses, and numerical superscript indicating the associated purple dot in panel A. Each column represents a single mouse. Full Pfam and KEGG annotations are given in **Table S7C**.

Figure S8. Effects of ETBF in lieu of NTBF on *Bacteroides thetaiotaomicron* gene expression in the context of the healthy donor's culture collection. . (A) Volcano plot illustrating differentially expressed loci in the *B. thetaiotaomicron* strain genomes in the context of an ETBF(+) NTBF(–) (upper right) or ETBF(–) NTBF(+) (upper left) healthy donor culture collection. Data were generated from cecal contents obtained from mice after 14 days of consumption of diet embodiment 2. The x-axis represents $\log_2$(expression fold-change) in mice colonized with ETBF(+) NTBF(+) compared to the ETBF(–) NTBF(+) healthy culture collection as the reference; the y-axis represents $\log_{10}$(FDR-corrected *p*-value of the significance of the difference as determined by the exact negative binomial test). (**B)** Z-score normalized transcript levels (counts per million) of differentially expressed genes represented in panel A with assigned both Pfam and KEGG annotations.

Figure S9. Effects of ETBF in lieu of NTBF on *Bacteroides caccae* gene expression in the context of the healthy donor's culture collection. (A) Volcano plot. (**B)** Heatmap.

Figure S10. Schematic of the *bft* locus and cloning strategy to generate the *bft* knockout of the isolated ETBF. (A) The *bft* locus with the flanking regions of the *B. fragilis* mVEW4 genome. **(B)** The pGERM suicide-vector mediated mutagenesis strategy used to disrupt expression of complete *bft* gene sequence.

SUPPLEMENTAL FIGURES

Figure S1.

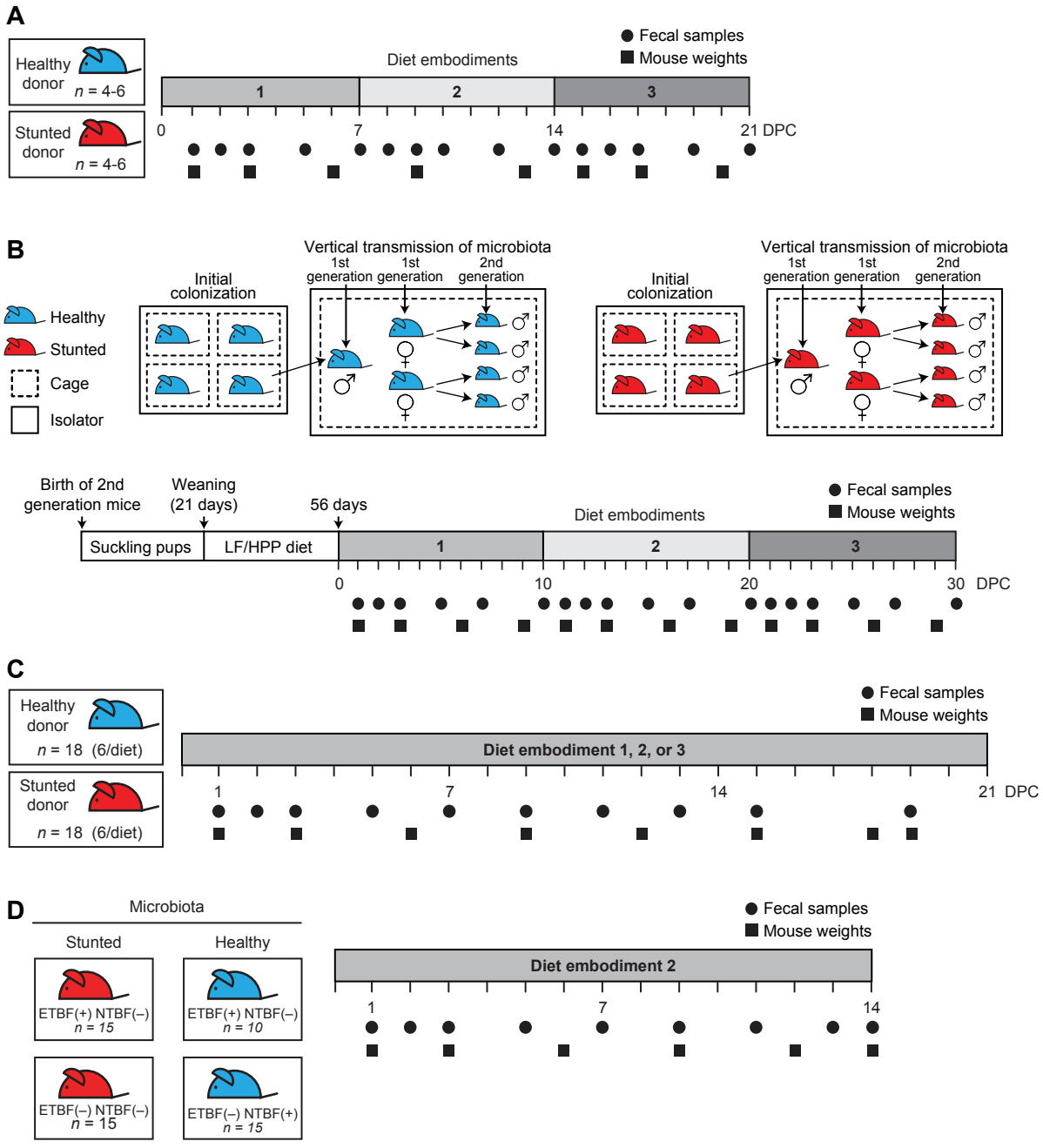

Figure S2.

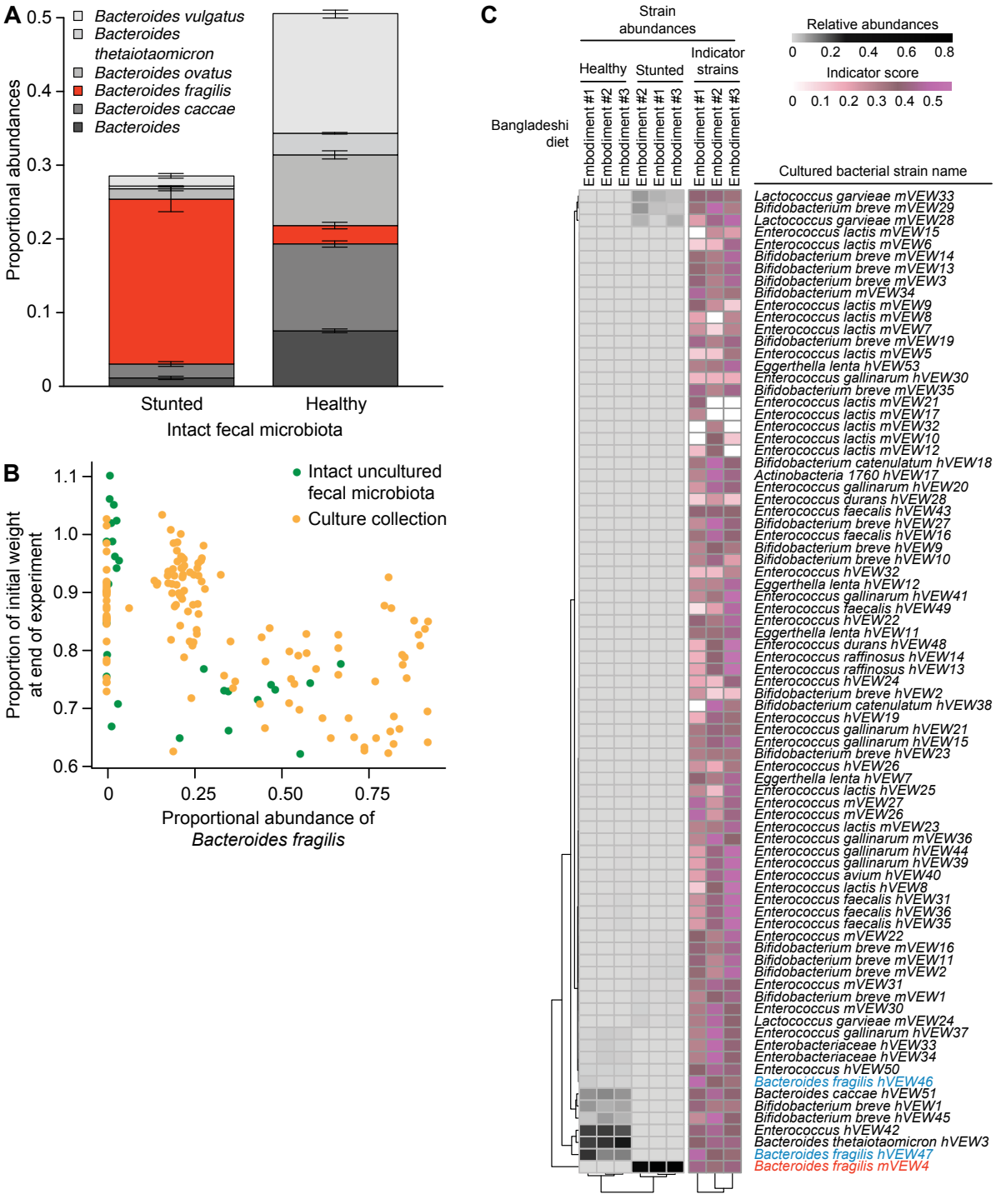

Figure S3.

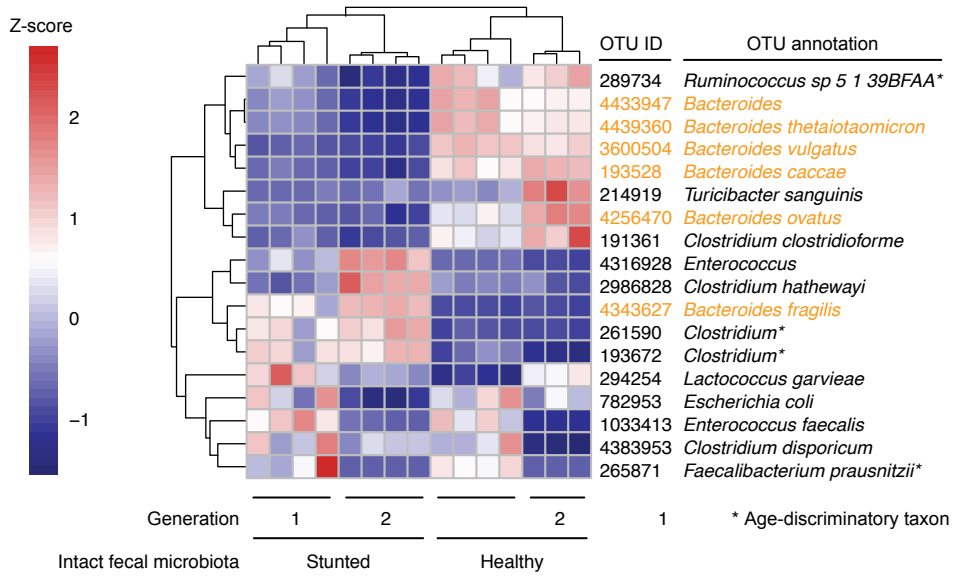

Figure S4.

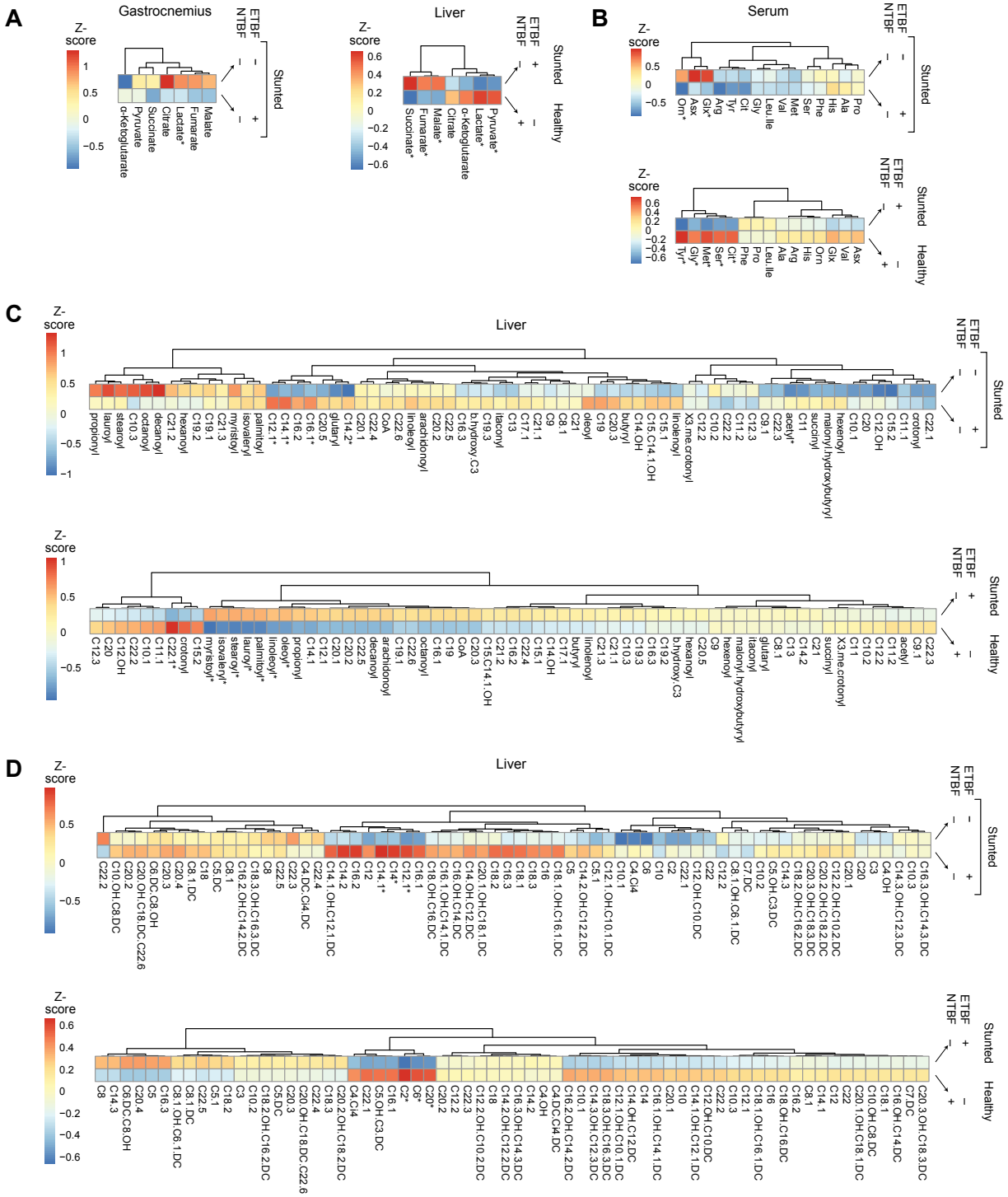

Figure S5.

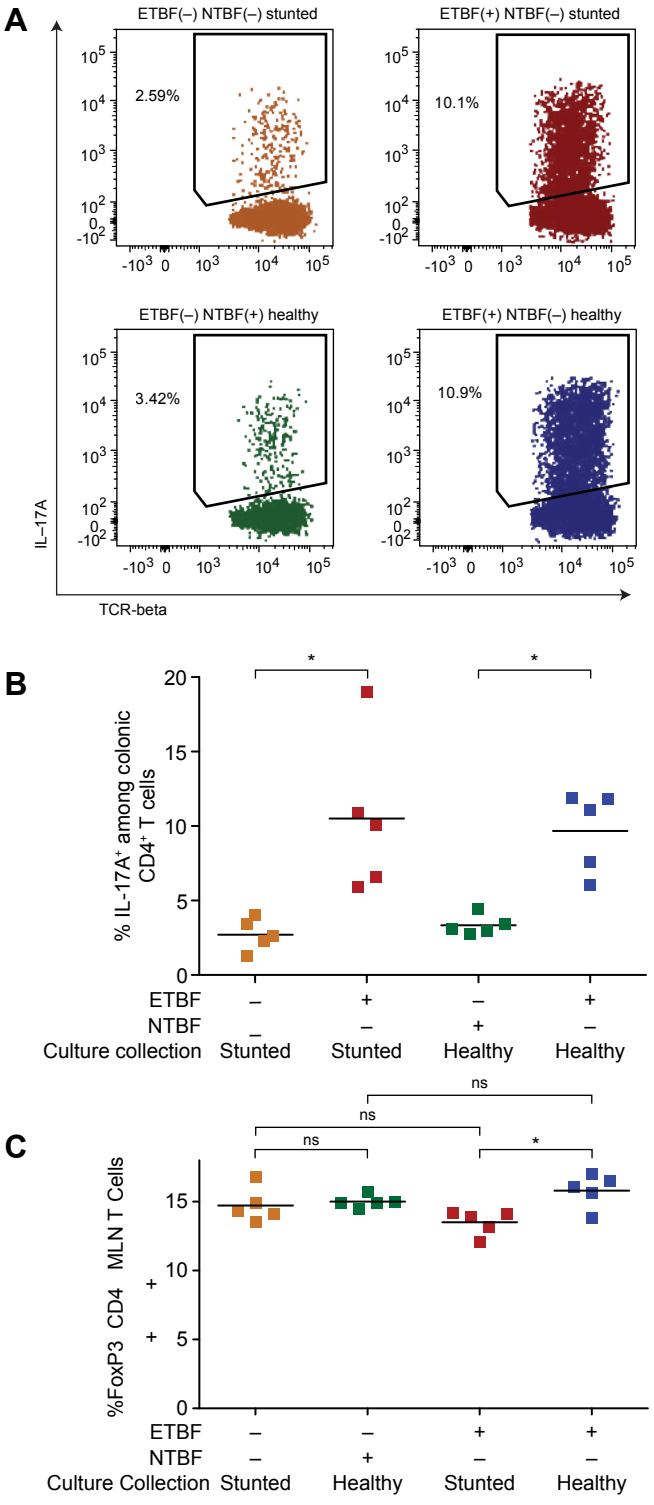

Figure S6.

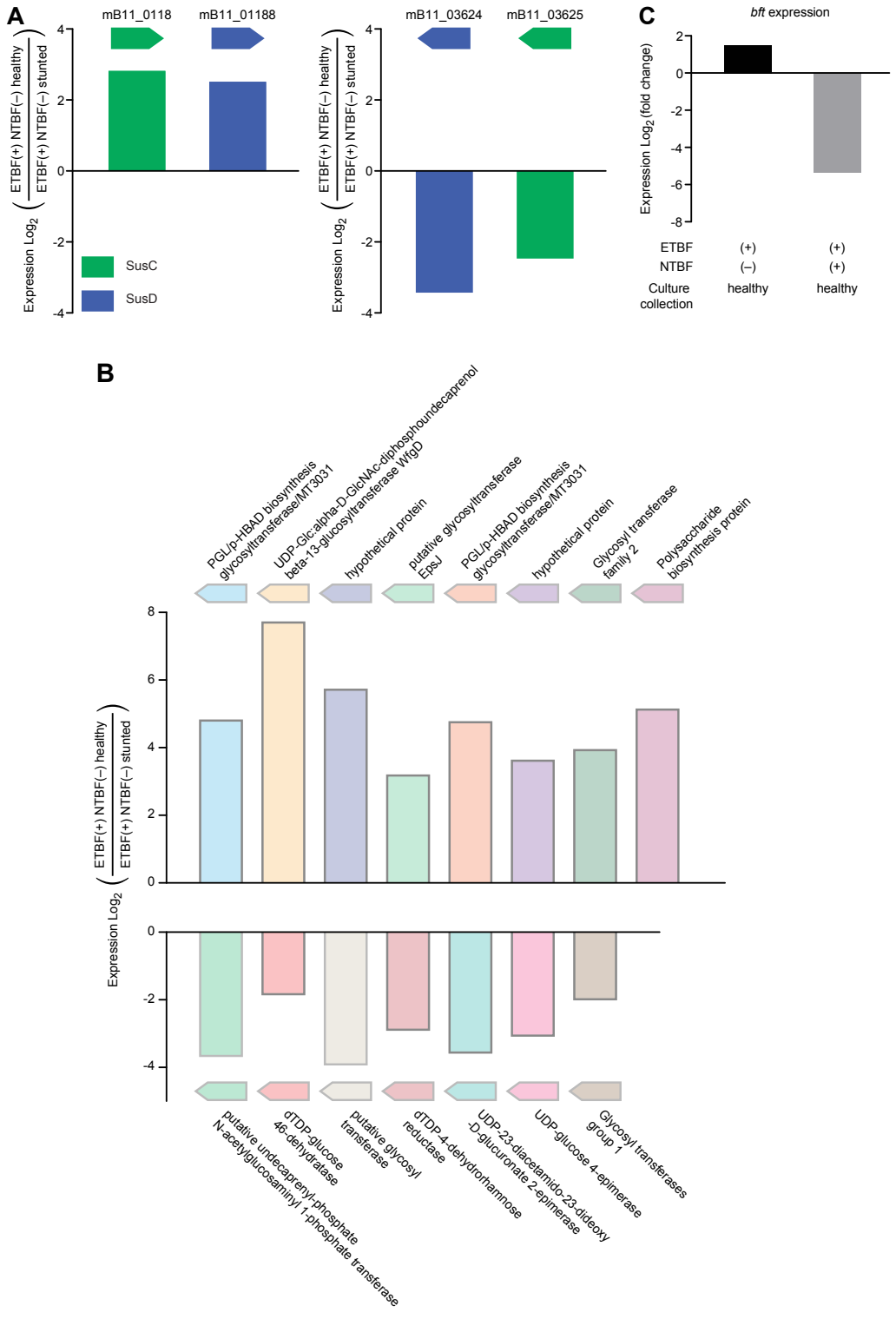

Figure S7A.

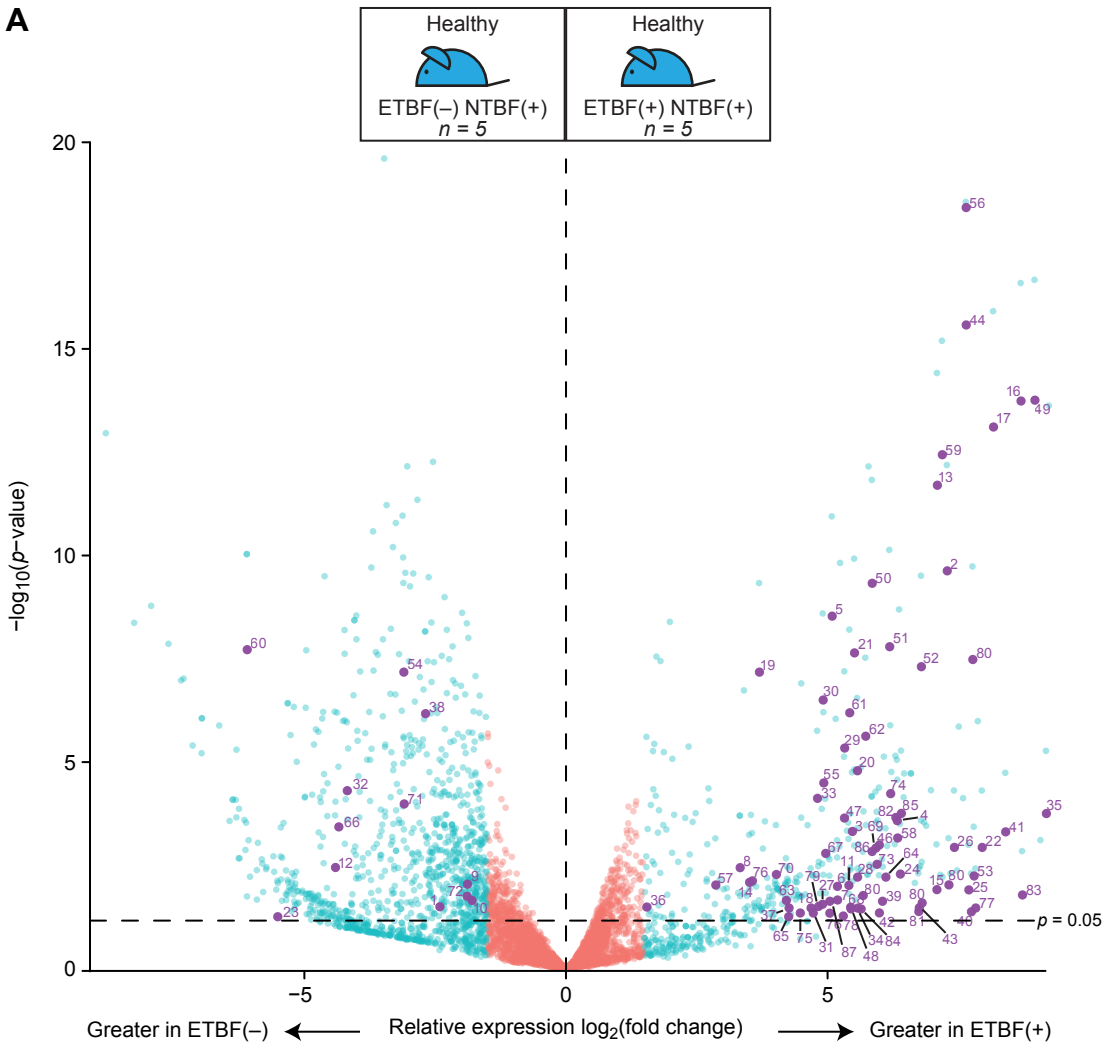

Figure S7B.

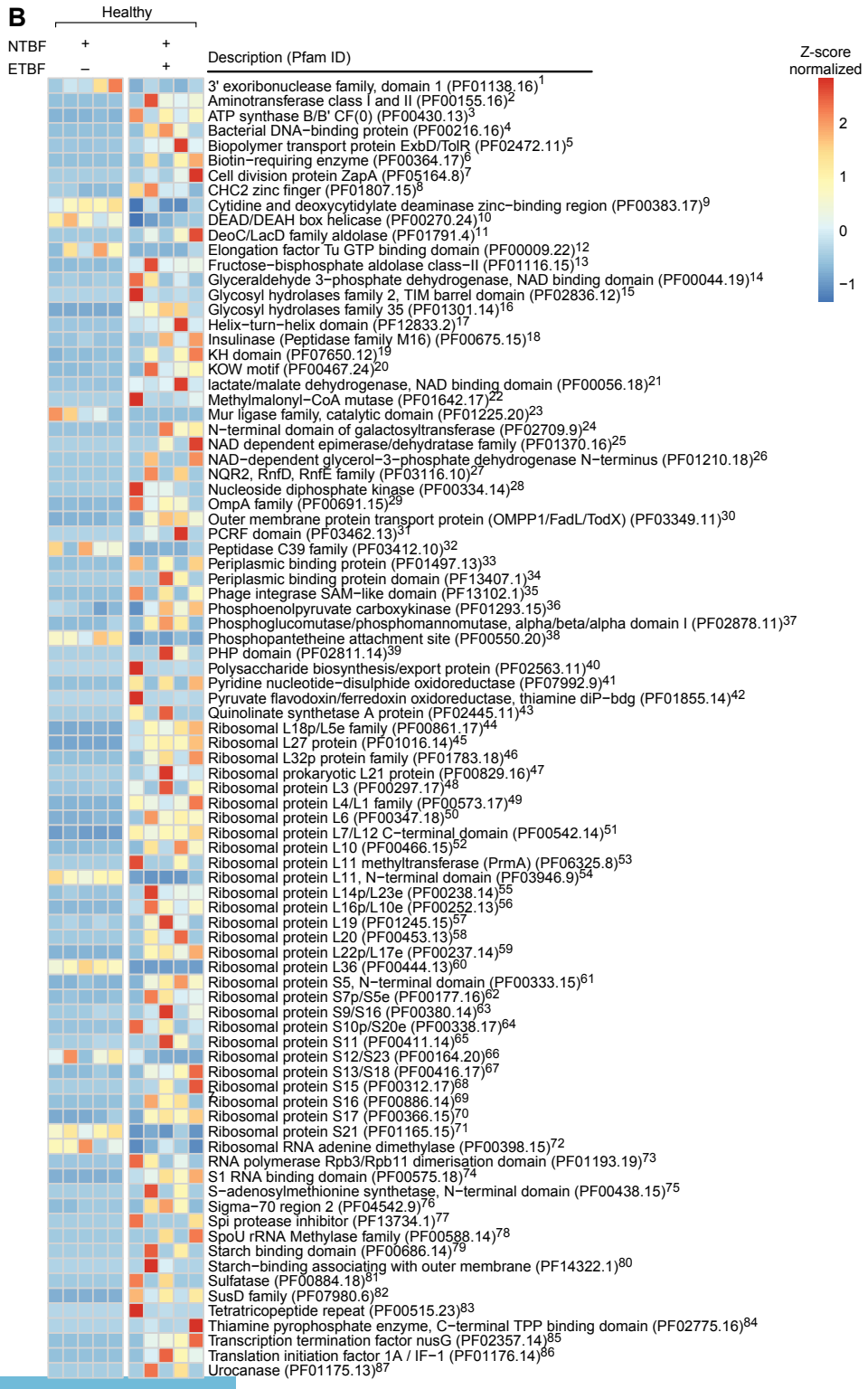

Figure S8A.

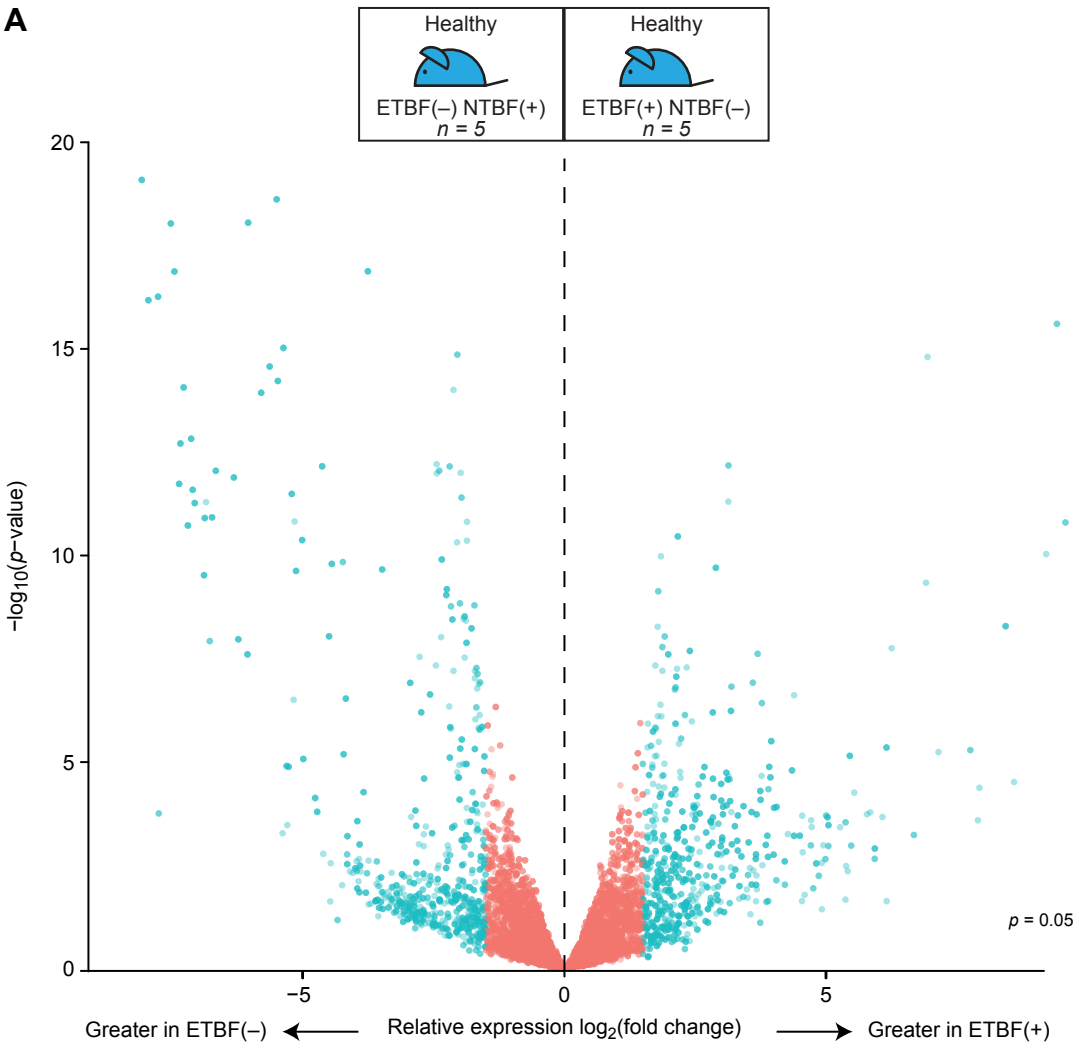

Figure S8B.

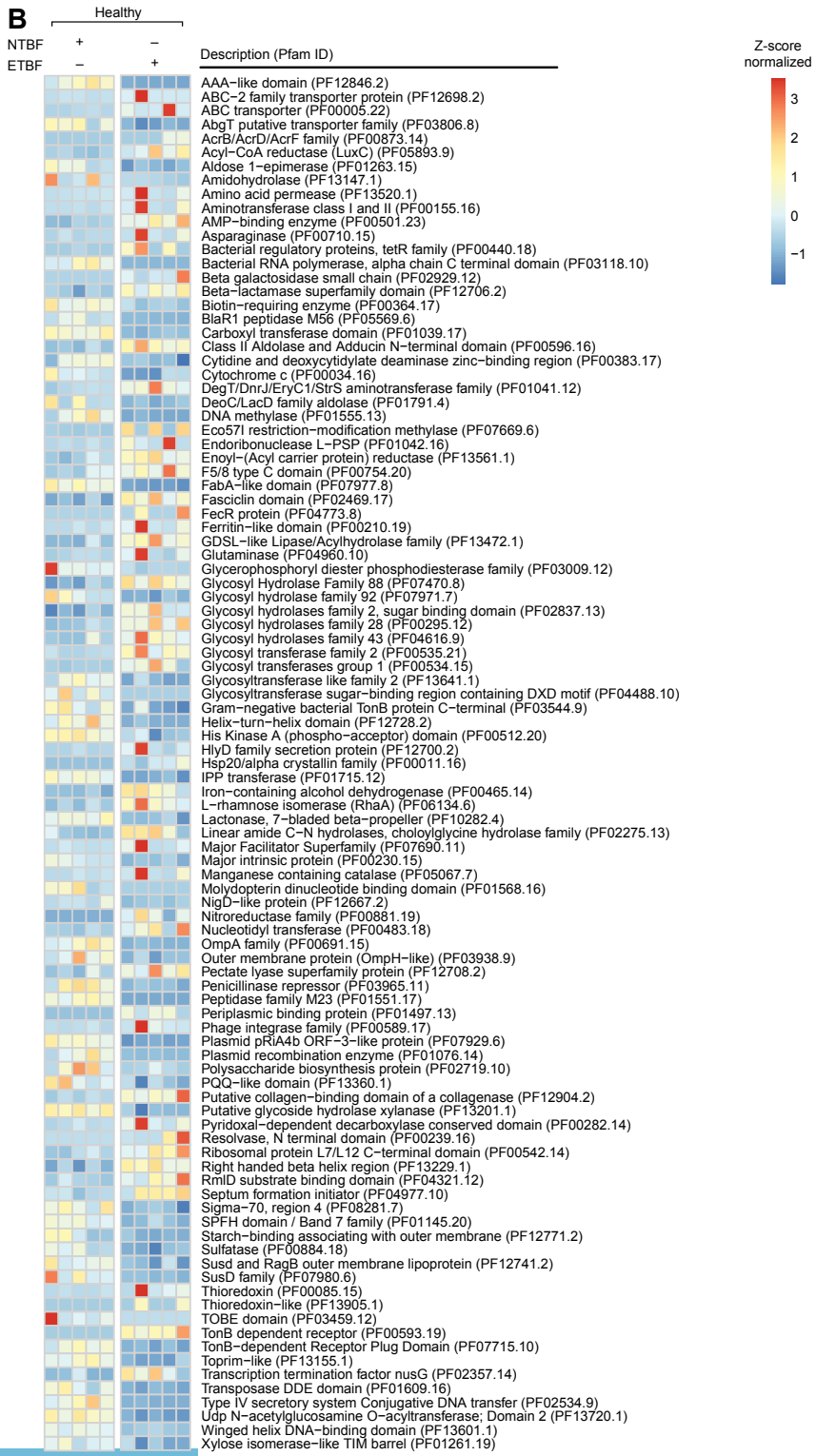

Figure S9A.

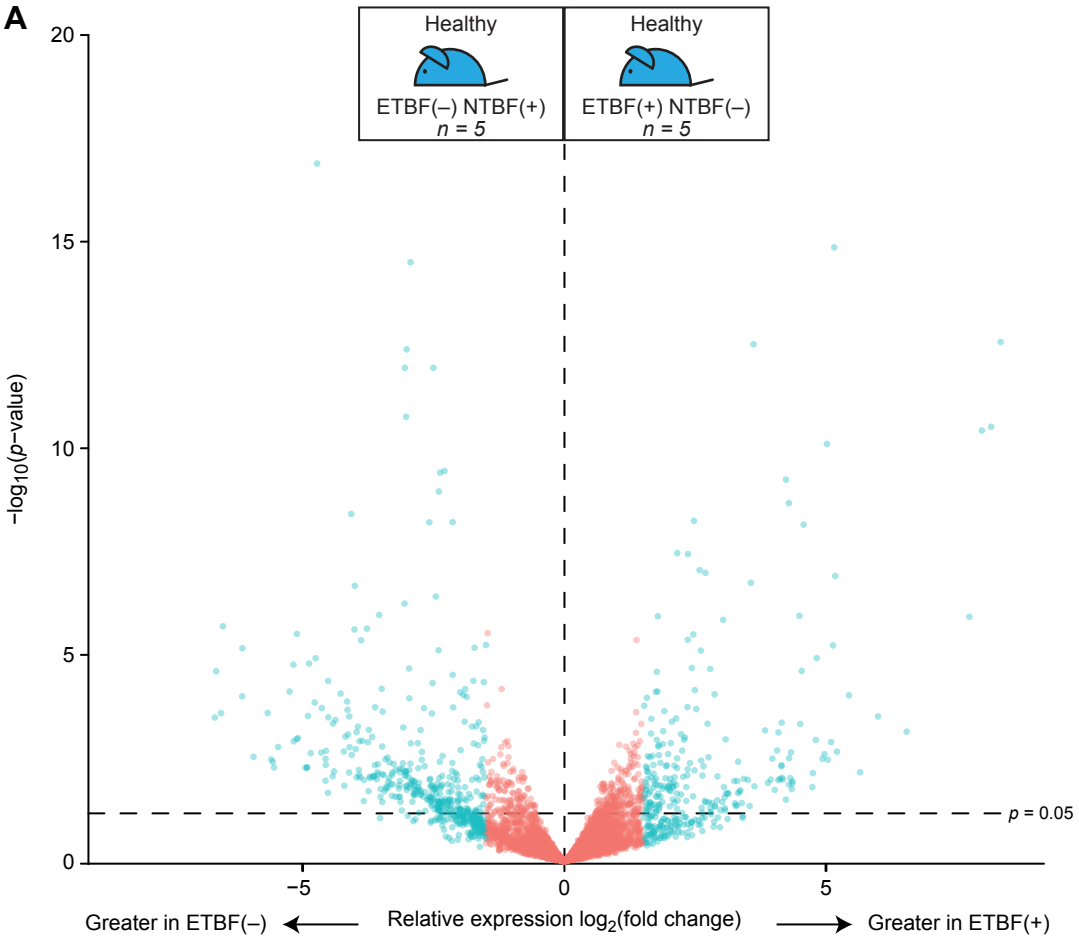

Figure S9B.

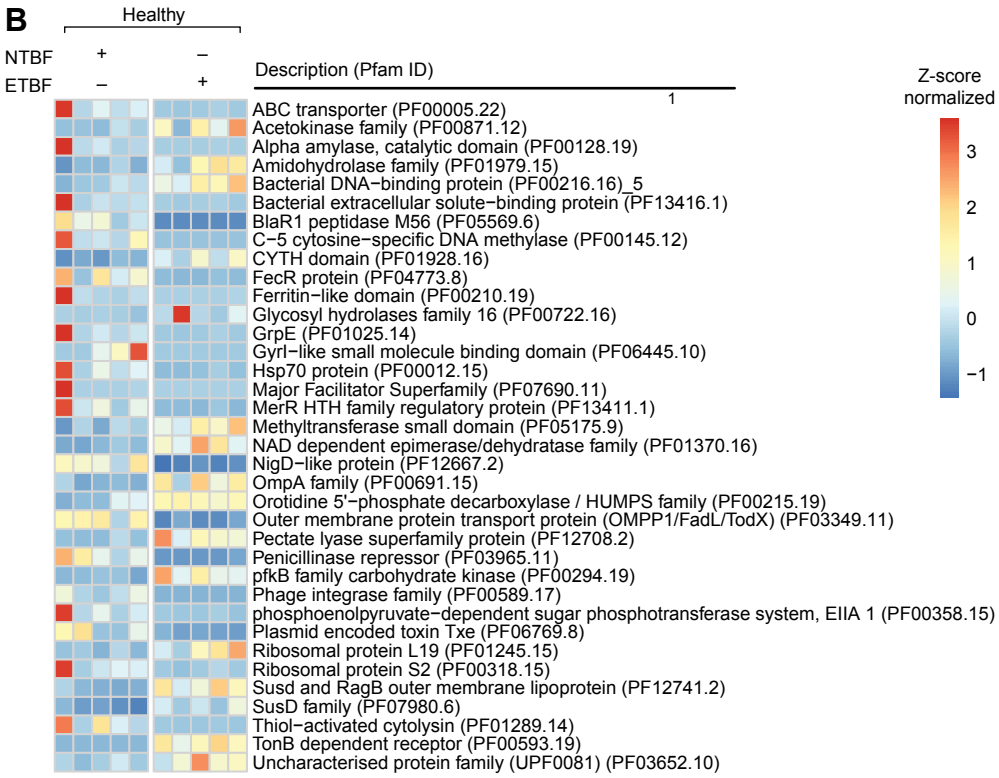

Figure S10.

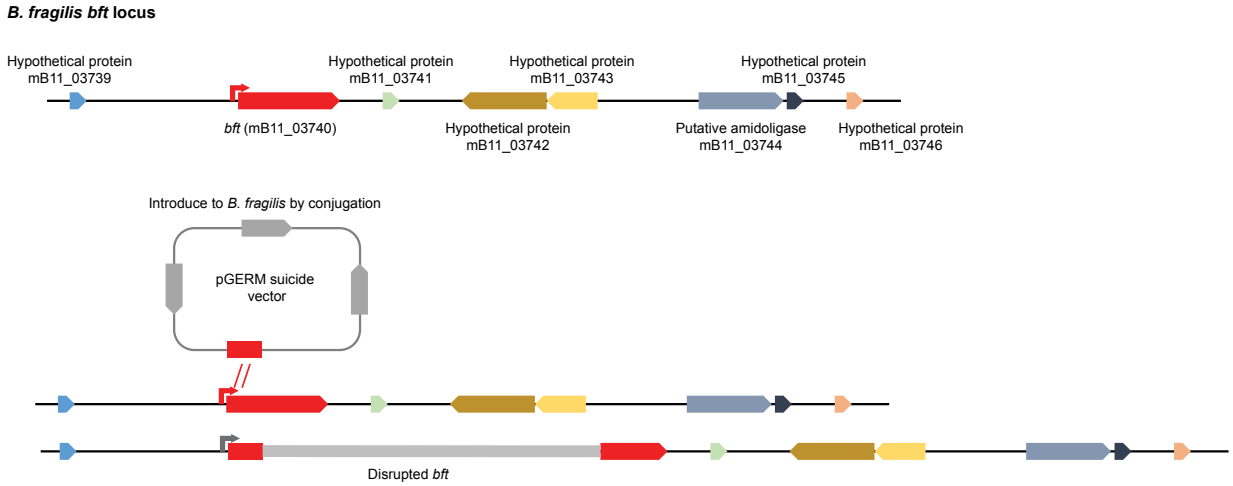

SUPPLEMENTAL TABLES

Table S1. Enterotoxigenic *B. fragilis* is variably present through time in a population of Bangladeshi children. (A) Two cultured bacterial isolates representing a single strain of *B. fragilis* (based on 96% genome sequence identity) harbor *bft* gene subtype 3. **(B)** Results of a *bft* PCR assay of fecal microbiota collected from members of a birth cohort of 100 Bangladeshi children at 18- and 24-months of age.

Table S2. Composition and nutritional content of Bangladeshi diet embodiments, and nutritional requirements of consumer mice and humans. A. Composition and nutritional content of the three Bangladeshi diet embodiments modeled after diets consumed by the populations from which donors were sampled. Diet embodiment composition is described by food category, item, and caloric representation of quantities added. **B.** (i) Daily nutritional requirements for mice and human children. (ii) Nutritional analysis of Bangladeshi diet embodiments.

Table S3. DNA and RNA sequencing datasets. (A) Human microbiota donor fecal bacterial V4-16S rRNA sequencing datasets. **(B)** Mouse fecal bacterial V4-16S rRNA datasets. **(C)** Mouse fecal bacterial shotgun sequencing datasets used for COPRO-Seq analyses. **(D)** Cecal microbial RNA-Seq datasets.

Table S4. Strains present in the culture collection generated from the fecal microbiota of a severely stunted/moderately underweight 2-year-old Bangladeshi child living in the Mirpur *thana* in Dhaka. (A) Strains based on ≥96% overall nucleotide sequence identity genome sequence identity among isolates, their taxonomic annotations (based on RDP classifications), and their designated names. **(B)** KEGG annotations.

Table S5. Weights of all individual mice as a function of diet, microbiota, and time. Weights are listed as both absolute measurements (grams) and relative to their weights prior to colonization (percentage). Metadata including microbiota donor information, MouseID, diet consumed, and days post colonization at the time of measurement are listed.

Table S6. Mass spectrometry based analyses of metabolites in host tissues, serum and the cecal microbiota obtained from mice in the different treatment groups (A) Amino acids in (i) cecum, (ii) gastrocnemius muscle, (iii) liver, and (iv) serum as measured by ultra-performance liquid chromatography (UPLC)-tandem mass spectrometry. (**B)** Organic acids in (i) cecum, (ii) gastrocnemius, and (iii) liver as measured by gas chromatography mass spectrometry (GC-MS). (**C)** Ceramides in (i) cecum, (ii) gastrocnemius muscle, and (iii) liver as measured by UPLC-tandem mass spectrometry. (**D)** Acylcarnitines in (i) cecum, (ii) gastrocnemius, (iii) liver, and (iv) serum as measured by UPLC-tandem mass spectrometry. (**E)** Acyl-CoAs in (i) gastrocnemius muscle and (ii) liver as measured by UPLC-tandem mass spectrometry. (**F**) Short-chain fatty acids in cecum as measured by GC-MS. (**G)** Bile acids in cecum as measured by (i) non-targeted and (ii) targeted UPLC-MS. (**H)** Concentrations or peak intensities of all metabolites measured (mean (± s.e.m) for each experimental group. A summary of significant differences between treatment groups is given to the right.

Table S7. Features of meta-transcriptomes in mice colonized with manipulated and unmanipulated culture collections. (A) ETBF genes differentially expressed in a healthy microbiota context compared to a stunted microbiota context: ETBF(+) NTBF(–) healthy vs ETBF(+) NTBF(–) stunted. (**B)** NTBF genes differentially expressed due to ETBF, in a healthy microbiota context: ETBF(+) NTBF(+) healthy vs ETBF(–) NTBF(+) healthy. (**C)** ETBF genes differentially expressed due to the presence of NTBF, in the context of the healthy culture collection: ETBF(+) NTBF(+) vs ETBF(+) NTBF(–). (**D)** *Bacteroides* genes (excluding *B. fragilis*) differentially expressed due to differences in the presence of ETBF versus NTBF in a healthy microbiota context: ETBF(–) NTBF(+) healthy vs ETBF(+) NTBF(–) healthy.

Table S8. Differentially expressed virulence factors in the cecal communities present in the various groups of gnotobiotic mice. (A) Virulence factor genes found in the genomes of strains comprising the stunted/underweight donor's culture collection. **(B)** Virulence factors expressed, but not significantly differently in the genomes of strains from the unmanipulated ETBF (+) versus manipulated ETBF(-) stunted/underweight donor's culture collection after transplantation into

gnotobiotic mice. (**C**) Virulence factor genes found in the genomes of the strains from the healthy culture collection. **(D)** Significantly differentially expressed virulence factors expressed in the genomes of the strains present in the unmanipulated ETBF (-) versus manipulated ETBF(+) NTBF(-) healthy donor-derived culture collection after transplantation into gnotobiotic mice.

Chapter 3

Regulators of gut motility revealed by a gnotobiotic model of travel-related diet changes

Regulators of gut motility revealed by a gnotobiotic model of travel-related diet changes

Neelendu Dey[1,2,3], Vitas E. Wagner[1,2], Laura V. Blanton[1,2], Jiye Cheng[1,2], Luigi Fontana[3], Rashidul Haque[4], Tahmeed Ahmed[4], and Jeffrey I. Gordon[1,2]*

[1]Center for Genome Sciences and Systems Biology, [2]Center for Gut Microbiome and Nutrition Research, and [3]Department of Medicine, Washington University School of Medicine, St. Louis, MO 63108, USA.

[4]Centre for Nutrition and Food Security, International Centre for Diarrhoeal Disease Research, Dhaka 1212, Bangladesh.

*Correspondence to: jgordon@wustl.edu

SUMMARY

Interactions between diets, consumers' gut microbiota, the enteric nervous system (ENS), and gut motility need better resolution to understand gut health. Using a gnotobiotic mouse model of short-term diet changes associated with international travel, microbiota from humans representing diverse cultural/culinary traditions were transplanted into animals that were fed a sequence of diets representing those of all donors. While correlations between bacterial species abundances and transit times were diet-dependent, unconjugated bile acids correlated with faster transit. Mice harboring 53 cultured bacterial strains from a Bangladeshi donor's microbiota and fed a Bangladeshi diet revealed that the commonly used spice, turmeric, slowed transit times. Wild-type and ENS-impaired *Ret*+/- mice, containing subsets of strains possessing high or low bile salt hydrolase activity, established that turmeric affects motility via bacterial bile acid deconjugation and Ret signaling. These results demonstrate how a traditional food ingredient interacts with a functional microbiota trait to regulate host physiology.

INTRODUCTION

Gut motility, a key physiologic parameter governing digestion and absorption of nutrients, is affected by diet (Cummings et al., 1976, 1978), gut microbes (Husebye et al., 1994, 2001; Wichmann et al., 2013), the enteric nervous system (ENS) (Edery et al., 1994; Romeo et al., 1994), and host genetics (Levy et al., 2000; Whorwell et al., 1986). At present, we lack detailed understanding of the complex and dynamic interrelationships between these factors, particularly in the global context of diverse cultural traditions concerning foods, their methods of preparation, and the varied human gut microbiota that have evolved under these dietary conditions. Intestinal transit times measured in >1000 healthy individuals representing diverse populations worldwide varied within and between groups, likely reflecting a culmination of these factors (Burkitt et al., 1972). The advent of culture-independent methods for characterizing the structure and expressed functions of a gut microbiota creates an opportunity to identify new approaches for understanding gut motility and for optimizing the nutritional benefits derived from different dietary practices.

In the present study, we began by modeling short-term diet changes associated with global human travel in gnotobiotic mice colonized with gut microbiota from healthy human donors from around the world. We hypothesized that with an international focus, we could conduct a screen of food types and microbiota for potential mediators of motility common to diverse diets and gut communities. Without making any assumptions regarding the healthiness of faster or slower motility, our strategy was to identify diets and microbiota whose interactions result in highly contrasting transit times in order to subsequently home in on specific dietary ingredients and microbiota-encoded metabolic capacities that affect motility. We reasoned that by generating clonally arrayed collections of bacterial strains cultured from donor microbiota that transmitted disparate motility phenotypes in different dietary settings, we could deliberately manipulate which members of the collection were used for colonization of mice based on specific metabolic attributes that could be identified from their genomes and confirmed by direct biochemical assays *in vitro*. Colonization with different subsets of the community could then be performed in the context of concurrently manipulated diets, either in wild-type animals or those with deliberately manipulated genetic fea-

tures known to affect ENS function. Our immediate goal for this type of preclinical modeling was to decipher the mechanisms by which diet-by-microbiota interactions can regulate gut motility. Our long-term goal was to implement an approach that could, in principle, be generalized to dissect the effects of interactions between (i) ingredients represented in established as well as emerging dietary traditions/trends, (ii) members of consumers' gut microbiota, and (iii) gut motility and potentially other aspects of human physiology.

RESULTS

Modeling diet and motility changes associated with global human travel in gnotobiotic mice

In an initial 'travel' experiment, intact uncultured fecal microbiota samples obtained from six healthy adults representing different geographic locations and cultural/culinary traditions were transplanted into adult germ-free C57BL/6 male mice (n=6 recipient mice/donor microbiota). Microbiota donors included (i) three residents of the USA (a twin pair stably discordant for obesity with both co-twins consuming an American diet without self-imposed dietary restrictions ($USA_{unrestricted}$) (Ridaura et al., 2013) plus another lean individual who had consumed a protein- and fat-rich primal diet for a number of years (USA_{primal})), (ii) an Amerindian living in a remote rural village in the Amazonas State of Venezuela (Yatsunenko et al., 2012), (iii) a Bangladeshi resident of an urban slum (Subramanian et al., 2014), and (iv) a Malawian from a rural village in the southern part of the country (Yatsunenko et al., 2012) (see **Table S1A** for a description of donor characteristics and **Table S1B** for analysis of microbiota transplantation efficiency). The six groups of transplant recipients were fed a sequence of six sterilized diets formulated to represent those consumed by the microbiota donors (**Figure S1, Table S1C,D**), in essence simulating the varying dietary experiences of humans and their microbiota during travel. In each case, the initial and final diets in the sequence represented the native or home diet of the donor, in order to characterize the longer term effects of dietary exposures during travel and the degree to which transit times recover; in between, travel diets were given in the same sequence, in an order chosen randomly but executed uniformly for all mice, as permitted by the type of home diet (**Figure 1A**). The starting and ending

home diets were given for 14 and 8 days, respectively, while each travel diet was administered for 8 days. Intestinal transit times were measured at the end of each diet phase by gavaging mice with non-absorbable red carmine dye and recording the time from gavage to first appearance of the dye in their feces (Kashyap et al., 2013; Li et al., 2011; Yano et al., 2015) (**Figure 1B**, **Table S2A**). Carmine dye does not perturb the structure of the gut bacterial community; 16S rRNA analysis of fecal samples, collected before and after carmine administration from 9-week-old gnotobiotic mice colonized with a fecal microbiota from a conventionally-raised C57BL/6 donor, showed no significant effect of the dye as judged by weighted UniFrac distances ($p>0.05$, two-tailed Student's *t*-test). Moreover, fecal samples collected on the days of transit time measurements were taken prior to carmine administration.

Aggregating data from all animals at all time points of this 6-phase travel experiment revealed a normal distribution of transit times (**Figure 1C**). The average within-mouse variance throughout the experiment was 27.7 minutes, while the average between-mouse variance at a given time point was 29.3 minutes. Repeated measures ANOVA in which transit time was the dependent variable demonstrated that diet ($p=5.6\text{x}10^{-5}$), the donor microbiota ($p=2.3\text{x}10^{-3}$), and the interaction of diet and microbiota ($p=2.6\text{x}10^{-3}$) were all significant factors (**Table S3A)**. The most contrasted diet-by-microbiota effects on transit times were documented in mice colonized with the Bangladeshi compared to the $\text{USA}_{unrestricted}$ microbiota when they consumed Bangladeshi and primal diets (**Figure 1D**). Specifically, mice colonized with the $\text{USA}_{unrestricted}$ microbiota had significantly faster motility (i.e., lower transit times) when consuming the Bangladeshi diet compared to primal diet ($p<0.002$, two-tailed Student's *t*-test); the opposite was observed in mice colonized with a Bangladeshi microbiota ($p<0.006$, two-tailed Student's *t*-test). We tested the robustness of these most contrasted motility phenotypes by colonizing animals ($n=5$ recipient mice/donor microbiota) with fecal microbiota obtained from three healthy Bangladeshi adults (including the donor tested in the first experiment) and three healthy $\text{USA}_{unrestricted}$ adults (a repeat of the obese co-twin in the discordant pair, plus a new obese and a new lean donor; see **Table S1A** for donor characteristics). Recipients were subjected to three diet phases beginning and ending with a 'lo-

cal' diet (i.e., the primal diet for mice colonized with a $USA_{unrestricted}$ microbiota or the Bangladeshi diet for mice colonized with a Bangladeshi microbiota) and including an interval 'non-native' diet (**Figure S2A**). The results of this 3-phase travel experiment confirmed that significantly contrasted transit times were imparted by the interactions of these diets and microbiota ($p<2.6x10^{-5}$, $F=19.8$, ANCOVA), although the effect size and statistical significance of differences in transit time varied by the individual microbiota donor (**Figure S2B, Table S2B**).

Correlations between the relative abundances of gut bacterial strains and transit times are diet-dependent

To identify relationships between specific bacterial taxa, diet, and transit time phenotypes, we sequenced PCR amplicons generated from the V4 region of bacterial 16S rRNA genes present in fecal microbiota collected throughout the course of the 6-phase as well as 3-phase travel experiments (984 fecal samples; 22,470±630 reads per sample [mean±s.e.m.]; **Table S4**). 16S rRNA reads were grouped into operational taxonomic units based on whether they shared ≥97% nucleotide sequence identity (97%ID OTUs). Principal coordinates analysis (PCoA) based on unweighted UniFrac, a phylogenetic metric that computes similarity between any two microbiota based on the degree to which their component OTUs share branch length on a bacterial tree (Lozupone and Knight, 2005), indicated that community assembly was rapid and highly reproducible within a given group of mice that received the same donor microbiota in both the 6-phase and 3-phase travel experiments (**Figure S3A,C**).

The microbiota donor was the predominant factor explaining variance in unweighted UniFrac distances between samples from the different experimental groups ($p<0.001$ within-group as compared to between-group similarity, PERMANOVA; **Figure S3B,D**). Nonetheless, diet had consistent effects across different treatment groups and phenotypes: 87 diet-discriminatory 97%ID OTUs that were robust to donor microbiota and motility phenotypes were identified by applying a machine learning algorithm (Random Forests) to the 16S rRNA dataset generated from all fecal microbiota samples collected from all mouse recipients of all human donor microbiota throughout

the 6-phase travel experiment (**Figure S4; Table S5**). We elected to apply a decision tree-based algorithm for feature selection (i.e., in this case, the most diet-discriminatory OTUs) so that we would not have to make any distributional assumptions regarding our dataset of proportional OTU abundances. The Random Forests-derived model predicted which diet was being consumed in the subsequent 3-phase travel experiment with a mean accuracy of 83%±0.02% (range 79%-86%; 10,000 replications), significantly better than the null distribution ($p<2.2x10^{-16}$). These 87 diet-discriminatory OTUs were not significantly correlated with transit times in either experiment. In an analysis of all 416 97%ID OTUs with relative abundances above the limit of detection (0.01%) in mouse fecal samples collected throughout both travel experiments, just a single OTU, *Parabacteroides gordonii* (OTU ID 240), was significantly correlated, after Bonferroni correction for multiple comparisons, with transit times *across* the highly contrasted diet-microbiota combinations (rho=0.3, p=0.02). This organism has not been reported to be associated with altered intestinal motility in humans.

In contrast, 27 OTUs present in both the $USA_{unrestricted}$ and Bangladeshi microbiota had significant diet-dependent correlations with transit times documented in the context of either the Bangladeshi or primal diets but not both (**Table S3B**). The relationships of bacteria to transit times were strain-specific: two strains of *Eubacterium desmolans* (OTU IDs 170124 and 158946) had opposing relationships with transit times within the setting of primal diet consumption. A single OTU, *E. desmolans* (OTU ID 158946), was significantly correlated with transit times in both diets, but remarkably the correlations were opposite in the Bangladeshi versus primal diet contexts ($p<9.3x10^{-6}$, F=9.6, ANCOVA testing interaction of *E. desmolans* abundance with diet). In the unrestricted USA diet context, yet another OTU in the $USA_{unrestricted}$ and Bangladeshi microbiota (*Clostridiales*, OTU ID 261590) was correlated with transit times (rho=-0.57, p=0.04). Hence, a hypothetical next-generation probiotic strain designed to impact motility would likely require simultaneous consumption of a specific diet or diet ingredient to exert its effect, much like leanness-conferring microbes have been demonstrated to transmit their phenotype in a diet-dependent manner (Ridaura et al., 2013).

Transit times at the ends of the initial and final home diets often varied. This finding could not be ascribed to increasing age (p=0.7, F=0.1, one-way ANOVA of transit time as a function of age). Mathematically, if we consider two functions $h(m)$ and $t(m)$, then $h(m)$ need not necessarily equal $h(t(h(m)))$. We postulated that if these two functions represent the effects of home (h) and travel (t) diets, respectively, on a microbiota m, then the result of a home diet may depend on whether intervening travel diets were consumed. Indeed, an analysis comparing fecal microbiota at the ends of the initial and final home phases in the 6-phase travel experiment disclosed that community structure, while largely similar, always exhibited statistically significant changes (p<0.05, paired two-tailed Student's t-test after Bonferroni correction) in the proportional abundances of one or more OTUs. For example, mice colonized with fecal microbiota from both $USA_{unrestricted}$ individuals exhibited a significant increase in the relative abundance of *Bacteroides ovatus* between the first and last home diet periods, while mice colonized with microbiota from the adult Bangladeshi donor exhibited significantly increased abundances of an OTU classified as *Clostridiales* and a decrease in *Ruminococcus obeum*.

The imperfect recovery of transit time following diverse dietary exposures during travel could reflect not only these structural differences but also functional differences in the microbiota. Therefore, we characterized metabolic features of the microbiota in the context of the most highly contrasted motility phenotypes.

Microbially deconjugated bile acid metabolites are correlated with faster gut transit

To identify metabolic features that correlate with motility phenotypes, we applied ultra high performance liquid chromatography mass spectrometry (UPLC-MS) to fecal samples collected from mice in the 3-phase travel experiment on the same days when their transit times were measured (3 $USA_{unrestricted}$ and 3 Bangladeshi donor microbiota; 5 mice/donor microbiota; 3 fecal samples analyzed/mouse). We observed >2,500 unique m/z peaks that were present in more than one mouse. Spearman's rank correlations (without Bonferroni correction) yielded 599 m/z peaks that were significantly correlated with transit times, of which 67 (11%) were putatively identified as bile acid

metabolites (**Tables S6A,S7A**). In mice, the predominant primary bile acids are beta-muricholic acid and cholic acid, while in humans they are chenodeoxycholic acid and cholic acid (Haslewood, 1967). Prior to secretion from hepatocytes into biliary canaliculi, bile acids are conjugated with either taurine (predominant in mice (Falany et al., 1997)) or glycine (predominant in humans (Falany et al., 1994)) to decrease passive absorption by intestinal enterocytes. Bile acids have microbicidal activity; members of the gut microbiota neutralize these effects by metabolizing host bile acids, beginning with deconjugation catalyzed by microbial bile salt hydrolases (BSH) (Drasar et al., 1966). Since bile acids are modified by the microbiota, we considered whether differences in bile acid metabolite profiles could explain discordant microbiota-associated motility phenotypes.

To gain insights into the relationships between OTUs and bile acid metabolites as they pertain to transit times, we calculated Spearman's rank correlation coefficients between the proportional abundances of 97%ID OTUs in fecal microbiota, the peak intensities of fecal bile acids, and transit times in the 3-phase travel experiment (**Figure 2**, **Table S7B**). After Bonferroni correction, we identified 118 OTUs with significant correlations between their abundances and levels of one or more fecal bile acids; only one of these OTUs, *Blautia* (OTU ID 296977), also had a significant correlation between its abundance and transit times (slower transit) (**Table S7B**). A sparse linear model, built after regressing transit times against all bile acid metabolite levels then simplified by applying stepwise backward feature selection, demonstrated that levels of just five bile acids (7-ketodeoxycholic acid, muricholic acid, taurocholic acid, tauro-beta-muricholic acid, and tauro-muricholic acid sulfate) accurately predicted transit times in the 3-phase travel experiment (rho=0.54, p=1.8x10^{-7}, Spearman's rank correlation), out-performing a linear model built with an equivalent number of randomly selected non-bile acid metabolites (rho=0.17, p=0.47, Spearman's rank correlation; mean values over 1,000 replications) (**Figure S5, Table S8**). Of these five bile acids, none was significantly associated with either diet. Only one bile acid species, tauro-muricholic acid sulfate, was significantly associated with the geographic origin of the microbiota donor; it was found at significantly higher concentrations in fecal specimens collected from mice colonized with subjects residing in Bangladesh (**Figure 2**). Bile acids that were correlated with faster transit times were unconjugated (7-ketodeoxycholic acid and muricholic acid), whereas those that correlated with slower transit times were conjugated (tauro-

beta-muricholic acid, taurocholic acid, and tauro-muricholic acid sulfate) (**Figure 2**, **Table S7B**). Multiple bile acids, including these five bile acids, were significantly correlated with multiple OTUs (**Figure 2**), underscoring the complexity of microbial bile acid metabolism.

Turmeric alters gut motility

Intestinal bile acid concentrations are largely dictated by dietary components (e.g., peptides and fats) that trigger intestinal signals (e.g., cholecystokinin), which, in turn, influence gallbladder contraction and release of bile into the lumen of the proximal small intestine. To further characterize interactions between specific OTUs, bile acid metabolism, and diet, we examined the effects of turmeric on transit time. We selected turmeric, a spice with cultural significance commonly used in Bangladeshi cuisine, because it has a dose-dependent cholekinetic effect; i.e., its active ingredient, curcumin, stimulates gallbladder contraction and thus increases luminal bile acid levels. The effect sizes of turmeric's cholekinesis vary between reported studies, possibly due to population-based differences (e.g., European versus Asian subjects) or differences in how the spice was administered (Marciani et al., 2013; Rasyid and Lelo, 1999; Rasyid et al., 2002). In a study using serial hydrogen breath tests to assess carbohydrate fermentation and small bowel transit time, investigators observed that turmeric-containing Japanese-style curry fed to Japanese individuals increased fermentation and shortened small bowel transit time compared to curry prepared without turmeric (Shimouchi et al., 2009). The microbial underpinnings of these observations in human subjects are unknown, as metagenomic or metabolomic analyses of their gut microbiota were not performed.

We initially defined the effect of turmeric in adult male C57BL/6 gnotobiotic mice colonized with a collection of anaerobic bacterial strains cultured from the fecal microbiota of a healthy 2-year-old Bangladeshi child (**Table S9**). We generated this culture collection from a child rather than an adult to avoid the potential confounding effects of chronic antecedent turmeric exposure on microbiota features. This child, like the three Bangladeshi adults whose microbiota were tested in the earlier experiments, lived in Mirpur, an urban sub-district of Dhaka. The sequenced, clonally arrayed bacterial culture collection gave us the capacity to perform follow-up experiments

in which specific strains were selected for colonization based on their capacity to metabolize bile acids.

Following gavage of the entire culture collection, composed of 53 bacterial strains (**Table S9**), mice were initially fed a Bangladeshi diet lacking turmeric for 10 days (diet phase 1), then the same diet containing turmeric for 10 days (diet phase 2), and finally the unsupplemented Bangladeshi diet again for 10 days (diet phase 3). A control group was maintained under germ-free conditions and subjected to the same sequence of diets (n=6 animals/group). To limit carryover of turmeric from the prior diet, old bedding was replaced with fresh new bedding at start of each diet phase.

Colonization was highly reproducible between animals with community assembly completed within 3-5 days after gavage. At the end of the first diet phase, 44±1.2 (mean±s.e.m.) of the 53 input strains were detectable in fecal samples collected from recipient animals, based on community profiling by shotgun sequencing (COPRO-Seq) of fecal DNA (see *Experimental Procedures*). Colonized mice had significantly faster transit times at each diet phase compared to their germ-free counterparts (p=5.0x10^{-6}, p<4.7x10^{-7}, and p<1.7x10^{-5} for diet phases 1, 2, and 3, respectively, two-tailed Student's t-test; **Table S2C**). Consumption of turmeric was associated with a significant slowing of motility (i.e., longer transit time) (**Table S2C**). UPLC-MS of fecal samples collected from germ-free mice at the end of each diet phase disclosed that ingestion of this cholekinetic spice was associated with significantly increased levels of taurohyodeoxycholic acid (p=0.003, one-tailed Student's t-test) and tauro-muricholic acid sulfate (p=0.03, one-tailed Student's t-test) compared to the period of unsupplemented diet consumption (**Table S6B**). As expected, no unconjugated bile acids were detected in the germ-free group during any of the diet phases. We included a curcumin standard in order to quantify fecal curcumin levels; however, curcumin was undetectable in all samples.

To directly test the hypothesis that microbiota with different capacities to deconjugate bile acids transmit distinct transit time phenotypes, we first used a UPLC-MS-based *in vitro* assay to

screen all members of the clonally arrayed culture collection for their bile salt hydrolase (BSH; EC 3.5.1.24) activities. The screen demonstrated that OTUs representing diverse phylotypes had the ability to deconjugate at least one of the two primary bile acids found in mice (**Table S9**). BLAST predictions, based on the presence in a strain's genome of a gene or genes homologous to known BSH genes (E-value threshold cutoff $\leq 10^{-5}$) were correct in predicting *in vitro* BSH enzymatic activity for 85% of the bacterial strains. Only 10 strains did not deconjugate either bile acid *in vitro* (6 members of the genus *Enterococcus*, 3 members of *Eggerthella*, and 1 belonging to *Enterobacteriaceae*). The strains with BSH activity were largely members of the genera *Bifidobacterium* and *Enterococcus*. We then assembled two bacterial consortia, each composed of seven strains representing the taxonomic diversity of the BSH-positive and BSH-negative subsets within the culture collection: the "BSH_{hi}" consortium contained four members of *Enterococcus* and three members of *Bifidobacterium*; the "BSH_{lo}" consortium had five members of *Enterococcus*, one *Eggerthella* species, and one *Enterobacteriaceae* (see **Table 10A** for a summary of KEGG-based annotations of the sequenced genomes of these 14 strains). Members of the two consortia had *in vitro* growth rates in rich medium that were not significantly different from one another (p=0.92, two-tailed Student's t-test).

Age-matched adult male C57BL/6 gnotobiotic mice were colonized with either the BSH_{hi} or BSH_{lo} consortium (assembled prior to gavage by combining equal numbers of colony forming units of each component strain). A positive control group was colonized with the entire culture collection. As before, mice in each of these three groups (n=5/group) were given the unsupplemented Bangladeshi diet for 3 days prior to gavage of the cultured organisms. Following gavage, mice were maintained on the unsupplemented Bangladeshi diet for 8 days, followed by the turmeric-supplemented diet for 8 days, and then returned to the starting Bangladeshi diet for another 8 days. The complete culture collection produced a transit time that was significantly faster than that measured with the BSH_{lo} consortium in all three diet phases (p<0.002, one-tailed Student's t-test; **Table S2D**). While mice harboring the BSH_{lo} consortium had the same transit time as the BSH_{hi}

consortium in the absence of turmeric, addition of this spice to the Bangladeshi diet produced significantly slower transit times in BSH_{lo} animals (p=0.02, one-tailed Student's t-test comparing phase 1 versus phase 2 transit times; **Figure 3A**) but no significant effects in BSH_{hi} mice (p=0.7, one-tailed Student's t-test). These findings indicate that a gut microbiota capable of deconjugating bile acids could modify the response to turmeric, which through its cholekinetic effects delivers increased amounts of conjugated bile acids to the proximal intestine.

Mice colonized with the BSH_{lo} consortium had significantly slower motility than BSH_{hi} animals only in the setting of turmeric (p<0.03, one-tailed Student's t-test; **Figure 3B**). UPLC-MS confirmed that BSH_{hi} mice had significantly higher total concentrations of fecal unconjugated bile acids (p=0.01, one-tailed Student's t-test) and significantly lower total concentrations of conjugated bile acids (p=0.02, one-tailed Student's t-test) compared to mice colonized with the BSH_{lo} consortium (**Figure 3C**, **Table S6D**). Total concentrations of the two unconjugated primary bile acids (cholic acid and beta-muricholic acid) were significantly negatively correlated with transit times (rho=-0.76, p=3.6×10^{-9}, Spearman's rank correlation). COPRO-Seq revealed that turmeric had no statistically significant effects on the representation of any strain in either consortium when compared to the unsupplemented diet phases (p>0.15, two-tailed Student's t-test).

Applying microbial RNA-Seq to fecal samples collected at the same time points as those used for the COPRO-Seq analysis, we confirmed significantly greater overall levels of community BSH expression in the BSH_{hi} compared to the BSH_{lo} consortium's meta-transcriptome (145-fold; p=0.006, two-tailed Student's t-test). However, turmeric did not result in significant changes in the levels of BSH transcripts in the fecal meta-transcriptomes of BSH_{lo} and BSH_{hi} animals (p>0.05, two-tailed Student's t-test). *Enterococcus faecalis* (isolate ID hG2) was the only member of the BSH_{lo} consortium that expressed BSH, albeit at low levels (thus explaining the presence of fecal unconjugated bile acids in these animals; **Figure 3C**). In the BSH_{hi} consortium, the principal contributors of BSH transcripts to the community meta-transcriptome were three *Bifidobacteria* (isolate IDs hB1, hB8, and hF8), which together accounted for 76%±1% (mean±s.e.m.) of these transcripts. In mice colonized with the BSH_{lo} consortium, turmeric resulted in significant reduc-

tions in expression of two transcripts in the meta-transcriptome assigned to the KEGG 'dioxin degradation pathway' (5.7-fold; p=0.004, two-tailed Student's t-test): salicylate 1-monooxygenase (EC 1.14.13.1, a oxidoreductase that produces catechol) and 4-oxalocrotonate tautomerase (EC 5.3.2.6; part of a metabolic pathway that generates TCA cycle intermediates). No KEGG pathways were significantly differentially expressed as a function of turmeric consumption in mice colonized with the BSH_{hi} consortium. Together, these results suggest that turmeric enhances the discordance in motility phenotypes between BSH_{lo} versus BSH_{hi} mice not by changing expression of bacterial BSH genes but rather through its cholekinetic effect, thereby providing conjugated bile acids to the two consortia with markedly different BSH gene content and deconjugation capacities.

Effects of turmeric on host gene expression

To assess the effects of turmeric on host gene expression, we focused on the BSH_{lo} consortium because, in the previous experiment, it transmitted a turmeric-responsive transit time phenotype. BSH_{lo} mice were monotonously fed either the unsupplemented or turmeric-supplemented Bangladeshi diet for 10 days. The capacity of turmeric to significantly slow motility was replicated in this new, single diet phase experiment (p=0.003, one-tailed Student's t-test comparing transit times between the two diet-treatment groups; **Figure 3D**). RNA-Seq datasets were generated from the liver and terminal ileum, essential components of the enterohepatic circulation. Differentially expressed genes were identified using the exact negative binomial test. Genes that satisfied our criteria for significant differences in expression (after correcting for multiple comparisons) are listed in **Table S11**. Transcriptional data generated from the livers of mice from the 10 day-long monotonous diet experiment indicated that turmeric consumption was followed by a homeostatic response designed to maintain bile acid pool size at constant levels: i.e., consistent with the increased fecal bile acid levels elicited by turmeric consumption, *Cyp7a1* (cholesterol 7α-hydroxylase) expression was 3.3-fold lower (p=0.00002). Cyp7A1 converts cholesterol into 7α-hydroxycholesterol in the rate-limiting first step of hepatic bile acid synthesis, a step subject to feedback inhibition by increased bile acid concentrations. In the terminal ileum, multiple genes involved in gut mucosal

immune/barrier function, including a subset implicated in protection against helminthic infections, exhibited significant differential expression in the face of turmeric consumption (**Table S11A;** see *Supplemental Information*).

Interplay of the microbiota, bile acids, and the ENS

To assess the degree to which the effect of turmeric on motility was dependent upon ENS-based signaling (Alemi et al., 2013), we turned to mice heterozygous for a null allele of the Ret receptor (Tsuzuki et al., 1995). *Ret,* which encodes a transmembrane protein that binds glial cell-derived neurotrophic factor family ligands, is the gene most commonly implicated in Hirschsprung's disease (Edery et al., 1994; Romeo et al., 1994), a developmental disorder associated with absent peristalsis in the distal colon. Heuckeroth and colleagues have reported that *Ret*+/- mice exhibit >90% reductions in longitudinal and circular gut muscle contractility and 70-95% reductions in the release of two neurotransmitters (substance P and VIP) compared to *Ret*+/+ animals despite having equivalent numbers of enteric neurons (Gianino et al., 2003). We found that conventionally raised wild-type (*Ret*+/+) mice have significantly slower transit times than their conventionally-raised heterozygous (*Ret*+/-) littermates (p=0.05, one-tailed Student's t-test; **Table S2F**).

We re-derived C57BL/6 *Ret*+/- mice as germ-free and colonized the heterozygotes and their wild-type littermates with either the 7-member BSH_{lo} or 7-member BSH_{hi} consortium. Animals were subjected to a three-phase diet oscillation as in the experiments described above (unsupplemented ➔ turmeric-supplemented ➔ unsupplemented Bangladeshi diet; 10 days/phase). We hypothesized that if enteric neurons were key mediators of the observed phenotypes, then the difference in transit times seen between wild-type mice colonized with the two different 7-member consortia (**Figure 3B**) might be mitigated in *Ret*+/- animals. Indeed, in contrast to wild-type mice, transit times were not significantly different between *Ret*+/- mice harboring the two different consortia (**Table S2D**) despite the same pattern of differences in fecal bile acids concentrations documented by UPLC-MS in wild-type mice: *Ret*+/- mice colonized with the BSH_{lo} consortium had significantly lower fecal concentrations of unconjugated bile acids compared to *Ret*+/- mice

colonized with the BSH_{hi} consortium in the setting of turmeric consumption (p=0.009, one-tailed Student's t-test). As in wild-type mice, COPRO-Seq analysis showed that no bacterial strains in the *Ret*+/- mice were significantly correlated with turmeric consumption. Notably, a significant difference in transit times between *Ret*+/- and wild-type mice was only seen in mice colonized with the BSH_{hi} bacterial consortium (diet phase 1: p=0.009, phase 2: p=0.02, phase 3: p=0.09, one-tailed Student's t-test; p>0.05 in all analogous comparisons of *Ret*+/- versus wild-type mice colonized with the BSH_{lo} consortium). Thus, while turmeric consumption has a cholekinetic effect in both wild-type and *Ret*+/- mice, the transit time phenotype it produces in wild-type mice is mediated by gut microbial bile acid metabolism and a functionally intact ENS.

DISCUSSION

Intestinal motility is a key physiologic parameter impacting nutritional status and gut health. The travel-associated diet changes that we model here is increasingly relevant to our daily lives during this period of rapid globalization, in which a day spent entirely in one's hometown may nonetheless consist of consumption of foods representing several of the world's cultures. A gnotobiotic mouse model of global travel might also incorporate additional factors that impact the gut microbiota, such as disruption of circadian rhythm (Thaiss et al., 2014) or the order in which different diets are experienced. Using gnotobiotic mice colonized with microbiota obtained from healthy individuals representing different geographic and cultural traditions and diets representative of those consumed by these donors, we were able to dissect factors that interact to define a motility phenotype. These diet-microbiota-metabolic interactions were resolved in the context of Bangladeshi microbiota through a multi-pronged strategy that involved (i) manipulating the dietary representation of a single culturally relevant spice, turmeric, (ii) selecting members of a clonally arrayed culture collection generated from a Bangladeshi donor's microbiota, based on whether they were or were not able to support BSH-mediated bile acid deconjugation, and (iii) colonizing germ-free mice with or without a mutation in *Ret*, a key regulator of ENS function, with a BSH_{hi} or BSH_{lo} consortium.

The simulation of global travel-associated short-term diet shifts revealed that (i) diet-discriminatory bacterial strains were represented across microbiota from individuals raised in environments that are geographically and culturally distinct, and (ii) correlations between individual bacterial species abundances and transit times are largely diet-dependent: e.g., a given bacterial strain can have contrasting correlations with transit times depending upon the diet context. These findings suggest that future use of bacterial strains derived from the human gut as probiotic agents for motility disorders will require thoughtful consideration of an individual's dietary practices and/or adjunct dietary recommendations. Reciprocally, our preclinical data suggest that dietary treatments for motility disorders need to be calibrated based on structural and functional features of an individual's microbiota. In this respect, we find that unconjugated bile acids resulting from bacterial metabolism are consistently correlated with faster transit times across different diets and microbiota. In patients with irritable bowel syndrome, a limited number of clinical trials have suggested that a subset of patients respond to oral administration of the unconjugated bile acid chenodeoxycholate with accelerated transit times (Odunsi-Shiyanbade et al., 2010; Rao et al., 2010), consistent with our observations. Our results point to fecal BSH activity as a functional microbiota parameter that could be useful for categorizing individuals with motility disorders, allowing correlation analyses to be performed between the levels of its conjugated substrates and/or its various unconjugated bile acid products and transit time. If significantly correlated within a population, this metabolic activity could be used as a target or biomarker in clinical studies testing the effects, both short and long-term, of various therapeutic interventions.

The imperfect recovery of transit times following consumption of 'travel' diets, initially noted in the context of the 6-phase and 3-phase travel experiments, was also seen in our experiments involving sequential presentation of an unsupplemented, turmeric-supplemented, and unsupplemented Bangladeshi diet. Across ecosystems, history (i.e., order and temporal features of perturbations) is well known to impact community structure and function (Chase, 2003; Fukami and Morin, 2003; Pagaling et al., 2014). In this context, turmeric may influence alternative stable states (Staver et al., 2011) of the gut microbiota and ENS. Despite our practice of changing bed-

ding between diet phases to limit carryover of ingredients, turmeric may have long-lived effects on host physiology. A sustained increase in total bile acid pool size evoked by turmeric's cholekinetic effects seems an unlikely explanation for these observations, as bile acid concentrations in the final diet phase returned to pre-turmeric levels (**Figure 3C**). Follow-up experiments examining the duration of turmeric's effects on the transcriptome of purified enteric neurons (including the TGR5 bile acid receptor (Alemi et al., 2013)) in combination with analyses of the microbiota and its metabolic features, localization of motility effects (i.e., gastric, small intestinal, and/or colonic), and production of neuroactive compounds such as serotonin by enteroendocrine cells (Yano et al., 2015), could reveal and help characterize this postulated turmeric-induced alternative stable state.

Other dietary ingredients (e.g., polysaccharides (Kashyap et al., 2013)) and products of bacterial metabolism (e.g., butyrate (Soret et al., 2010)) have been previously described to impact motility in mouse models. Populations experiencing shifting cultural/culinary traditions through travel, immigration or emigration, are susceptible to marked changes in their gut microbiota, both structural and functional, which may have downstream health consequences. In principle, our approach could be used to identify and characterize the biological activities and microbiota interactions of dietary components characteristic of dietary/cultural traditions established over centuries but now vulnerable to diminished use due to Westernization. Their exclusion from modern diets may represent a loss of key food ingredients that could be used to promote health in contemporary societies. These ingredients may also serve as valuable tools for identifying and characterizing mechanisms by which food and the microbiota interact to affect various features of our physiology.

EXPERIMENTAL PROCEDURES

Measurement of gastrointestinal transit times using non-absorbable red carmine dye

Carmine red (Sigma-Aldrich, St. Louis, MO) was prepared as a 6% (w/v) solution in 0.5% methylcellulose (Sigma-Aldrich) and autoclaved prior to import into gnotobiotic isolators. Mice were maintained on a strict 12h light cycle (lights on between 06:00 and 18:00) and gavaged with 150 µL of the carmine solution between 08:00 and 08:30 local time. Animals were not fasted before-

hand. Feces were collected every 30 minutes (up to 8 hours from time of gavage) and streaked across a sterile white napkin to assay for the presence of the red carmine dye. The time from gavage to initial appearance of carmine in the feces was recorded as the total intestinal transit time for that animal.

Generating a clonally arrayed culture collection of anaerobic bacterial strains from the fecal microbiota of a healthy 24-month-old Bangladeshi child

A clonally arrayed culture collection was generated using methods described in an earlier publication (Goodman et al., 2011). A given well of the 96-well plate used to archive the collection contained a monoculture of a single isolate. Each isolate's genome was sequenced using an Illumina MiSeq or HiSeq instrument [250 nucleotide (nt) and 101 nt paired end reads, respectively; 53±4.8-fold (mean±s.e.m.) genome coverage]. Genomes were assembled using MIRA (Chevreux et al., 1999) (N50 contig length: 23,253± 2,669 bp; range, 735-112,622 bp). Assemblies were annotated using Prokka (version 1.10) (Seemann, 2014). Predicted genes were mapped to KEGG pathways by querying the KEGG reference database (release 72.1) and assigning their protein products to KEGG Ortholog (KO) groups (BLAST 2.2.29+, blastp E-value threshold $\leq 10^{-10}$, single best hit defined by E-value and bit score) (Kanehisa and Goto, 2000; Kanehisa et al., 2014). Species-level taxonomic identities of bacterial isolates were defined by Sanger capillary sequencing of full-length 16S rRNA gene amplicons generated using the universal 8F and 1391R PCR primers, with classifications performed using the Ribosomal Database Project (RDP) version 2.4 classifier (Ridaura et al., 2013). Strain-level taxonomic classifications were subsequently determined based on a minimum 96% genome identity [calculated by the software package *NUCmer* (Kurtz et al., 2004)] between sequenced isolates bearing the same 16S rRNA-based taxonomy. A total of 53 unique strains were identified using this 96% identity cutoff threshold and grown in modified gut microbiota medium (mGMM) containing ingredients described in a previous publication (Goodman et al., 2011) but without short chain fatty acid supplementation. Strains were stored at -80°C in 15% glycerol (v/v) in reduced PBS until used for gavage of germ-free mice.

In vitro assays for bile acid deconjugation

We screened each of the 91 isolates, comprising 53 strains, in the clonally arrayed culture collection for their capacity to deconjugate bile acids. The two predominant primary bile acids in mice, taurocholic acid (TCA; Sigma-Aldrich, St. Louis, MO) and tauro-beta-muricholic acid (TbMCA; Santa Cruz Biotechnology, Santa Cruz, CA), were dissolved in water at concentrations of 100 mg/mL and 10 mg/mL, respectively. Each isolate was first incubated in 1 mL of mGMM containing 100 µM TCA for 48 h in an anaerobic Coy chamber (75% N_2, 20% CO_2, and 5% H_2) with growth monitored based on OD_{600}. Cells were then pelleted by centrifugation (17,900 x g for 7 minutes at 4°C), and the resulting supernatant subjected to ultra high performance liquid chromatography-mass spectrometry (UPLC-MS; see details below) to assess levels (peak intensities) of unconjugated and conjugated bile acids (cholic acid and taurocholic acid [TCA], respectively). For the vast majority of isolates, bile acid profiles at 48 hours were either all conjugated or unconjugated. Growth of bacterial isolates was simultaneously assessed by measuring optical densities at 600 nm to ensure that a lack of deconjugation was not simply a reflection of a lack of bacterial viability. If no deconjugation was observed, we performed a secondary screen where isolates were incubated in 1 mL of mGMM containing 100 µM tauro-beta-muricholic acid (TbMCA) for 48 hours in an anaerobic chamber, followed by UPLC-MS quantitation of the levels of unconjugated (beta-muricholic acid) and conjugated (TbMCA) bile acids. Bacterial isolates that did not deconjugate either bile acid *in vitro* were considered as eligible for the BSH_{lo} consortium. See *Supplemental Information* for additional protocols.

ACKNOWLEDGEMENTS

We are grateful to Robert Heuckeroth (University of Pennsylvania) for generously providing *Ret*+/- mice, Maria Gloria Dominguez-Bello (New York University) for her leadership in obtaining fecal samples from Amerindians in an earlier collaborative study, Andreea Soare for her assistance in obtaining fecal samples and diet records from individuals consuming a primal diet, David O'Donnell and Maria Karlsson for their assistance with gnotobiotic husbandry, Sabrina Wagoner, Janaki Lelwala-Guruge, Martin Meier, and Jessica Hoisington-Lopez for their invaluable technical assistance, and Vanessa Ridaura, Sathish Subramanian, Ansel Hsiao, Matthew Hibberd, Nicholas Griffin, Nathan McNulty, Philip Ahern, and other members of the Gordon lab for their helpful suggestions. This work was supported by grants from the NIH (DK30292, DK70977, DK078669), the Bill and Melinda Gates Foundation, and the Crohn's and Colitis Foundation of America. N.D. is the recipient of a Young Investigator Grant for Probiotics Research from the Global Probiotics Council. J.I.G. is cofounder of Matatu Inc., a company characterizing the role of diet-by-microbiota interactions in animal health.

ACCESSION NUMBERS

Bacterial V4-16S rRNA amplicon datasets, whole genome shotgun sequencing datasets from cultured bacterial strains, plus microbial and host RNA-Seq datasets have been deposited in the European Nucleotide Archive (ENA) under the study accession number PRJEB9169.

AUTHOR CONTRIBUTIONS

N.D., L.V.B., J.C., and J.I.G. designed the experiments; N.D., V.E.W., L.V.B, and J.C. generated the data; V.E.W. generated the clonally arrayed bacterial culture collection; L.F. provided microbiota samples and dietary data from primal dieters; T.A. and R.H. provided microbiota samples and dietary data from Bangladeshi individuals; N.D. and J.I.G. analyzed the data and wrote the paper.

REFERENCES

Alemi, F., Poole, D.P., Chiu, J., Schoonjans, K., Cattaruzza, F., Grider, J.R., Bunnett, N.W., and Corvera, C.U. (2013). The receptor TGR5 mediates the prokinetic actions of intestinal bile acids and is required for normal defecation in mice. Gastroenterology *144*, 145–154.

Burkitt, D.P., Walker, A.R.P., and Painter, N.S. (1972). Effect of dietary fibre on stools and the transit-times, and its role in the causation of disease. The Lancet *300*, 1408–1411.

Chase, J.M. (2003). Community assembly: when should history matter? Oecologia *136*, 489–498.

Chevreux, B., Wetter, T., and Suhai, S. (1999). Genome Sequence Assembly Using Trace Signals and Additional Sequence Information. Comput. Sci. Biol. Proc. Ger. Conf. Bioinforma. GCB *99*, 45–56.

Cummings, J.H., Jenkins, D.J., and Wiggins, H.S. (1976). Measurement of the mean transit time of dietary residue through the human gut. Gut *17*, 210–218.

Cummings, J.H., Wiggins, H.S., Jenkins, D.J., Houston, H., Jivraj, T., Drasar, B.S., and Hill, M.J. (1978). Influence of diets high and low in animal fat on bowel habit, gastrointestinal transit time, fecal microflora, bile acid, and fat excretion. J. Clin. Invest. *61*, 953–963.

Drasar, B.S., Hill, M.J., and Shiner, M. (1966). The deconjugation of bile salts by human intestinal bacteria. Lancet *1*, 1237–1238.

Edery, P., Lyonnet, S., Mulligan, L.M., Pelet, A., Dow, E., Abel, L., Holder, S., Nihoul-Fékété, C., Ponder, B.A., and Munnich, A. (1994). Mutations of the RET proto-oncogene in Hirschsprung's disease. Nature *367*, 378–380.

Falany, C.N., Johnson, M.R., Barnes, S., and Diasio, R.B. (1994). Glycine and taurine conjugation of bile acids by a single enzyme. Molecular cloning and expression of human liver bile acid CoA:amino acid N-acyltransferase. J. Biol. Chem. *269*, 19375–19379.

Falany, C.N., Fortinberry, H., Leiter, E.H., and Barnes, S. (1997). Cloning, expression, and chromosomal localization of mouse liver bile acid CoA:amino acid N-acyltransferase. J. Lipid Res. *38*, 1139–1148.

Fukami, T., and Morin, P.J. (2003). Productivity-biodiversity relationships depend on the history of community assembly. Nature *424*, 423–426.

Gianino, S., Grider, J.R., Cresswell, J., Enomoto, H., and Heuckeroth, R.O. (2003). GDNF availability determines enteric neuron number by controlling precursor proliferation. Development *130*, 2187–2198.

Goodman, A.L., Kallstrom, G., Faith, J.J., Reyes, A., Moore, A., Dantas, G., and Gordon, J.I. (2011). Extensive personal human gut microbiota culture collections characterized and manipulated in gnotobiotic mice. Proc. Natl. Acad. Sci. U. S. A. *108*, 6252–6257.

Haslewood, G.A. (1967). Bile salt evolution. J. Lipid Res. *8*, 535–550.

Husebye, E., Hellström, P.M., and Midtvedt, T. (1994). Intestinal microflora stimulates myoelectric activity of rat small intestine by promoting cyclic initiation and aboral propagation of migrating myoelectric complex. Dig. Dis. Sci. *39*, 946–956.

Husebye, E., Hellström, P.M., Sundler, F., Chen, J., and Midtvedt, T. (2001). Influence of microbial species on small intestinal myoelectric activity and transit in germ-free rats. Am. J. Physiol. - Gastrointest. Liver Physiol. *280*, G368–G380.

Kanehisa, M., and Goto, S. (2000). KEGG: kyoto encyclopedia of genes and genomes. Nucleic Acids Res. *28*, 27–30.

Kanehisa, M., Goto, S., Sato, Y., Kawashima, M., Furumichi, M., and Tanabe, M. (2014). Data, information, knowledge and principle: back to metabolism in KEGG. Nucleic Acids Res. *42*, D199–D205.

Kashyap, P.C., Marcobal, A., Ursell, L.K., Larauche, M., Duboc, H., Earle, K.A., Sonnenburg, E.D., Ferreyra, J.A., Higginbottom, S.K., Million, M., et al. (2013). Complex interactions among

diet, gastrointestinal transit, and gut microbiota in humanized mice. Gastroenterology *144*, 967–977.

Kurtz, S., Phillippy, A., Delcher, A.L., Smoot, M., Shumway, M., Antonescu, C., and Salzberg, S.L. (2004). Versatile and open software for comparing large genomes. Genome Biol. *5*, R12.

Levy, R.L., Whitehead, W.E., Korff, M.R.V., and Feld, A.D. (2000). Intergenerational transmission of gastrointestinal illness behavior. Am. J. Gastroenterol. *95*, 451–456.

Li, Z., Chalazonitis, A., Huang, Y., Mann, J.J., Margolis, K.G., Yang, Q.M., Kim, D.O., Côté, F., Mallet, J., and Gershon, M.D. (2011). Essential Roles of Enteric Neuronal Serotonin in Gastrointestinal Motility and the Development/Survival of Enteric Dopaminergic Neurons. J. Neurosci. *31*, 8998–9009.

Lozupone, C., and Knight, R. (2005). UniFrac: a new phylogenetic method for comparing microbial communities. Appl. Environ. Microbiol. *71*, 8228–8235.

Marciani, L., Cox, E.F., Hoad, C.L., Totman, J.J., Costigan, C., Singh, G., Shepherd, V., Chalkley, L., Robinson, M., Ison, R., et al. (2013). Effects of various food ingredients on gall bladder emptying. Eur. J. Clin. Nutr. *67*, 1182–1187.

Odunsi-Shiyanbade, S.T., Camilleri, M., McKinzie, S., Burton, D., Carlson, P., Busciglio, I.A., Lamsam, J., Singh, R., and Zinsmeister, A.R. (2010). Effects of chenodeoxycholate and a bile acid sequestrant, colesevelam, on intestinal transit and bowel function. Clin. Gastroenterol. Hepatol. Off. Clin. Pract. J. Am. Gastroenterol. Assoc. *8*, 159–165.

Pagaling, E., Strathdee, F., Spears, B.M., Cates, M.E., Allen, R.J., and Free, A. (2014). Community history affects the predictability of microbial ecosystem development. ISME J. *8*, 19–30.

Rao, A.S., Wong, B.S., Camilleri, M., Odunsi-Shiyanbade, S.T., McKinzie, S., Ryks, M., Burton, D., Carlson, P., Lamsam, J., Singh, R., et al. (2010). Chenodeoxycholate in females with

irritable bowel syndrome-constipation: a pharmacodynamic and pharmacogenetic analysis. Gastroenterology *139*, 1549–1558, 1558.e1.

Rasyid, A., and Lelo, A. (1999). The effect of curcumin and placebo on human gall-bladder function: an ultrasound study. Aliment. Pharmacol. Ther. *13*, 245–249.

Rasyid, A., Rahman, A.R.A., Jaalam, K., and Lelo, A. (2002). Effect of different curcumin dosages on human gall bladder. Asia Pac. J. Clin. Nutr. *11*, 314–318.

Ridaura, V.K., Faith, J.J., Rey, F.E., Cheng, J., Duncan, A.E., Kau, A.L., Griffin, N.W., Lombard, V., Henrissat, B., Bain, J.R., et al. (2013). Gut Microbiota from Twins Discordant for Obesity Modulate Metabolism in Mice. Science *341*, 1241214.

Romeo, G., Ronchetto, P., Luo, Y., Barone, V., Seri, M., Ceccherini, I., Pasini, B., Bocciardi, R., Lerone, M., and Kääriäinen, H. (1994). Point mutations affecting the tyrosine kinase domain of the RET proto-oncogene in Hirschsprung's disease. Nature *367*, 377–378.

Seemann, T. (2014). Prokka: rapid prokaryotic genome annotation. Bioinforma. Oxf. Engl. *30*, 2068–2069.

Shimouchi, A., Nose, K., Takaoka, M., Hayashi, H., and Kondo, T. (2009). Effect of dietary turmeric on breath hydrogen. Dig. Dis. Sci. *54*, 1725–1729.

Soret, R., Chevalier, J., De Coppet, P., Poupeau, G., Derkinderen, P., Segain, J.P., and Neunlist, M. (2010). Short-Chain Fatty Acids Regulate the Enteric Neurons and Control Gastrointestinal Motility in Rats. Gastroenterology *138*, 1772–1782.

Staver, A.C., Archibald, S., and Levin, S. (2011). Tree cover in sub-Saharan Africa: rainfall and fire constrain forest and savanna as alternative stable states. Ecology *92*, 1063–1072.

Subramanian, S., Huq, S., Yatsunenko, T., Haque, R., Mahfuz, M., Alam, M.A., Benezra, A., DeStefano, J., Meier, M.F., Muegge, B.D., et al. (2014). Persistent gut microbiota immaturity in malnourished Bangladeshi children. Nature *510*, 417–421.

Thaiss, C.A., Zeevi, D., Levy, M., Zilberman-Schapira, G., Suez, J., Tengeler, A.C., Abramson, L., Katz, M.N., Korem, T., Zmora, N., et al. (2014). Transkingdom control of microbiota diurnal oscillations promotes metabolic homeostasis. Cell *159*, 514–529.

Tsuzuki, T., Takahashi, M., Asai, N., Iwashita, T., Matsuyama, M., and Asai, J. (1995). Spatial and temporal expression of the ret proto-oncogene product in embryonic, infant and adult rat tissues. Oncogene *10*, 191–198.

Whorwell, P.J., McCallum, M., Creed, F.H., and Roberts, C.T. (1986). Non-colonic features of irritable bowel syndrome. Gut *27*, 37–40.

Wichmann, A., Allahyar, A., Greiner, T.U., Plovier, H., Lundén, G.Ö., Larsson, T., Drucker, D.J., Delzenne, N.M., Cani, P.D., and Bäckhed, F. (2013). Microbial Modulation of Energy Availability in the Colon Regulates Intestinal Transit. Cell Host Microbe *14*, 582–590.

Yano, J.M., Yu, K., Donaldson, G.P., Shastri, G.G., Ann, P., Ma, L., Nagler, C.R., Ismagilov, R.F., Mazmanian, S.K., and Hsiao, E.Y. (2015). Indigenous bacteria from the gut microbiota regulate host serotonin biosynthesis. Cell *161*, 264–276.

Yatsunenko, T., Rey, F.E., Manary, M.J., Trehan, I., Dominguez-Bello, M.G., Contreras, M., Magris, M., Hidalgo, G., Baldassano, R.N., Anokhin, A.P., et al. (2012). Human gut microbiome viewed across age and geography. Nature *486*, 222–227.

FIGURE LEGENDS

Figure 1. Diet and microbiota significantly impact intestinal transit times. **(A)** Schematic of 6-phase travel experiment. Groups of adult germ-free C57BL/6 mice were colonized with fecal microbiota from six healthy donors and fed diets representative of those consumed by all donors in the sequence shown in panel B. **(B)** The central squares of this heat map represent means of transit times for each diet-microbiota combination as measured by carmine red dye assay; the frames of the squares represent s.e.m. (n=6 mice/donor microbiota). Microbiota are represented along rows, diet phases along columns. Each group of mice consumed human diets in the order shown from left to right; home diets were always consumed during the initial and final diet phases but skipped in the intervening travel diet progression (primal diet ➔ unrestricted American diet ➔ Bangladeshi diet ➔ Malawian diet ➔ Amerindian diet). **(C)** Histogram showing distribution of all transit times recorded throughout the 6-phase travel experiment. (**D**) The most contrasted diet-by-microbiota effects on transit times were observed in mice colonized with a Bangladeshi or $USA_{unrestricted}$ microbiota and fed Bangladeshi versus primal diets. Results for $USA_{unrestricted}$ (lean) and $USA_{unrestricted}$ (obese) were aggregated and are represented together as $USA_{unrestricted}$. Results from the 'home' and 'return home' phases for mice colonized with a Bangladeshi microbiota and fed a Bangladeshi diet were also aggregated. Statistical significance was determined using a two-tailed Student's t-test; *, $p<0.05$. See also **Figures S1,S2,S3,S4** and **Tables S1,S2,S3,S4,S5**.

Figure 2. Significant correlations between fecal bile acid metabolite concentrations and the relative abundances of bacterial 97%ID OTUs. Bile acid metabolite profiling and 16S rRNA analysis was performed on fecal samples collected from mice in the 3-phase travel experiment (**Figure S2**). Spearman rank correlations were calculated between bile acid concentrations and relative abundances of 97%ID OTUs. Unsupervised hierarchical clustering was applied. Significant associations ($p<0.05$ calculated by two-tailed Student's t-test, with Bonferroni correction) between microbiota/diet and bile acids/OTUs are represented in the vertical and horizontal side panels. Associations between bile acids and motility were calculated by linear modeling with stepwise

backward feature selection, as detailed in the text and *Supplemental Experimental Procedures*. See also **Figures S2,S5** and **Tables S4,S6,S7,S8**.

Figure 3. An interaction between diet, bile acid metabolism, and gut motility revealed by colonizing germ-free mice with a BSH_{hi} or BSH_{lo} consortium and feeding them a representative Bangladeshi diet with or without turmeric. **(A)** Turmeric consumption resulted in significantly slower motility in mice colonized with the BSH_{lo} but not the BSH_{hi} consortium. **(B)** While consuming the turmeric-supplemented Bangladeshi diet, BSH_{hi} mice had transit times comparable to mice colonized with the complete 53 strain culture collection ("CC") and faster motility (i.e., shorter transit times) than BSH_{lo} mice (n=5 animals/microbiota). **(C)** Turmeric consumption is associated with a significant increase in total fecal unconjugated bile acid concentrations in gnotobiotic wild-type mice colonized with the BSH_{hi} consortium but not the BSH_{lo} consortium. **(D)** Transit times (mean±s.e.m.) measured for two groups of gnotobiotic mice colonized with BSH_{lo} consortium and fed the unsupplemented or turmeric-containing Bangladeshi diet. Measurements occurred at the end of the single (monotonous) 10-day diet experiment. Statistical significance was determined using a one-tailed Student's t-test. *, $p<0.05$. See also **Tables S4,S6,S9,S10,S11**.

FIGURES

Figure 1.

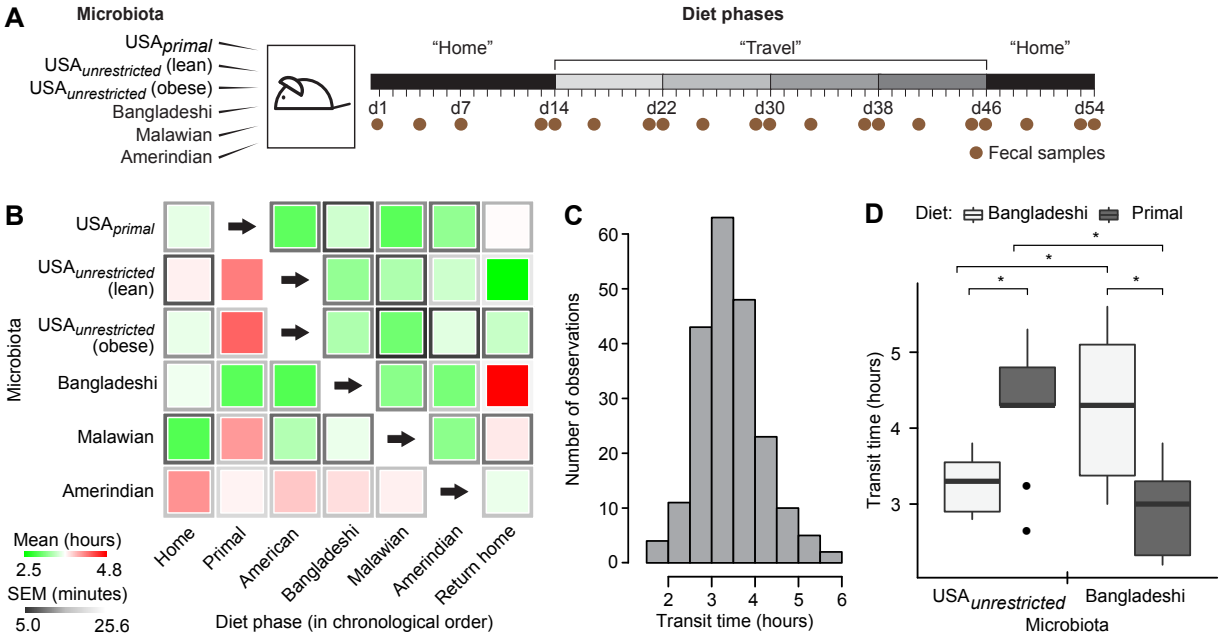

Figure 2.

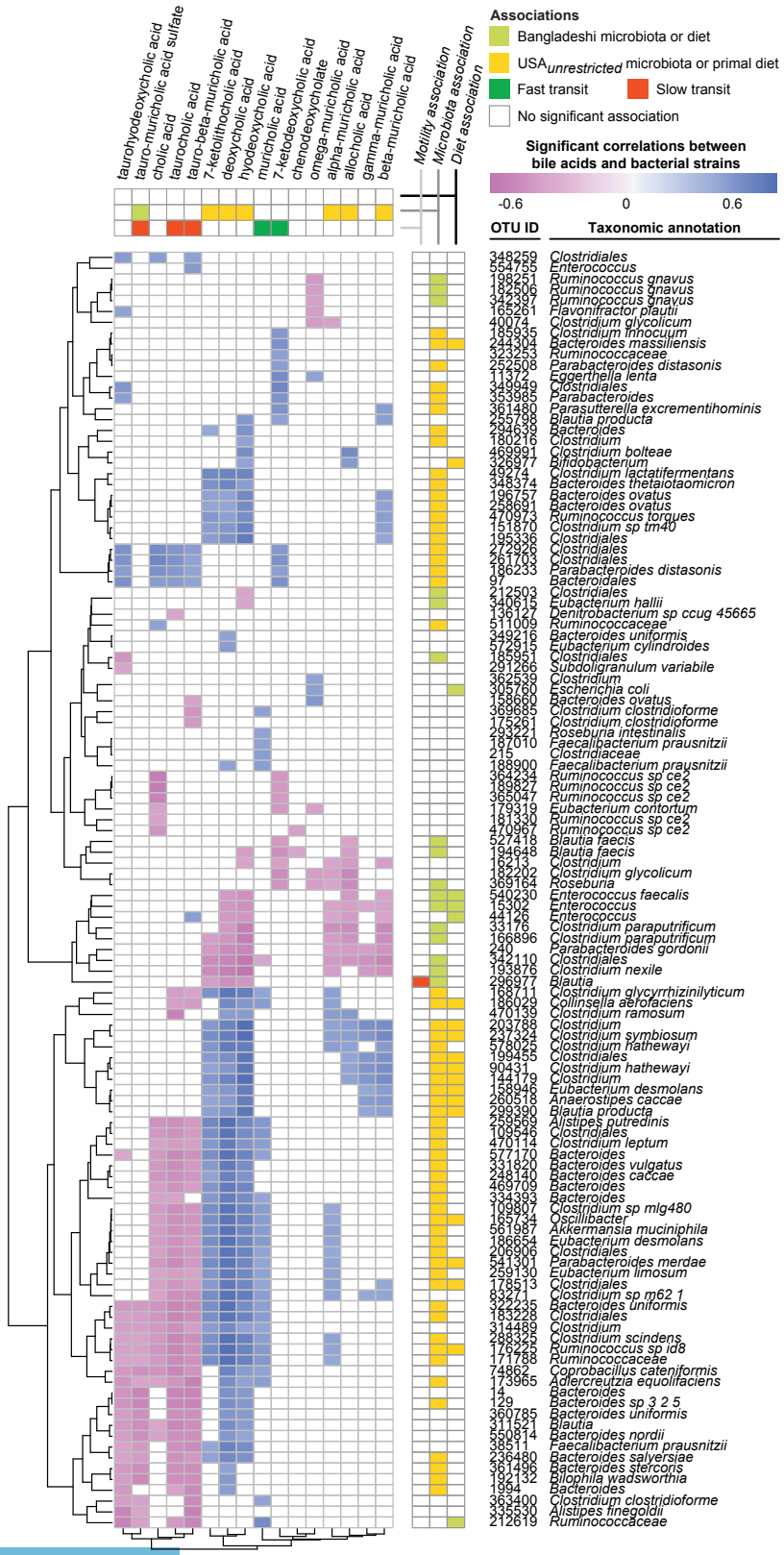

Figure 3.

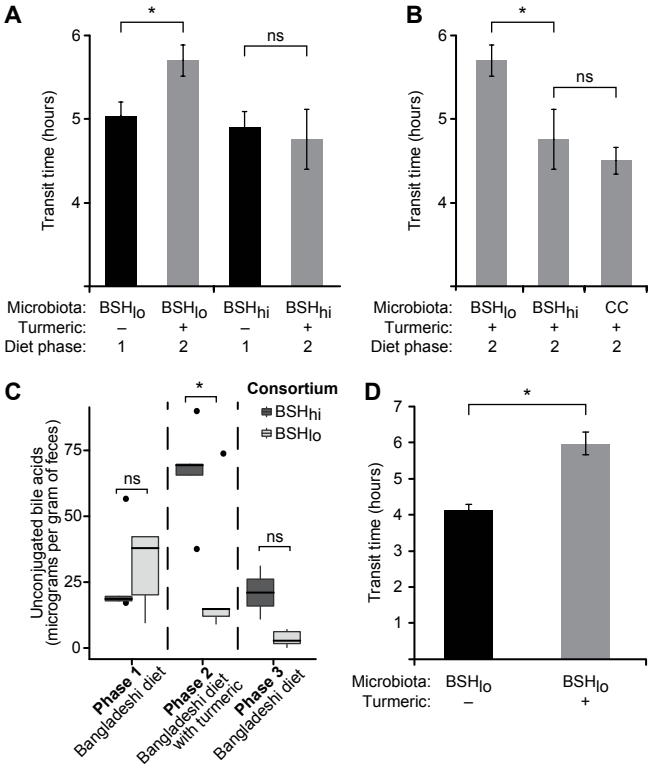

SUPPLEMENTAL INFORMATION

SUPPLEMENTAL DATA

Turmeric alters ileal expression of anti-helminthic immune functions

In the terminal ileum, a total of 96 genes exhibited significant differential expression in the face of turmeric consumption (**Table S11A**), including genes involved in gut mucosal immune/barrier function: (i) 410-fold higher expression (p=0.003) of *Retnlb* (resistin-like molecule β), (ii) 23-fold higher expression (p=0.0009) of *Siglec5* (sialic acid binding Ig-like lectin 5, an eosinophil marker), (iii) 15-fold higher expression (p=0.009) of *Fut2* [α-1,2-fucosyltransferase; a null allele of this gene in humans confers non-secretor status and is associated with Crohn's disease (Franke et al., 2010; Tong et al., 2014) while Fut2 deficiency in mice enhances susceptibility to infection with eukaryotic and bacterial pathogens (Goto et al., 2014; Hurd and Domino, 2004)], (iv) 7.8-fold higher expression (p=0.0004) of *Nfil3* [nuclear factor, interleukin 3, a transcription factor that directs development of innate lymphoid cells (ILC) (Geiger et al., 2014; Klose et al., 2014; Seillet et al., 2014; Yu et al., 2014)], (v) 4.3-fold greater expression (p=0.00006) of *Cd55* (involved in regulation of the complement cascade), (vi) 2.8-fold higher expression (p=0.02) of *Tnfrsf21* (tumor necrosis factor receptor superfamily member 21 involved in T helper cell function), and (vii) 2.2-fold higher expression (p=0.02) of *Irf2* (interferon regulatory factor 2).

Retnlb is expressed by intestinal goblet cells and enterocytes (Hogan et al., 2006) and appears to have various effects on immunity, including maintenance of mucosal barrier function (Hogan et al., 2006), macrophage activation to produce TNF-α (McVay et al., 2006; Steinbrecher et al., 2011), and protection from gut helminthic infections [e.g., by inhibiting migration of worms (Artis et al., 2004; Herbert et al., 2009)]. Eosinophils, which, as noted above, express *Siglec5*, contribute to protective immunity against parasites (Knott et al., 2007). *Nfil3* expression is linked to ILC accumulation; group 2 ILCs have been implicated in development of protective immunity to parasites (Oliphant et al., 2014) while group 3 ILCs promote *Fut2* expression and mediate resistance to bacterial pathogens such as *Salmonella* (Goto et al., 2014). Turmeric's ability to modulate

the distal ileal transcriptome is interesting in light of the South Asian Ayurvedic tradition of using crushed turmeric as an anti-helminthic (Handral et al., 2013; Nadkarni and Nadkarni, 1976). The burden of parasitic infection in this population is great (Roy et al., 2011); our findings offer one potential biological insight about why turmeric came to be ubiquitously represented in Bangladeshi cuisine. Though it is unclear whether these findings relate to our observed motility phenotypes, they may be of anthropologic significance.

SUPPLEMENTAL EXPERIMENTAL PROCEDURES

Collection of fecal samples from human microbiota donors

Human fecal specimens were collected, de-identified, and stored in a biorepository in accordance with protocols approved by the Washington University Human Research Protection Office and local IRBs for now completed observational studies conducted in the United States, Bangladesh, Malawi, and Venezuela (Yatsunenko et al., 2012; Ridaura et al., 2013; Subramanian et al., 2014; Mondal et al., 2012; Smith et al., 2013; Turnbaugh et al., 2009). Specimens were maintained at -80°C until use. Except for the fecal samples acquired from 10 raw primal dieters for the present study, all previously collected samples had been analyzed by 16S rRNA sequencing and the results described in previous reports (Yatsunenko et al., 2012; Ridaura et al., 2013; Subramanian et al., 2014).

A subset of samples from healthy adult microbiota donors representing each geographic region and culinary tradition were selected from our biorepository using the following criteria: (i) the donor was in his/her third-to-fifth decade of life; (ii) if female, the donor was not known to be pregnant or was greater than 6 months post-partum; (iii) the body mass index of the donor was greater than 21 kg/m^2; (iv) there was no reported past medical history of systemic or gastrointestinal diseases; (v) the donor was on his/her current diet for at least five years; (vi) the donor was not known to have consumed antibiotics or probiotics for at least three months prior to sampling; and (vii) the bacterial phylogenetic configuration of the sample was representative of samples collected from the geographic/culinary cohort (i.e., near the centroid of their cohort in principal

coordinates space based on unweighted UniFrac analysis of fecal bacterial 16S rRNA datasets). "Primal" dieters were defined as group that had consumed a "raw primal" diet (i.e., raw meats and vegetables) for 8 to 11 years. In addition to adult microbiota donors, a fecal microbiota sample was obtained from a 24-month-old Bangladeshi child from the Mirpur thana of Dhaka city (23.8042°N 90.3667°E) who had a healthy growth phenotype as defined by serial anthropometry (Subramanian et al., 2014). Microbiota donor features are reported in **Table S1a**.

Production of gnotobiotic mouse diets representative of those consumed by the human microbiota donors

Diets used in the current study are described in **Figure S2** and **Table S1b**. All ingredients were purchased at local grocery stores (Whole Foods Market, Global Foods Market, and Schnuck's Markets, all in St. Louis, MO). Organic products were purchased whenever possible to minimize any effects of residual fertilizers and pesticides. Fruits, vegetables, and meats were de-pitted or de-boned as needed and then chopped manually. Any requisite cooking was performed at this point. All ingredients were ultimately ground and mixed for 10 minutes in an industrial food processor (Robot Coupe Model R23, Jackson, MS), then further homogenized in an industrial mixer (Globe Equipment Company, Port Washington, NY).

The *Bangladeshi diet* was based on dietary analyses performed by the Institute of Nutrition and Food Science at the University of Dhaka (Islam et al., 2010). Rice was cooked in a standard commercial rice cooker. Tilapia fish was simmered on a hot plate (Corning Life Sciences, Tewksbury, MA; heat setting of 2) for 30 minutes with minimal water added to prevent burning prior to the addition of the vegetables (potato, spinach, tomato, cauliflower, okra, and Indian cucumber). Yellow lentils were cooked separately in a glass beaker on a hot plate for 90 minutes, with occasional stirring and minimal water periodically added to prevent burning. Ingredients were then mixed as above. For experiments involving turmeric, the Bangladeshi diet was split into two portions immediately after it was cooked. One portion was set aside as the "unsupplemented" diet. Turmeric was heated in vegetable oil (at a 1:1 volume-to-weight ratio, e.g., 1.0 mL oil to 1.0 g

turmeric) in a glass beaker on a hot plate for 10 min with occasional stirring, then added to the Bangladeshi diet and mixed in the industrial mixer for an additional 10 minutes. The amount of turmeric added to the Bangladesh diet (0.8 mg/g diet) was equivalent to 20 times the median daily consumption in South Asia (Ferrucci et al., 2010). The *raw primal diet* was based on an analysis of the most commonly consumed foods and overall nutritional intake gleaned from the food diaries of seven individuals living in the USA. Ingredients were not cooked in keeping with the food preparation habits of these people. An *American diet* was based on analyses of food journals, obtained from four individuals living in the USA with no self-imposed dietary restrictions, detailing 31 cumulative days of food intake (eight days each from three subjects and seven days from another). A dietician analyzed these journals with the Nutrition Data System for Research (NDS-R; version 4.03_31) to quantify the macronutrients and micronutrients consumed by each subject. The means of daily consumption of dietary energy (kilocalories), carbohydrates, proteins and fats were calculated. These mean values served as the benchmarks against which *in silico* menus were evaluated. Randomly generated menus were created by sampling 41 of the journal entries. Thousands of randomized menus were produced; the representative diet used for our study was the one whose calculated values was closest to the means. All *in silico* diet design was conducted in software R version 3.1.2 (R Development Core Team, 2013). The *Malawian diet* was based on staple foods consumed by individuals living in rural southern Malawi, and cooked using procedures described in an earlier publication (Smith et al., 2013). The *Amerindian diet* was based on foods consumed by individuals from the Guahibo Amerindian families living in villages near Puerto Ayacucho in the Amazonas State of Venezuela (Yatsunenko et al., 2012). Catfish and eggs were simmered on a hot plate for 20 minutes with minimal water added to prevent burning, prior to addition of the remaining ingredients (corn flour, cassava flour, and powdered whole milk). Minimal modifications to the recipes were made as needed to ensure that all diets satisfied the recommended daily intake of macro- and micronutrients for mice (National Research Council (US) Subcommittee on Laboratory Animal Nutrition, 1995).

Aliquots (250 g or 500 g) of each diet type were double-sealed (vacuum packed) and double-bagged before sterilization by irradiation (dose 20-50 kGy; Steris Isomedix Corporation, Chicago, IL). Sterility was confirmed by (i) spore strips (North American Science Associates Inc, Northwood, OH) that were placed in each box of bagged food prior to irradiation and (ii) culturing aliquots of a representative bag from each irradiated box for 7 days at 35°C under aerobic conditions in BHI broth (BD Diagnostics, Sparks, MD), nutrient broth (BD Diagnostics, Sparks, MD), and Sabouraud dextrose broth (BD Diagnostics, Sparks, MD) prior to plating on blood agar plates. The nutritional content of diets was confirmed by direct analyses of micronutrients and macronutrients (N-P Analytic Laboratories, Nestlé Purina Petcare, St. Louis, MO; see **Table S1b)**. Irradiated, vacuum-packed diets were stored at 4°C until use.

Preparation of human fecal microbiota for transplantation into gnotobiotic mice

Clarified fecal microbiota suspensions were prepared from previously frozen human fecal samples in an anaerobic chamber (Coy Lab Products, Grass Lake, MI; atmosphere composed of 75% N_2, 20% CO_2, and 5% H_2) using a protocol detailed in an earlier report (Ridaura et al., 2013) that was modified as follows: in place of pulverization with a mortar and pestle, samples (500 mg) were diluted in 15 mL of reduced PBS (PBS supplemented with 0.1% Resazurin (w/v) and 0.05% L-cysteine-HCl), homogenized in a blender for 1 minute, and passed through a 40 μm pore diameter nylon cell strainer (BD Falcon, Franklin Lakes, NJ). Clarified fecal microbiota suspensions were stored in reduced PBS with 15% glycerol at -80°C until use.

Animal husbandry

All gnotobiotic mouse experiments were performed using protocols approved by the Washington University Animal Studies Committee. Conventionally raised C57BL/6 *Ret* +/- mice were re-derived as germ-free by embryo transfer (Faith et al., 2011) and maintained in sterile, flexible, plastic gnotobiotic isolators (Class Biologically Clean Ltd., Madison, WI) under a strict 12-hour cycle. All mice used in our experiments were 8-12 weeks old.

In each of the experiments described this report, feeding of the initial diet was started three days prior to colonization with uncultured fecal microbiota samples or with cultured bacterial consortia. Age-matched male germ-free C57BL/6 mice within a given isolator were gavaged with the same bacterial community, or maintained as germ-free. Mice were co-housed as described below. Autoclaved Aspen hardwood lab bedding (NEPCO, Warrensburg, NY) was replaced with new bedding at the start of each new diet phase to limit carryover of ingredients from the prior diet phase. Total intestinal transit times were measured at the end of each diet phase by gavaging mice with red carmine dye and recording the time from gavage to first appearance of the dye in their feces (see below for details)

Six-phase travel experiment. Six groups of mice (*n*=6 mice per group) were colonized with uncultured fecal microbiota samples obtained from six healthy adults representing different cultural/culinary traditions and geographic locations. Each group of mice designated to receive the same donor's microbiota was placed in a separate gnotobiotic isolator prior to gavage; within each isolator, mice were triply housed (*n*=3 mice per cage). Mice were fed a sequence of sterilized diets formulated to represent those consumed by the microbiota donors (ingredients and preparation detailed above). The starting and ending 'home' diets were given for 14 and 8 days, respectively, while each of the four intermediate 'travel' diets was administered for 8 days.

Three-phase travel experiment. Six groups of mice (*n*=5 mice per group) were colonized with uncultured fecal microbiota samples obtained from healthy adults living in Bangladesh (*n*=3 donors) and the USA (specifically, $USA_{unrestricted}$; *n*=3 donors). Each group of mice resided in a separate flexible film gnotobiotic isolator where they were co-housed in two cages (*n*=2-3 mice per cage). Mice were fed a sequence of sterilized Bangladeshi and primal diets with the starting and ending diet representing a 'local' diet of the microbiota donor: mice colonized with a $USA_{unrestricted}$ microbiota were fed the primal diet, while mice colonized with a Bangladeshi microbiota were fed the Bangladeshi diet. The starting and ending phase diets were given for 14 and 8 days, respectively, while the second (intermediate) phase 'non-native' diet was administered for 8 days.

Assessing the effects of turmeric in germ-free mice versus those colonized with the clonally arrayed bacterial culture collection. Two groups of mice (*n*=6 mice per group) were either maintained as germ-free or colonized with the clonally arrayed culture collection derived from the fecal microbiota of the Bangladeshi child with a healthy growth phenotype. Each group of mice resided in a separate gnotobiotic isolator (*n*=3 mice per cage). Mice were fed a sequence of sterilized diets formulated to represent Bangladeshi diet, with or without turmeric. Each diet phase was 10 days in length. The starting and ending diets were unsupplemented (i.e., lacked turmeric), while the intermediate phase diet contained turmeric.

Comparing the effects of BSH_{hi} and BSH_{lo} consortia with and without turmeric in wild-type Ret+/+ and heterozygous Ret+/- C57BL6/J mice. Three groups of mice (*n*=5 mice per group) were colonized with (i) the entire clonally arrayed culture collection, (ii) the 7-member BSH_{hi} consortium, or (iii) the 7-member BSH_{lo} consortium. Each group of mice was housed in a separate gnotobiotic isolator containing two cages (*n*=2-3 mice per cage). Mice were fed a sequence of sterilized diets formulated to represent the Bangladeshi diet, with or without turmeric. Each diet phase was 8 days in length. The starting and ending diets were unsupplemented while the intermediate diet contained turmeric. Two additional groups of *Ret*+/- mice (*n*=5 mice per group) were colonized with either the BSH_{hi} or BSH_{lo} consortium. Recipient mice containing a given consortium were housed in the same isolators (but in separate cages) as wild-type mice harboring the same consortium (*n*=2-3 mice per cage).

Effects of turmeric on host gene expression in mice harboring the BSH_{lo} consortium. Two groups of wild-type mice (*n*=3-4 mice per group; 1 cage per group) were colonized with the "BSH_{lo}" consortium. Mice were fed the Bangladeshi diet, with or without turmeric, over the course of a single diet phase that was 10 days long. Distal ileum and liver samples collected at the time of sacrifice were used for mouse RNA-Seq, performed as described below.

Sample collection from gnotobiotic mice

Before colonization and throughout each experiment, fecal pellets were collected from mice at pre-established time points, including on the days of transit time measurements, with care taken to collect pellets prior to the passage of carmine dye. Samples were snap frozen in liquid nitrogen within 30 minutes of their collection and stored at -80°C until use. At the conclusion of each experiment (>48 hours after the last carmine dye assay), the following biospecimens were procured after weighing and sacrificing each animal: liver, small intestine, cecal contents, colon, and feces. The small intestine was partitioned into 8 equal-sized segments. Segment 8 was operationally defined as 'terminal ileum'. Samples were immediately snap frozen in liquid nitrogen and stored at -80°C until use.

Multiplex sequencing and analysis of PCR amplicons generated from bacterial 16S rRNA genes

Genomic DNA was extracted from mouse fecal pellets as described previously (Turnbaugh et al., 2009). Primers 515F and 806R with sample-specific barcodes were used to generate PCR amplicons spanning variable region 4 (V4) of bacterial 16S rRNA genes present in the fecal samples. Libraries of these V4-16S rRNA amplicons were subjected to multiplex sequencing on the Illumina MiSeq platform (250 nt paired-end reads; see **Table S4** for details regarding multiplexing and sequencing depth). Paired-end reads were trimmed to 200 base pairs to retain the highest-quality sequences, and aligned using the flash aligner (Magoč and Salzberg, 2011). 16S rRNA reads were grouped into operational taxonomic units based on whether they shared ≥97% nucleotide sequence identity (97%ID OTUs). We employed an open-reference OTU-picking strategy (QIIME; version 1.5.0) (Caporaso et al., 2010), where reads were clustered against the Greengenes reference database (DeSantis et al., 2006) using the UCLUST algorithm (Edgar, 2010). Any reads that did not match entries in the reference dataset were clustered *de novo*. OTUs were picked using the combined V4-16S rRNA sequence datasets from all mouse experiments, so that OTU IDs and associated taxonomic annotations would be uniform across the corresponding analyses. OTUs with

proportional abundances of at least 0.1% in at least 1% of all samples were retained for downstream analysis. Taxonomy was assigned to OTUs using the Ribosomal Database Project (RDP) version 2.4 classifier, which enabled classifications at the phylum, class, order, family, genus, and species level (Ridaura et al., 2013). Samples were rarefied to a depth of 4080 reads per sample. Unweighted and weighted UniFrac was used to calculate beta diversity indices; principal coordinates analysis (PCoA) plots were generated using these data.

Community profiling by sequencing (COPRO-Seq)

Genomic DNA was extracted from mouse fecal pellets (Turnbaugh et al., 2009) that had been collected throughout experiments involving mice colonized with either the complete culture collection, or the BSH_{hi} or BSH_{lo} consortia. Multiplexed DNA libraries were prepared from genomic DNA samples as described (Faith et al., 2011; McNulty et al., 2011) and subjected to shotgun sequencing using an Illumina MiSeq platform to generate 75 nt unidirectional reads (see **Table S4** for details regarding multiplexing and sequencing depth). The analytic pipeline described in a previous publication (McNulty et al., 2011), and available at https://github.com/nmcnulty/COPRO-Seq, was used to map reads to the sequenced genomes of members of the culture collection and calculate their relative abundances in the fecal microbiota of gnotobiotic mice.

Profiling the fecal meta-transcriptomes of gnotobiotic mice using microbial RNA-Seq

Bacterial community transcriptional responses to turmeric were profiled in fecal samples collected from eight male age-matched wild-type C57BL/6 mice, colonized with the 7-member BSH_{hi} or BSH_{lo} 7- consortia, at two time points (8 and 16 days after gavage, which corresponded to periods where animals were consuming the Bangladeshi diet lacking and containing turmeric, respectively). Multiplexed cDNA libraries were prepared as described previously (Faith et al., 2011; McNulty et al., 2011; Ridaura et al., 2013) with the following modification: after removal of 5S rRNA and tRNA with a MEGAclear column (Life Technologies, Carlsbad, CA) remaining rRNA was depleted using the Ribo-Zero™ rRNA Removal Kit for Bacteria (Epicentre, Madison, WI). Multiplexed libraries were sequenced using a Illumina NextSeq instrument to generate 75 nt uni-

directional reads (see **Table S4** for details regarding multiplexing and sequencing depth). Analysis was performed as previously described (Ridaura et al., 2013) with the custom reference database consisting of the 14 genomes of the 14 strains that comprised the two BSH consortia. Following gene assignments, pathway analysis was performed using the KEGG reference database (release 72.1) (Kanehisa and Goto, 2000; Kanehisa et al., 2014).

Profiling the host transcriptome using RNA-Seq

We used RNA-Seq to characterize gene expression in the livers and ileums of seven age-matched wild-type C57BL/6 mice colonized with the BSH_{lo} consortium and fed the Bangladeshi diet with or without turmeric. For each sample, 20-30 mg of tissue was placed in pre-cooled RNAlater®-ICE (Life Technologies, Carlsbad, CA) and stored at -20°C for at least 16 hours. Total RNA was extracted using the RNeasy Mini Kit (Qiagen, Venlo, Limburg) after tissue disruption and homogenization (TissueLyser, Qiagen). 5S rRNA and tRNA were depleted from the sample (MEGAclear column purification) followed by treatment with RNase-free TURBO™ DNase (Life Technologies). Cytoplasmic and mitochondrial rRNA were then depleted using the Ribo-Zero™ rRNA Removal Kit for Human/Mouse/Rat (Epicentre, Madison, WI). (This approach was used rather than poly(A) enrichment to obtain more even coverage since Ribo-Zero™ does not have a 3' end bias). RNA was precipitated with ethanol, followed by a second DNase treatment (Baseline-ZERO™ DNase; Epicentre, Madison, WI). First strand cDNA synthesis was accomplished using SuperScript II Reverse Transcriptase (Life Technologies), followed by second strand cDNA synthesis with *E. coli* DNA polymerase, *E. coli* DNA ligase, and RNase H (all from New England Biolabs, Ipswich, Massachusetts). Double-stranded cDNA was purified using QIAquick purification columns (Qiagen) before shearing (BioRuptor XL sonicator; Diagenode, Denville, NJ). ~250 bp fragments were size-selected by extraction from 2% agarose gels. Multiplex libraries were prepared and subjected to sequencing on the Illumina NextSeq platform to generate 75 nt unidirectional reads.

Analysis was limited to reads that contained exact 5' sequence matches to barcodes utilized for multiplexing and no more than 1 expected error, as calculated by Q scores via usearch (version 8.0.1517) (Edgar, 2010). (See **Table S4** for details regarding multiplexing, sequencing depth, filtering, and mapping of the resulting high-quality sequences). Reads were mapped to the *Mus musculus* C57BL/6J strain genome (UCSC mm10) using Bowtie2 (version 2.2.4) (Langmead and Salzberg, 2012), with subsequent alignment and splice junction mapping (TopHat2, version 2.0.13) (Kim et al., 2013). 81.8%- 89.0% of input sequences could be mapped. These data were imported into R (version 3.1.2) (R Development Core Team, 2013) for analysis using the *edgeR* package (version 3.8.5) (Robinson et al., 2010). Separate analyses were conducted for liver and distal ileum RNA-Seq datasets. Low-expression genes were filtered out: only those with an abundance of at least 1 count per million reads in more than one sample and at least 10 counts per million reads in one sample were retained. Trimmed mean of M-values (TMM) normalization was applied. The coefficient of biological variation (the square root of dispersion under the negative binomial model) was estimated across the entire dataset for each tissue and for each gene. Differentially expressed genes were then identified using the exact negative binomial test, which is appropriate since a single variable (turmeric consumption) was being investigated. Significance was corrected for multiple comparisons using the method of Benjamini-Hochberg (Benjamini and Hochberg, 1995), as reported in **Table S11**.

Ultra High Performance Liquid Chromatography-Mass Spectrometry (UPLC-MS)

Sample processing - Frozen fecal samples were combined with 20 volumes of ice cold methanol and 1 volume of cholic acid-$^{13}C_1$ (200 mg/ml; Sigma-Aldrich, St. Louis, MO), and then shaken for 2 minutes in a bead beater (Biospec Products; maximal setting; no beads added) before incubation at -20°C for 1 hour. Samples were then centrifuged at 4°C for 10 minutes at 20,800 x g. The supernatant (200 µL) was collected and dried in a SpeedVac at room temperature (requiring a spin time of 2-3 hours). Dried samples were re-suspended in 100 µL of 5% ethanol (in water) by a combination of pipetting, vigorous shaking in a bead beater, and sonication. After centrifugation for 5 minutes at 20,800 x g at 4°C, the supernatant was separated for UPLC-MS. Analyses were

performed on a Waters Acquity I Class UPLC system (Waters Corp., Milford, MA) coupled to an LTQ-Orbitrap Discovery (Thermo Fisher Corporation). For the 150 mm x 2.1 mm Waters BEH C18 1.7 mm particle column, injection volume was 5 µL, and the flow rate was 0.3 mL per minute. Mobile phases for positive ion mode were (i) 0.1% formic acid in water and (ii) 0.1% formic acid in acetonitrile, whereas negative ion mode used (i) 5 mM ammonium bicarbonate in water and (ii) 5 mM ammonium bicarbonate in 95/5 acetonitrile/water. The capillary column was maintained at 325°C with a sheath gas flow of 40 (arbitrary units), an aux gas flow of 5 (arbitrary units) and a sweep gas flow of 3 (arbitrary units) for both positive and negative injections. The spray voltage was 4.5 kV for the positive ion injection and 4 kV for the negative ion injection.

Data pre-processing - Data in instrument specific format (.D) were converted to common data format (.cdf) files using MSD ChemStation (E02.01, Agilent Technologies, Santa Clara, CA). The .cdf files were extracted using Bioinformatics Toolbox in MATLAB 7.1 (The MathWorks, Inc., Natick, MA), along with custom scripts (Cheng et al., 2011) for alignment of data in the time domain, automatic integration, and extraction of peak intensities. The resulting three-dimension data set included sample information, peak retention time, and peak intensities. Data were then mean-centered and unit variance-scaled for multivariate analysis, which was performed in R (version 3.1.2) (R Development Core Team, 2013) using custom scripts.

Quality control of metabolomics data - Pooled quality control (QC) samples were prepared from 8-10 µL aliquots of 10 samples and analyzed together with the other samples. QC samples were inserted and analyzed every 10 samples. Metabolite identification was done by co-characterization of standards.

Statistical analyses

Routine statistical analyses were performed in R (version 3.1.2) (R Development Core Team, 2013) using custom scripts that are available upon request. Linear modeling, including stepwise backward feature selection, statistical correlations and comparisons, and Bonferroni corrections for multiple comparisons were performed using functions within the default *stats* package (version

3.1.2).

Diet-discriminatory OTUs were identified using the Random Forests supervised machine learning algorithm as implemented in the *randomForest* package (version 4.6-10) (Liaw and Wiener, 2002) following 100 replications per diet-microbiota combination (parameters: ntree, 1000; importance scores tracked; otherwise default values). Initial modeling was performed to identify diet-discriminatory taxa in fecal samples obtained from mice colonized with the same donor microbiota. Mean importance scores were then aggregated, and hierarchical clustering was applied to examine whether OTUs were diet-discriminatory across different microbiota. The accuracy of the model built on the basis of the 6-phase travel experiment results was tested on experimental data from the 3-phase travel using 10,000 replications (parameters: ntree, 1000; importance scores tracked; otherwise default values). Out-of-bag error estimations were determined by iterating through OTUs that had been ranked by mean importance score to determine the performances of the resulting Random Forests models.

Figures were generated using R, employing for several figures *ggplot2* (version 1.0.0) (Wickham, 2009) and *pheatmap* (version 0.7.7) (Kolde, 2013) packages.

REFERENCES

Artis, D., Wang, M.L., Keilbaugh, S.A., He, W., Brenes, M., Swain, G.P., Knight, P.A., Donaldson, D.D., Lazar, M.A., Miller, H.R.P., et al. (2004). RELMbeta/FIZZ2 is a goblet cell-specific immune-effector molecule in the gastrointestinal tract. Proc. Natl. Acad. Sci. U. S. A. *101*, 13596–13600.

Benjamini, Y., and Hochberg, Y. (1995). Controlling the False Discovery Rate: A Practical and Powerful Approach to Multiple Testing. J. R. Stat. Soc. Ser. B Methodol. *57*, 289–300.

Caporaso, J.G., Kuczynski, J., Stombaugh, J., Bittinger, K., Bushman, F.D., Costello, E.K., Fierer, N., Peña, A.G., Goodrich, J.K., Gordon, J.I., et al. (2010). QIIME allows analysis of high-throughput community sequencing data. Nat. Methods *7*, 335–336.

Cheng, J., Xia, Y., Zhou, Y., Guo, F., and Chen, G. (2011). Application of an ultrasound-assisted surfactant-enhanced emulsification microextraction method for the analysis of diethofencarb and pyrimethanil fungicides in water and fruit juice samples. Anal. Chim. Acta *701*, 86–91.

DeSantis, T.Z., Hugenholtz, P., Larsen, N., Rojas, M., Brodie, E.L., Keller, K., Huber, T., Dalevi, D., Hu, P., and Andersen, G.L. (2006). Greengenes, a chimera-checked 16S rRNA gene database and workbench compatible with ARB. Appl. Environ. Microbiol. *72*, 5069–5072.

Edgar, R.C. (2010). Search and clustering orders of magnitude faster than BLAST. Bioinformatics *26*, 2460–2461.

Faith, J.J., McNulty, N.P., Rey, F.E., and Gordon, J.I. (2011). Predicting a human gut microbiota's response to diet in gnotobiotic mice. Science *333*, 101–104.

Ferrucci, L.M., Daniel, C.R., Kapur, K., Chadha, P., Shetty, H., Graubard, B.I., George, P.S., Osborne, W., Yurgalevitch, S., Devasenapathy, N., et al. (2010). Measurement of spices and seasonings in India: Opportunities for cancer epidemiology and prevention. Asian Pac. J. Cancer Prev. APJCP *11*, 1621–1629.

Franke, A., McGovern, D.P.B., Barrett, J.C., Wang, K., Radford-Smith, G.L., Ahmad, T., Lees, C.W., Balschun, T., Lee, J., Roberts, R., et al. (2010). Genome-wide meta-analysis increases to 71 the number of confirmed Crohn's disease susceptibility loci. Nat. Genet. *42*, 1118–1125.

Geiger, T.L., Abt, M.C., Gasteiger, G., Firth, M.A., O'Connor, M.H., Geary, C.D., O'Sullivan, T.E., van den Brink, M.R., Pamer, E.G., Hanash, A.M., et al. (2014). Nfil3 is crucial for development of innate lymphoid cells and host protection against intestinal pathogens. J. Exp. Med. *211*, 1723–1731.

Goto, Y., Obata, T., Kunisawa, J., Sato, S., Ivanov, I.I., Lamichhane, A., Takeyama, N., Kamioka, M., Sakamoto, M., Matsuki, T., et al. (2014). Innate lymphoid cells regulate intestinal epithelial cell glycosylation. Science *345*, 1254009.

Handral, H.K., Duggi, S., Handral, R., G, T., and D, S.S. (2013). Turmeric: Nature's precious medicine. Asian J. Pharm. Clin. Res. *6*, 10–16.

Herbert, D.R., Yang, J.-Q., Hogan, S.P., Groschwitz, K., Khodoun, M., Munitz, A., Orekov, T., Perkins, C., Wang, Q., Brombacher, F., et al. (2009). Intestinal epithelial cell secretion of RELM-beta protects against gastrointestinal worm infection. J. Exp. Med. *206*, 2947–2957.

Hogan, S.P., Seidu, L., Blanchard, C., Groschwitz, K., Mishra, A., Karow, M.L., Ahrens, R., Artis, D., Murphy, A.J., Valenzuela, D.M., et al. (2006). Resistin-like molecule β regulates innate colonic function: Barrier integrity and inflammation susceptibility. J. Allergy Clin. Immunol. *118*, 257–268.

Hurd, E.A., and Domino, S.E. (2004). Increased susceptibility of secretor factor gene Fut2-null mice to experimental vaginal candidiasis. Infect. Immun. *72*, 4279–4281.

Islam, S.N., Khan, M.N.I., and Akhtaruzzaman, M. (2010). A Food Composition Database for Bangladesh with Special reference to Selected Ethnic Foods (INFS-NFPCSP-FAO, Dhaka, Bangladesh).

Kanehisa, M., and Goto, S. (2000). KEGG: kyoto encyclopedia of genes and genomes. Nucleic Acids Res. *28*, 27–30.

Kanehisa, M., Goto, S., Sato, Y., Kawashima, M., Furumichi, M., and Tanabe, M. (2014). Data, information, knowledge and principle: back to metabolism in KEGG. Nucleic Acids Res. *42*, D199–D205.

Kim, D., Pertea, G., Trapnell, C., Pimentel, H., Kelley, R., and Salzberg, S.L. (2013). TopHat2: accurate alignment of transcriptomes in the presence of insertions, deletions and gene fusions. Genome Biol. *14*, R36.

Klose, C.S.N., Flach, M., Möhle, L., Rogell, L., Hoyler, T., Ebert, K., Fabiunke, C., Pfeifer, D., Sexl, V., Fonseca-Pereira, D., et al. (2014). Differentiation of type 1 ILCs from a common progenitor to all helper-like innate lymphoid cell lineages. Cell *157*, 340–356.

Knott, M.L., Matthaei, K.I., Giacomin, P.R., Wang, H., Foster, P.S., and Dent, L.A. (2007). Impaired resistance in early secondary Nippostrongylus brasiliensis infections in mice with defective eosinophilopoeisis. Int. J. Parasitol. *37*, 1367–1378.

Kolde, R. (2013). pheatmap: Pretty Heatmaps.

Langmead, B., and Salzberg, S.L. (2012). Fast gapped-read alignment with Bowtie 2. Nat. Methods *9*, 357–359.

Liaw, A., and Wiener, M. (2002). Classification and Regression by randomForest. R News *2*, 18–22.

Magoč, T., and Salzberg, S.L. (2011). FLASH: fast length adjustment of short reads to improve genome assemblies. Bioinforma. Oxf. Engl. *27*, 2957–2963.

McNulty, N.P., Yatsunenko, T., Hsiao, A., Faith, J.J., Muegge, B.D., Goodman, A.L., Henrissat, B., Oozeer, R., Cools-Portier, S., Gobert, G., et al. (2011). The Impact of a Consortium of Fermented Milk Strains on the Gut Microbiome of Gnotobiotic Mice and Monozygotic Twins. Sci. Transl. Med. *3*, 106ra106.

McVay, L.D., Keilbaugh, S.A., Wong, T.M.H., Kierstein, S., Shin, M.E., Lehrke, M., Lefterova, M.I., Shifflett, D.E., Barnes, S.L., Cominelli, F., et al. (2006). Absence of bacterially induced RELMbeta reduces injury in the dextran sodium sulfate model of colitis. J. Clin. Invest. *116*, 2914–2923.

Mondal, D., Minak, J., Alam, M., Liu, Y., Dai, J., Korpe, P., Liu, L., Haque, R., and Petri, W.A. (2012). Contribution of enteric infection, altered intestinal barrier function, and maternal malnutrition to infant malnutrition in Bangladesh. Clin. Infect. Dis. Off. Publ. Infect. Dis. Soc. Am. *54*, 185–192.

Nadkarni, K.M., and Nadkarni, A.K. (1976). In Indian Materia Medica, Mumbai, M/S Popular Prakashan Pvt, (Ltd), pp. 1175–1181.

National Research Council (US) Subcommittee on Laboratory Animal Nutrition (1995). Nutrient Requirements of Laboratory Animals (Washington, D.C.: National Academies Press).

Oliphant, C.J., Hwang, Y.Y., Walker, J.A., Salimi, M., Wong, S.H., Brewer, J.M., Englezakis, A., Barlow, J.L., Hams, E., Scanlon, S.T., et al. (2014). MHCII-mediated dialog between group 2 innate lymphoid cells and CD4(+) T cells potentiates type 2 immunity and promotes parasitic helminth expulsion. Immunity *41*, 283–295.

R Development Core Team (2013). R: A language and environment for statistical computing (Vienna, Austria: R Foundation for Statistical Computing).

Ridaura, V.K., Faith, J.J., Rey, F.E., Cheng, J., Duncan, A.E., Kau, A.L., Griffin, N.W., Lombard, V., Henrissat, B., Bain, J.R., et al. (2013). Gut Microbiota from Twins Discordant for Obesity Modulate Metabolism in Mice. Science *341*, 1241214.

Robinson, M.D., McCarthy, D.J., and Smyth, G.K. (2010). edgeR: a Bioconductor package for differential expression analysis of digital gene expression data. Bioinforma. Oxf. Engl. *26*, 139–140.

Roy, E., Hasan, K.Z., Haque, R., Haque, A.F., Siddique, A.K., and Sack, R.B. (2011). Patterns and risk factors for helminthiasis in rural children aged under 2 in Bangladesh. South Afr. J. Child Health *5*, 78–84.

Seillet, C., Rankin, L.C., Groom, J.R., Mielke, L.A., Tellier, J., Chopin, M., Huntington, N.D., Belz, G.T., and Carotta, S. (2014). Nfil3 is required for the development of all innate lymphoid cell subsets. J. Exp. Med. *211*, 1733–1740.

Smith, M.I., Yatsunenko, T., Manary, M.J., Trehan, I., Mkakosya, R., Cheng, J., Kau, A.L., Rich, S.S., Concannon, P., Mychaleckyj, J.C., et al. (2013). Gut Microbiomes of Malawian Twin Pairs Discordant for Kwashiorkor. Science *339*, 548–554.

Steinbrecher, K.A., Harmel-Laws, E., Garin-Laflam, M.P., Mann, E.A., Bezerra, L.D., Hogan, S.P., and Cohen, M.B. (2011). Murine guanylate cyclase C regulates colonic injury and inflammation. J. Immunol. *186*, 7205–7214.

Subramanian, S., Huq, S., Yatsunenko, T., Haque, R., Mahfuz, M., Alam, M.A., Benezra, A., DeStefano, J., Meier, M.F., Muegge, B.D., et al. (2014). Persistent gut microbiota immaturity in malnourished Bangladeshi children. Nature *510*, 417–421.

Tong, M., McHardy, I., Ruegger, P., Goudarzi, M., Kashyap, P.C., Haritunians, T., Li, X., Graeber, T.G., Schwager, E., Huttenhower, C., et al. (2014). Reprograming of gut microbiome energy metabolism by the FUT2 Crohn's disease risk polymorphism. ISME J.

Turnbaugh, P.J., Hamady, M., Yatsunenko, T., Cantarel, B.L., Duncan, A., Ley, R.E., Sogin, M.L., Jones, W.J., Roe, B.A., Affourtit, J.P., et al. (2009). A core gut microbiome in obese and lean twins. Nature *457*, 480–484.

Wickham, H. (2009). ggplot2: elegant graphics for data analysis (Springer New York).

Yatsunenko, T., Rey, F.E., Manary, M.J., Trehan, I., Dominguez-Bello, M.G., Contreras, M., Magris, M., Hidalgo, G., Baldassano, R.N., Anokhin, A.P., et al. (2012). Human gut microbiome viewed across age and geography. Nature *486*, 222–227.

Yu, X., Wang, Y., Deng, M., Li, Y., Ruhn, K.A., Zhang, C.C., and Hooper, L.V. (2014). The basic leucine zipper transcription factor NFIL3 directs the development of a common innate lymphoid cell precursor. eLife *3*.

SUPPLEMENTAL FIGURE LEGENDS

Figure S1. Compositions of diets used in the 6-phase travel experiment (related to Figure 1). In the foreground, word clouds convey the specific ingredients used: font sizes depict the weight-based proportional representations of ingredients within each diet. Pie charts in the background present the macromolecular compositions.

Figure S2. Three-phase travel experiment (related to Figures 1D, 2). (A) Experimental design. Six groups of gnotobiotic mice (n=5 animals/donor microbiota) were colonized with intact fecal microbiota from one of six healthy adults (three from Bangladesh, three from the USA) and then subjected to the three serial diet phases shown. **(B)** The most contrasted diet-by-microbiota effects originally observed in the 6-phase travel experiment (**Figure 1D**) were reproducible across microbiota donors living in a given geographic area. The results from the initial and final 'local' phases were aggregated. *, p<0.05 (two-tailed Student's t-test).

Figure S3. Fecal microbiota transplantation is reproducible and results in significant within-group similarity (related to Figures 1). Principal coordinates analysis (PCoA) plots of unweighted UniFrac distances calculated from the fecal microbiota 16S rRNA profiles of gnotobiotic mice in the 6-phase travel experiment **(A,B)** and the 3-phase travel experiment **(C,D)**. PC1, the principal coordinate that explains the greatest amount of variance, is shown as a function of days post gavage of the donor microbiota, with diet phases annotated (panels A and C) and with relation to PC2 (panels B and D). Each dot represents a single fecal sample, color-coded by microbiota donor. Microbiota donor is the major determinant of clustering of fecal microbiota in recipient mice.

Figure S4. Diet-discriminatory OTUs are robust to different donor microbiota and motility phenotypes (related to Figure 1). (A) Out-of-bag estimated error rates in a Random Forests model for predicting diet, stratified by donor microbiota, as a function of numbers of diet-discriminatory OTUs. For each microbiota, 40 OTUs were sufficient to discriminate diet, yielding a total of 87 unique OTUs across six microbiota donors from five cultural/dietary traditions in the 6-phase travel experiment. **(B)** Evidence for the robustness of diet-discriminatory OTUs to donor micro-

biota and motility phenotype. Feature importance scores of 87 diet-discriminatory OTUs in each diet-microbiota context are represented in this heat map. A sparse Random Forests model built using these diet-discriminatory OTUs accurately predicted diet in the 3-phase travel experiment.

Figure S5. Fecal bile acid levels predict gut transit time (related to Figure 2). In the 3-phase travel experiment representing six microbiota donors from two cultural/dietary traditions, a linear model built using fecal levels of five bile acids (7-ketodeoxycholic acid, muricholic acid, tauro-cholic acid, tauro-beta-muricholic acid, and tauro-muricholic acid sulfate) can predict transit times accurately, out-performing a linear model built using five randomly selected metabolites that were not individually correlated with transit times.

SUPPLEMENTAL FIGURES

Figure S1.

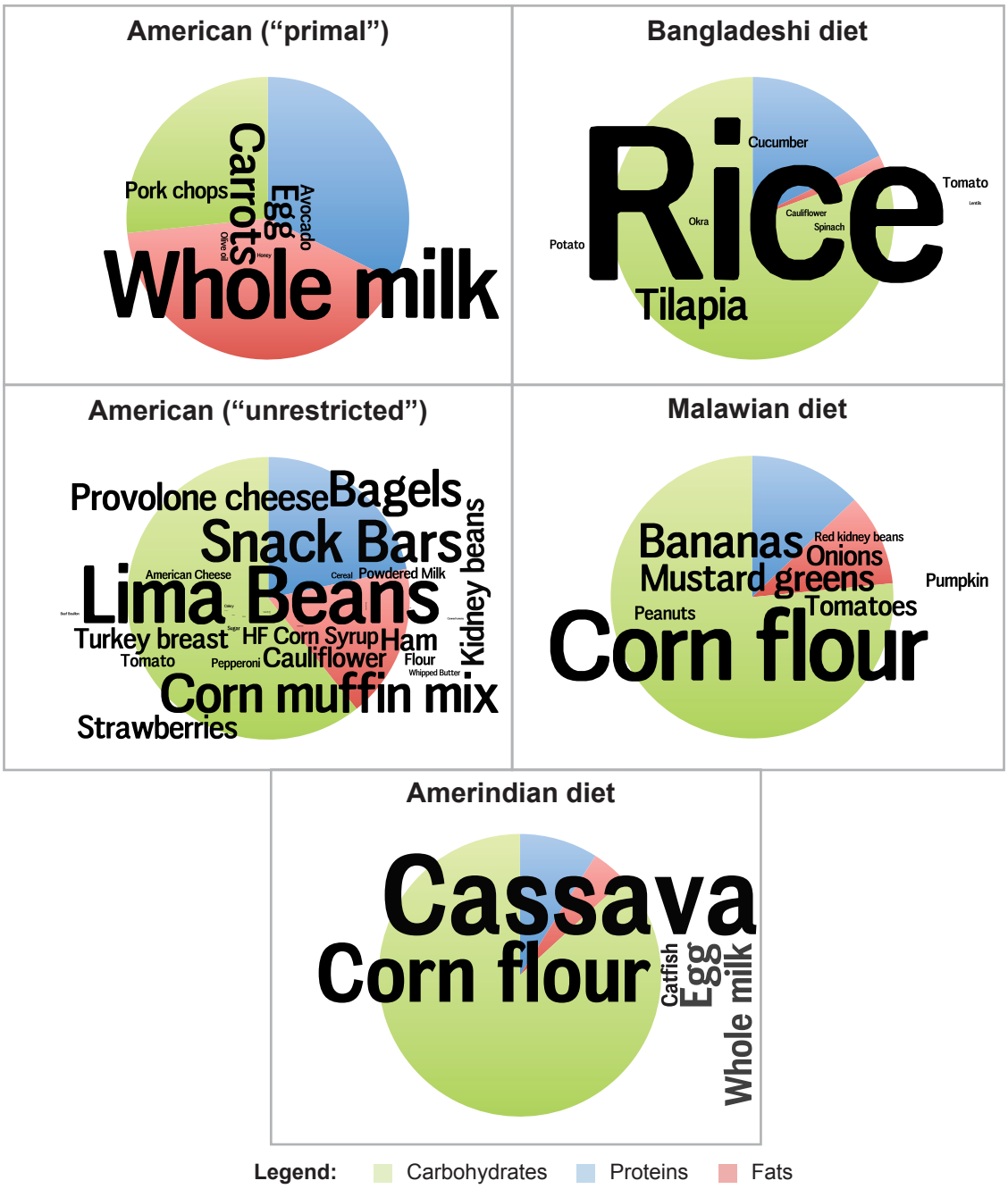

Figure S2.

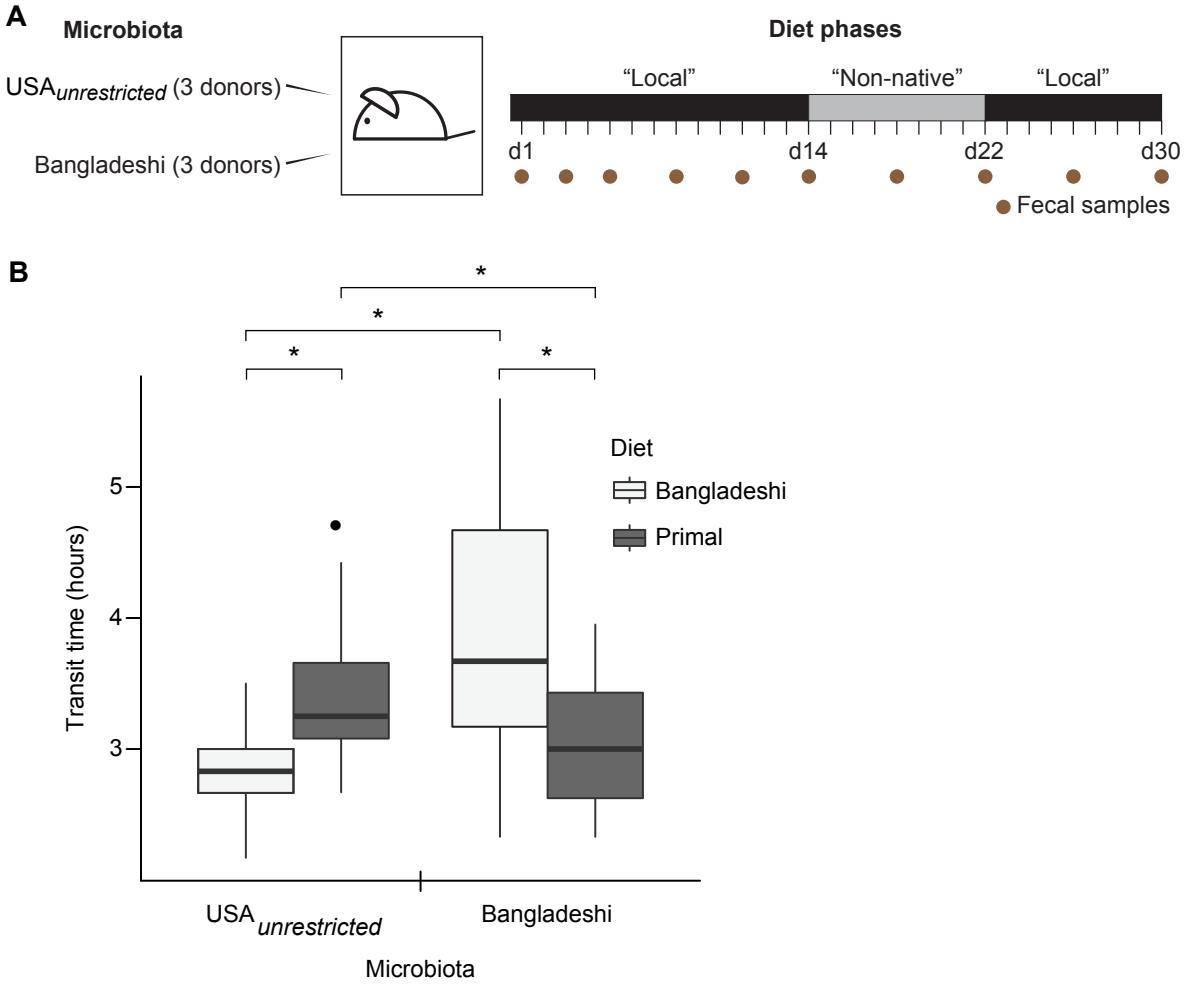

Figure S3.

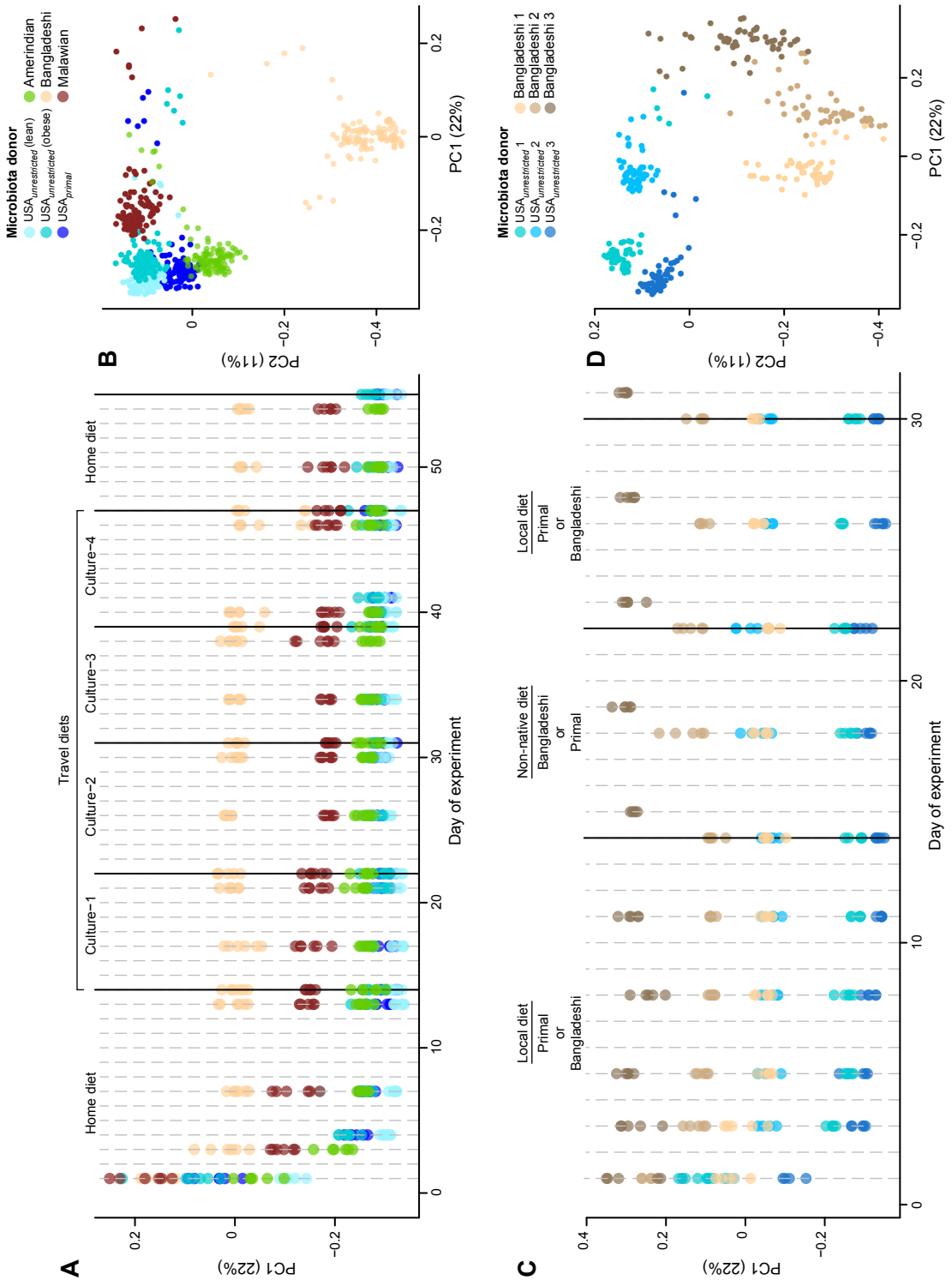

Figure S4.

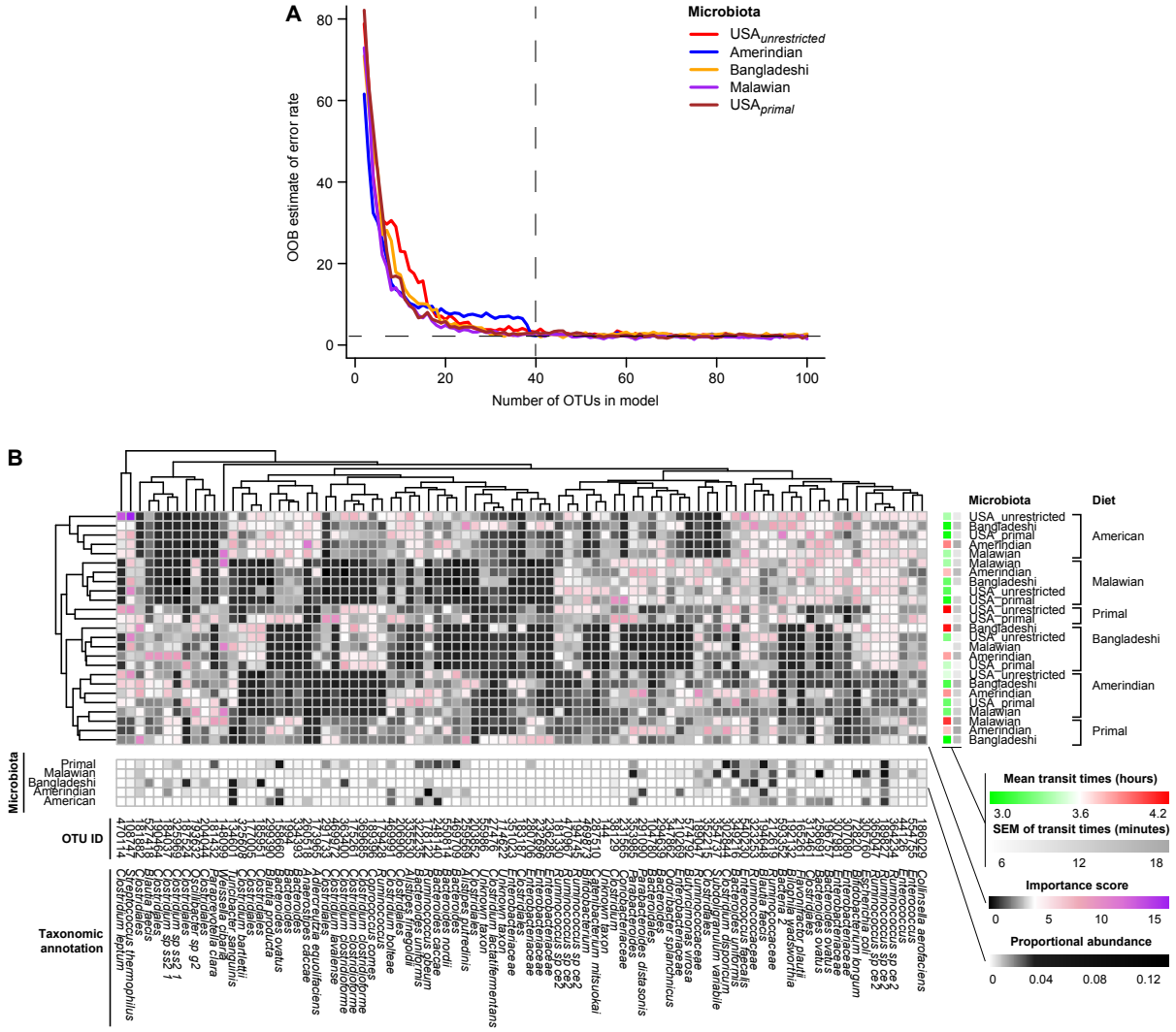

Figure S5.

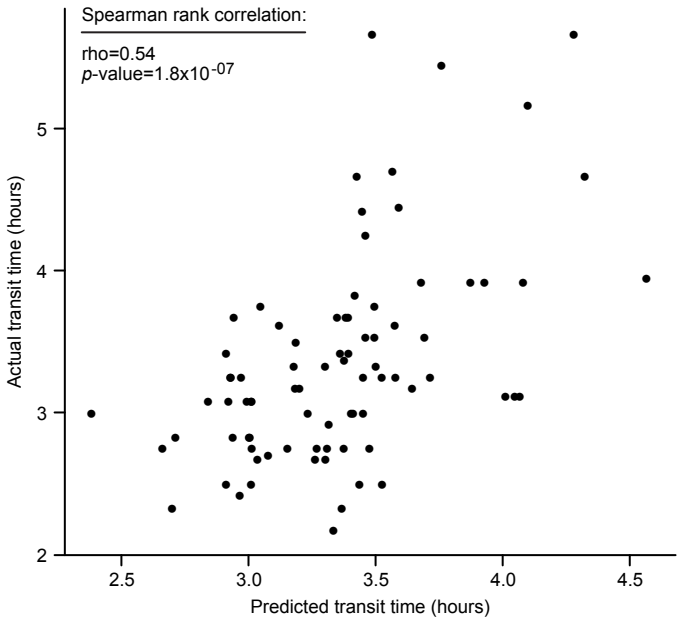

SUPPLEMENTAL TABLES

Table S1. Donor features and diets used in all experiments (related to Figure 1). **(A)** Demographics and IDs of microbiota donors. **(B)** Bacterial 16S rRNA-based analysis of the efficiency of transplantation of 97%ID OTUs present in the donors' microbiota in the 6-phase travel experiment. **(C)** Compositions of diets modeled after those consumed by microbiota donors. **(D)** Nutritional analyses of diets modeled after those consumed by microbiota donors, performed immediately after sterilization by irradiation and again after storage at 4°C for 2 months.

Table S2. Transit times and body weights of individual mice (related to Figure 1). (A) The 6-phase travel experiment. **(B)** The 3-phase travel experiment. **(C-E)** Experiments assessing the effects of turmeric on transit time. **(F)** Experiment comparing conventionally-raised specified pathogen free wild-type (*Ret*+/+) versus *Ret*+/- littermates.

Table S3. Diet, microbiota, and their interaction are significant factors impacting transit times (related to Figure 1). (A) Analysis of factors impacting transit times in 6-phase travel experiment: Repeated measures ANOVA. **(B)** 97%ID OTUs with significant diet-dependent correlations with transit times in an analysis of the highly contrasted diet-microbiota combinations (Bangladeshi/primal diets and Bangladeshi/$USA_{unrestricted}$ microbiota).

Table S4. DNA and RNA sequencing datasets from the 6-phase travel experiment, the 3-phase travel experiment, and experiments assessing the effects of turmeric (related to Figures 1-3). **(A)** Mouse fecal bacterial V4-16S rRNA datasets. **(B)** Mouse fecal bacterial COPRO-Seq datasets. **(C)** Mouse fecal microbial RNA-Seq dataset. **(D)** Mouse liver and distal ileum RNA-Seq sequencing dataset.

Table S5. Diet-discriminatory bacterial 97%ID OTUs identified by Random Forests (machine learning) analysis of datasets from 6-phase travel experiment (related to Figure 1). **(A)** For a given microbiota, the top 40 diet-discriminatory OTUs (n=5 diets tested). **(B)** 87 diet-discriminatory OTUs across, robust to microbiota and motility phenotypes.

Table S6. UPLC-MS analysis of bile acids in feces collected from gnotobiotic mice (related to Figure 2-3). **(A)** The 3-phase travel experiment, described in **Figure S2A**, involving wild-type C57BL/6 mice colonized with intact uncultured fecal microbiota from adult $USA_{unrestricted}$ or Bangladeshi donors fed Bangladeshi or primal diets. **(B)** Germ-free wild-type mice fed a Bangladeshi diet with and without turmeric. **(C)** Mice from the same experiment as in panel B but colonized with all members of the clonally arrayed bacterial culture collection from a Bangladeshi donor. **(D)** Mice from the 3-phase diet experiment described in **Figure 3A** colonized with either all members of the culture collection or the BSH_{hi} or BSH_{lo} consortium and fed the Bangladeshi diet with or without turmeric. **(E)** Wild-type mice were colonized with the BSH_{lo} consortium and fed a Bangladeshi diet ± turmeric in a 10-day single phase diet experiment.

Table S7. Identifying correlations between fecal metabolites, OTUs and transit times that are robust to diet (related to Figure 2). Untargeted UPLC-MS analysis of metabolites in the fecal microbiota of mice colonized with the uncultured fecal microbiota from adult $USA_{unrestricted}$ or Bangladeshi donors and fed Bangladeshi or primal diets. **(A)** Metabolites whose peak intensities are significantly correlated (by Spearman rank correlation) with transit times in the 3-phase travel experiment. Unadjusted *p*-values and Bonferroni-corrected *p*-values are shown. **(B)** Significant correlations (after Bonferroni corrections for multiple comparisons) between 97% ID OTUs, bile acids, and transit times in the 3-phase travel experiment.

Table S8. Analysis of the relationships between fecal bile acids and transit times (related to Figure 2). Linear models of transit times were regressed against fecal bile acid levels, with simplification by applying stepwise backward feature selection. **(A)** Results from the 3-phase travel experiment described in **Figure S2A** involving mice colonized with intact uncultured $USA_{unrestricted}$ and Bangladeshi microbiota and fed Bangladeshi and primal diets. **(B)** Analysis of datasets generated from the experiment in which mice colonized with the complete culture collection from a Bangladeshi child and germ-free controls were subjected to a 3-phase diet oscillation consisting of the Bangladeshi diet ± turmeric.

Table S9. Bacterial culture collection generated from the fecal microbiota of a healthy Bangladeshi child (related to Figure 3). List of 53 bacterial strains and their BSH enzyme activities as measured by an *in vitro* UPLC-MS based assay described in *Experimental Procedures*.

Table S10. KEGG-annotated genome features (related to Figure 3). Members of **(A)** the two 7-strain consortia and **(B)** the clonally arrayed bacterial culture collection generated from the fecal microbiota of a healthy 2-year-old Bangladeshi child from which the consortia were derived.

Table S11. Host genes whose expression is significantly affected by turmeric consumption in mice colonized with the BSH_{lo} consortium (related to Figure 3D). RNA-Seq datasets were generated from tissues harvested at the time of sacrifice. Animals were given a monotonous Bangladeshi diet either with or without turmeric for ten days. (**A**) Distal ileum. (**B**) Liver.

Chapter 4

Future Directions

One goal of using preclinical models of the type described in this thesis is to characterize microbe-microbe and microbe-host interactions under highly controlled conditions where dietary, microbial community and host manipulations can be performed in order to (i) characterize microbe-microbe interactions, microbe-host interactions, (ii) identify mechanisms that underlie these interactions and affect disease pathogenesis, and (iii) provide preclinical proof of concept that specific manipulations may mitigate or prevent disease (*1*, *2*).

Chapter 2 of this thesis supports the idea that intra- and interspecific competition plays a key role in preventing adverse outcomes from colonization with an enteropathogen such as enterotoxigenic *B. fragilis*. Using more specific knowledge about the nature of these competitive interactions may provide insight into building tools—whether they be specific bacterial strains, dietary ingredients, or both—that allow for extirpation or control of organisms without the risks inherent in broad-spectrum antibiotic treatment (*3*-*5*).

One series of experiments can be envisioned that directly tests whether any of the putative competitor species revealed when ETBF was co-colonized with the healthy culture collection can prevent the weight loss seen in mice receiving the complete culture collection from the severely stunted/underweight child while consuming a Bangladeshi diet. A first test would be to colonize mice with the stunted donor culture collection plus the NTBF strains from the healthy donor's culture collection, with the hypothesis being that NTBF-ETBF interactions and/or other interactions between NTBF strains and the stunted/underweight community members are sufficient to mitigate the ETBF-dependent weight loss and metabolic phenotypes transmitted through colonization with the underweight donor's culture collection. However, given that ETBF did not induce weight loss in mice harboring the healthy culture collection ±NTBF, other taxa from the healthy donor's culture collection may be required to prevent or ameliorate the ETBF-dependent phenotypes transmitted to recipient mice by the stunted/underweight culture collection. Recently, Faith and Ahern described a screening method that helps overcome the large combinatorial challenge of identifying which strain or set of strains from the healthy donor culture collection might achieve this effect (*6*). Their approach involves generating random subsets of strains from a clonally arrayed culture

collection with overlapping membership and testing their effects on a given phenotype in a given microbial community context. Subsets of nominal size (e.g., 3-10 members, etc.) are generated with each subset of a given size representing a consortium of unique composition *but* overlapping membership. Biological repetition for each strain is achieved because subsets have overlapping membership. Strains whose presence in a consortium best explain phenotypic variation are advanced to a validation step where they alone, or in combination are tested.

After determining whether an individual strain or a small consortium of strains from the healthy donor's culture collection could mitigate weight-loss transmitted by the ETBF (+) stunted/underweight donor culture collection, follow-up experiments could test the generalizability of the findings. In particular, hypotheses worthy of follow-up include: do other strains of ETBF from other Bangladeshi donors have the same community and host effects as the ETBF strain from the stunted donor in the context of that donor's culture collection; do other strains of ETBF have the same effects on host phenotypes and community gene expression (including virulence gene expression) in the context of the healthy donor's culture collection; do other NTBF strains or strains, identified via the previously described combinatorial screen, from other healthy individuals have the same effects on ETBF and ETBF-dependent transmissible host phenotypes in the context of the stunted/underweight donor's community described in my thesis? Probiotic leads identified from studies involving culture collections could be advanced to testing intact uncultured microbiota from undernourished children with ETBF (and other enteropathogens) ± evidence of EED living in Mirpur, from other areas of Bangladesh, or conceivably from other countries where the burden of undernutrition is high.

These types of studies would require a variety of methods, a number of which were applied during the course of the work described in this thesis. A comprehensive analysis could include (i) comparative genomics of the strains to be tested, (ii) body composition phenotyping (using quantitative magnetic resonance) to ascertain the effects on adiposity versus lean body mass, (iii) microbial RNA-Seq of the various communities harbored by colonized gnotobiotic mice, (iv) careful monitoring of food consumption (using pelleted embodiments of the Bangladeshi diets)

and bomb calorimetry of feces (to define the efficiency of energy extraction from the diet by the microbiota), (v) serum assays of regulators of energy balance/nutrient utilization/immunoinflammatory responses); (vi) transcriptional profiling via RNA-Seq of distal intestine/colon, liver and gastrocnemius muscle (to better define host responses including those involving components of the innate and adaptive immune system, metabolic signaling, metabolic pathways critical for nutrient processing and biosynthesis), (vii) mass spectrometry-based profiling of microbial community and host metabolism (to validate and discover new discriminatory biomarkers of host responses, and (viii) FACS-based studies characterizing immune cell populations and gut barrier function. Implementation of (ii)-(viii) would initially be prioritized based on those microbial manipulations that have the greatest effect size weight and identified discriminatory metabolic biomarkers.

Other studies would involve diet manipulations. The intergenerational transmission experiments described in Chapter 2 allude to a diet dependency of the pathogenic effects of ETBF. Developing more efficacious food interventions for treating children with undernutrition is currently an active area of investigation. As noted in Chapter 1, while a number of protocols have been developed (*7*), efficacy has been limited for treating stunting, neurodevelopmental abnormalities and immune defects such as poor vaccine responsiveness. (*1*, *8*-*10*). Adding additional experimental arms where diet is a variable should help identify locally sourced and culturally acceptable foods that can be used as complimentary feeding therapies along with, or potentially in lieu of, treatment with a targeted probiotic. These avenues of experimentation should enhance our understanding of the interactions of diet, the gut microbiota, and the enteric dysfunction that is often associated with severe stunting. Exploration of nutritional therapies along with newly identified probiotic candidates in preclinical animal models will hopefully guide clinical researchers toward mechanistically-informed standardized methods for restoring healthy gut microbiota function to mitigate the long-term sequelae of childhood stunting precipitated by undernutrition.

Finally, an intriguing finding obtained from the microbial RNA-Seq studies described in Chapter 2 was that expression of a large set of putative virulence factors from multiple strains comprising the healthy donor's culture collection was significantly affected by ETBF (virulence

gene expression was not affected by the presence or absence of ETBF in the context of the stunted/ underweight culture collection which shared only one strain with the healthy culture collection). These findings raise the question: What are the underlying mechanisms by which ETBF influences expression of these factors in members of the healthy culture collection? Quorum sensing regulates microbial gene expression in response to population density (*11*) and plays an integral role in signaling among the gut microbiota (*12*) as well as between the commensal gut bacteria and the enteropathogen *Vibrio cholera* (*13*). Quorum sensing regulates microbial gene expression in response to population density (*11*) and plays an integral role in signaling among the gut microbiota (*12*) as well as between the commensal gut bacteria and the enteropathogen Vibrio cholera (13). The quorum-sensing pathway identified by RNA-Seq was the LuxQ pathway that senses signaling pathways occur through the autoinducer 2 (AI-2) pathway, also encoded by numerous Bacteroides species (*14*). At low cell density, and thus low concentrations of of AI-2, LuxQ has kinase activity, while at high cell density, in the presence of AI-2, kinase activity is inactivated and the LuxQ switches to a phosphatase activity. These changes between LuxQ enzymatic activities are responsible for transmitting information about the surrounding environment to the cytoplasm (*15*). Expression of luxQ in ETBF was dramatically increased by the presence of NTBF in the healthy culture collection context: this finding is of interest given the lower relative abundances of the *B. thetaiotaomicron, E. avium,* and *B. caccae* strains as a result of ETBF and NTBF co-colonization. LuxQ is not a well-characterized AI-2 sensing kinase in *Bacteroides fragilis* and presents an interesting target for genetic manipulation in both ETBF and NTBF to ascertain its role in regulating community structure and gene expression; especially in light of recent work demonstrating *E. coli* engineered to express high levels of AI2 dramatically lowered the relative abundance of *Bacteroidetes in vivo* (*12*).

Both avenues of research may offer deeper insight into mechanistic interactions of the gut microbiota and its influence on host health. Through a better mechanistic understanding of the gut microbiota, we should be able to develop therapeutics using dietary and microbial interventions that target health-related factors influenced by the microbiota.

REFERENCES

1. S. Subramanian *et al.*, Perspective, *Cell* **161**, 36–48 (2015).

2. J. I. Gordon, K. G. Dewey, D. A. Mills, R. M. Medzhitov, The human gut microbiota and undernutrition, *Science Translational Medicine* **4**, 137ps12–137ps12 (2012).

3. L. M. Cox *et al.*, Altering the Intestinal Microbiotaduring a Critical Developmental Window Has Lasting Metabolic Consequences, *Cell* **158**, 705–721 (2014).

4. F. Marra *et al.*, Antibiotic Use in Children Is Associated With Increased Risk of Asthma, *PEDIATRICS* **123**, 1003–1010 (2009).

5. L. Dethlefsen, S. Huse, M. L. Sogin, D. A. Relman, J. A. Eisen, Ed. The Pervasive Effects of an Antibiotic on the Human Gut Microbiota, as Revealed by Deep 16S rRNA Sequencing, *PLoS Biol* **6**, e280 (2008).

6. J. J. Faith, P. P. Ahern, V. K. Ridaura, J. Cheng, J. I. Gordon, Identifying gut microbe-host phenotype relationships using combinatorial communities in gnotobiotic mice, *Science Translational Medicine* **6**, 220ra11 (2014).

7. L. L. Iannotti, I. Trehan, K. L. Clitheroe, M. J. Manary, Diagnosis and treatment of severely malnourished children with diarrhoea, *J Paediatr Child Health* **51**, 387–395 (2015).

8. C. Y. Chang *et al.*, Children Successfully Treated for Moderate Acute Malnutrition Remain at Risk for Malnutrition and Death in the Subsequent Year after Recovery, *J Nutr* **143**, 215–220 (2013).

9. I. Trehan *et al.*, Antibiotics as part of the management of severe acute malnutrition, *N Engl J Med* **368**, 425–435 (2013).

10. S. Subramanian *et al.*, Persistent gut microbiota immaturity in malnourished Bangladeshi children, *Nature* (2014).

11. M. B. Miller, B. L. Bassler, Quorum sensing in bacteria, *Annual Reviews in Microbiology* (2001).

12. J. A. Thompson, R. A. Oliveira, A. Djukovic, C. Ubeda, K. B. Xavier, Manipulation of the Quorum Sensing Signal AI-2 Affects the Antibiotic-Treated Gut Microbiota, *CellReports* **10**, 1861–1871 (2015).

13. A. Hsiao *et al.*, Members of the human gut microbiota involved in recovery from Vibrio cholerae infection, *Nature* **515**, 423–426 (2014).

14. L. C. M. Antunes *et al.*, Bacteroides species produce Vibrio harveyi autoinducer 2-related molecules, *Anaerobe* **11**, 295–301 (2005).

15. M. B. Neiditch, M. J. Federle, S. T. Miller, B. L. Bassler, F. M. Hughson, Regulation of LuxPQ Receptor Activity by the Quorum-Sensing Signal Autoinducer-2, *Molecular Cell* **18**, 507–518 (2005).